AD_____

GRANT NUMBER: DAMD17-93-J-3018

TITLE: Triplex Forming Therapeutic Agents for Breast Cancer

PRINCIPAL INVESTIGATOR: Donald M. Miller, M.D., Ph.D.

CONTRACTING ORGANIZATION: University of Alabama at Birmingham
Birmingham, Alabama 35294

REPORT DATE: December 1995

TYPE OF REPORT: Final

PREPARED FOR: Commander
U.S. Army Medical Research and Materiel Command
Fort Detrick, Frederick, Maryland 21702-5012

REPORT DOCUMENTATION PAGE

Form Approved
OMB No. 0704-0188

1. AGENCY USE ONLY *(Leave blank)*	2. REPORT DATE	3. REPORT TYPE AND DATES COVERED
	December 1995	Final (15 Dec 92 - 16 Nov 95)

4. TITLE AND SUBTITLE
Triplex Forming Therapeutic Agents for Breast Cancer

5. FUNDING NUMBERS
DAMD17-93-J-3018

6. AUTHOR(S)
Donald M. Miller, M.D., Ph.D.

7. PERFORMING ORGANIZATION NAME(S) AND ADDRESS(ES)
University of Alabama at Birmingham
Birmingham, Alabama 35294

8. PERFORMING ORGANIZATION REPORT NUMBER

9. SPONSORING/MONITORING AGENCY NAME(S) AND ADDRESS(ES)
Commander
U.S. Army Medical Research and Materiel Command
Fort Detrick, Frederick, Maryland 21702-5012

10. SPONSORING/MONITORING AGENCY REPORT NUMBER

11. SUPPLEMENTARY NOTES

12a. DISTRIBUTION / AVAILABILITY STATEMENT
Approved for public release; distribution unlimited

12b. DISTRIBUTION CODE

13. ABSTRACT *(Maximum 200*

The overall goal of this proposal was to develop sequence specific DNA binding compounds which are targeted to the promoters of the c-myc, c-Ha-ras, and neu genes. Inhibition of expression of these genes, which appear to play an important role in the development of the malignant phenotype of breast carcinoma cells would be expected to inhibit cellular proliferation and possibly induce apoptosis. During the period of funding we have demonstrated sequence specific triplex formation for the c-myc P1 and P2, neu, cyclin D1, and Ki-ras promoters. We have developed new methods to demonstrate the uptake of triplex forming oligonucleotides by single cells. We have developed a transgenic model with which to test the effects of c-myc targeted oligonucleotides. We have begun to create vectors which will express "triplex forming transcripts" and which may have utility as gene therapy vectors. We have demonstrated that the use of DNA binding drugs and triplex forming oligonucleotides may be compelementary. These unexpected observations have substantially enhanced the likelihood that this approach to breast cancer will be successful. Our laboratory group has published 25 manuscripts which are directly relevant to this grant during its three year period of funding.

14. SUBJECT TERMS	15. NUMBER OF PAGES
Triplex, breast cancer	71
	16. PRICE CODE

17. SECURITY CLASSIFICATION OF REPORT	18. SECURITY CLASSIFICATION OF THIS PAGE	19. SECURITY CLASSIFICATION OF ABSTRACT	20. LIMITATION OF ABSTRACT
Unclassified	Unclassified	Unclassified	Unlimited

FOREWORD

Opinions, interpretations, conclusions and recommendations are those of the author and are not necessarily endorsed by the US Army.

___ Where copyrighted material is quoted, permission has been obtained to use such material.

___ Where material from documents designated for limited distribution is quoted, permission has been obtained to use the material.

___ Citations of commercial organizations and trade names in this report do not constitute an official Department of Army endorsement or approval of the products or services of these organizations.

___ In conducting research using animals, the investigator(s) adhered to the "Guide for the Care and Use of Laboratory Animals," prepared by the Committee on Care and Use of Laboratory Animals of the Institute of Laboratory Resources, National Research Council (NIH Publication No. 86-23, Revised 1985).

___ For the protection of human subjects, the investigator(s) adhered to policies of applicable Federal Law 45 CFR 46.

___ In conducting research utilizing recombinant DNA technology, the investigator(s) adhered to current guidelines promulgated by the National Institutes of Health.

___ In the conduct of research utilizing recombinant DNA, the investigator(s) adhered to the NIH Guidelines for Research Involving Recombinant DNA Molecules.

___ In the conduct of research involving hazardous organisms, the investigator(s) adhered to the CDC-NIH Guide for Biosafety in Microbiological and Biomedical Laboratories.

PI - Signature Date

Table of Contents

INTRODUCTION

The overall goal of this three year grant was to develop sequence specific DNA binding compounds which are targeted to the promoters of the c-myc, c-Ha-ras, and neu genes. Inhibition of expression of these genes, which appear to play an important role in the development of the malignant phenotype of breast carcinoma cells, would be expected to inhibit cellular proliferation and possibly induce apoptosis. The experiments which were originally proposed were based largely on our extensive experience with the transcriptional inhibitory effects of G-C specific DNA binding drugs such as mithramycin. During the period of funding, we have made several unexpected observations which have substantially enhanced the likelihood that this approach to breast cancer will be successful. Our laboratory group has published 25 manuscripts which are directly relevant to this grant during its three year period of funding, six of those resulted from the work supported by this grant..

BODY

Specific Aim 1: To determine whether neu, c-myc, and c-Ha-ras targeted acridine-oligonucleotide conjugates inhibit expression of the target genes in breast cancer cells in culture.

1. Triplex Formation by the human neu promoter inhibits regulatory protein binding and transcriptional activity. (J. Clin. Invest. 92:2433-2439, 1993). The HER-2/neu oncogene promoter sequence contains a polypurine region from -42 to -69 upstream of the transcription start site which is a potential triplex forming sequence. Gel shift analysis shows that a 28-mer oligonucleotide which is identical to the target sequence but in antiparallel orientation will form triplex DNA with the target duplex in a concentration dependent manner **(Figure 1)**. Triplex formation occurs at 100 fold excess of TFO, but does not occur with a control parallel oligonucleotide. The Kd of triplex formation by the TFO is 4.5 x 10^5 M. The sequence specificity of this intermolecular triplex in the HER-2/neu promoter was confirmed by DNAse I protection footprinting. A gel mobility shift experiment in which a HeLa nuclear extract was added to the HER-2/neu promoter demonstrates that triplex formation prevents nuclear protein binding **(Figure 2)**. This indicates that triplex formation prevents the binding of one or more nuclear proteins to the HER-2/neu promoter. In addition, triplex formation by this sequence results in specific inhibition of in vitro

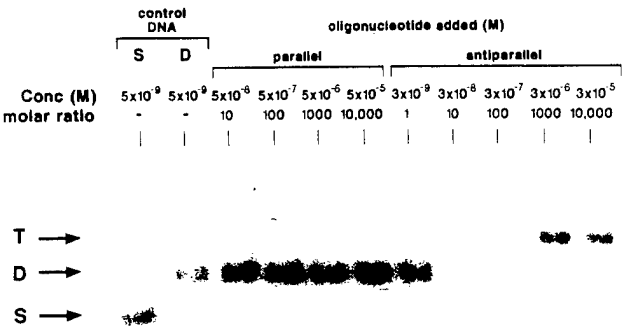

Gel mobility shift analysis showing concentration dependent triplex formation. In all lanes, the 28-base pyrimidine rich strand of the target sequence is labeled. The labeled strand was annealed to its purine-rich complement, and the parallel or antiparallel purine rich oligonucleotides were added as described in Methods. Single and double strand controls were included. The concentration of the target sequence was constant at 5×10^{-9} M for the control lane and parallel lanes and at 3.3×10^{-9} M (numbers in figure have been truncated for clarity) in the antiparallel lanes. The oligonucleotide added, its concentration, and its molar ratio to the target DNA are indicated. *S*, single strand DNA; *D*, duplex DNA; *T*, triplex DNA.

Figure 1.

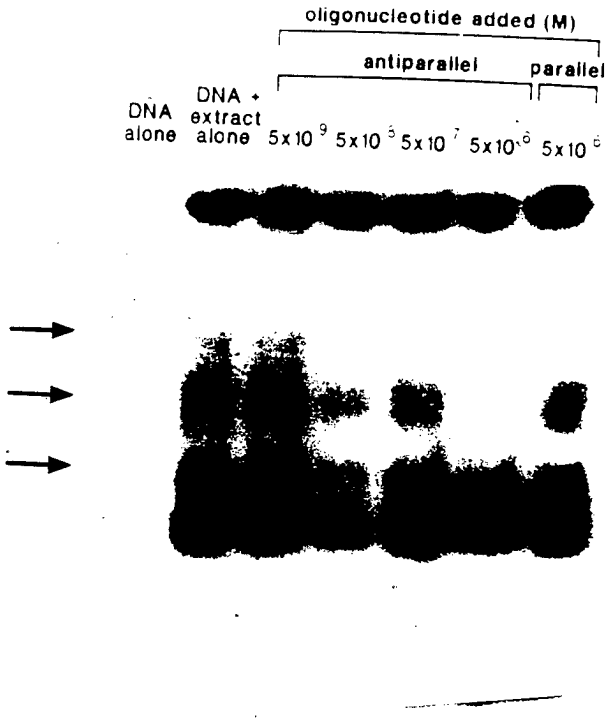

Gel mobility shift analysis demonstrating protein binding by a nuclear extract to the HER-2/neu promoter. A 119-bp fragment of the HER-2/neu promoter was labeled and incubated with a HeLa nuclear extract as described. In the "oligonucleotide added" lanes, the DNA was preincubated with the antiparallel or parallel purine-rich oligonucleotides at the concentrations indicated. Arrows indicate protein-DNA complexes that are prevented by the triplex formation.

Figure 2.

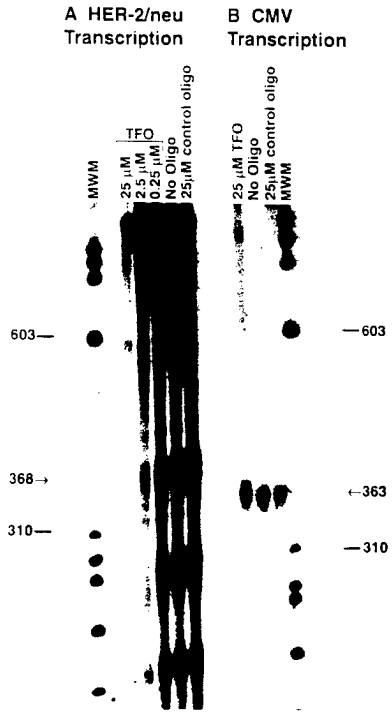

In vitro transcription assay demonstrating specific inhibition of HER-2/neu transcription. (*A*) Transcription from a digested plasmid containing the HER-2/neu promoter-template. (*B*) Transcription from a purified CMV promoter template. Oligonucleotides were added to the template DNA as described at the concentrations indicated above each lane. HER-2/neu transcription yields a full-length 368-base RNA transcript (*arrow*), as well as two smaller prematurely terminated transcripts of ~ 250 and 150 bases. These transcripts are inhibited by triplex formation with the antiparallel 28 base oligonucleotide in a concentration dependent fashion. A purine-rich oligonucleotide antiparallel to an adjacent target site does not form triplex and has no effect on in vitro transcription (control oligo). Large molecular weight bands in *A* at 600 and 1,500 bases represent interaction of the HeLa extract with the plasmid backbone and are not HER-2/neu transcripts. CMV transcription with a purified promoter template yields a single 363-base transcript (*arrow, B*). Neither the TFO nor the control oligonucleotide have an effect on CMV transcription. *MWM*, ϕX174/HaeIII molecular weight marker with the 310 and 603 base standards indicated.

Figure 3.

transcription of the neu promoter **(Figure 3)**. The triplex target site in the neu promoter is one of importance to the transcription of the HER-2/neu oncogene since it lies between the CCAAT and TATA boxes, binding sites for two factors necessary for transcription.

2. Inhibition of in vitro transcription by a triplex forming oligonucleotide targeted to the human c-myc P2 promoter (Biochemistry 34:8165-8171).

Triplex-forming oligonucleotides (TFOs) have been shown to bind in a sequence-specific manner to polypurine/polypyrimidine sequences in several human gene promoters, including the c-myc P1 promoter. TFOs have been shown to inhibit transcription in vitro and the expression of target genes in cell culture. The human c-myc protooncogene contains a 23 base pair purine-pyrimidine-rich motif (-62 to -40) within its predominant promoter, P2, that is a potential target for purine-purine-pyrimidine triplex formation. Using electrophoretic mobility shift analysis (EMSA) and competition experiments, we have demonstrated that a MAZ (myc-associated zinc

finger protein) consensus sequence is capable of competing with the purine-pyrimidine motif for the binding of a HeLa nuclear protein **(Figure 4)**. We have shown the formation of an intermolecular triplex using a 23-base purine-rich oligonucleotide antiparallel to the purine-rich target

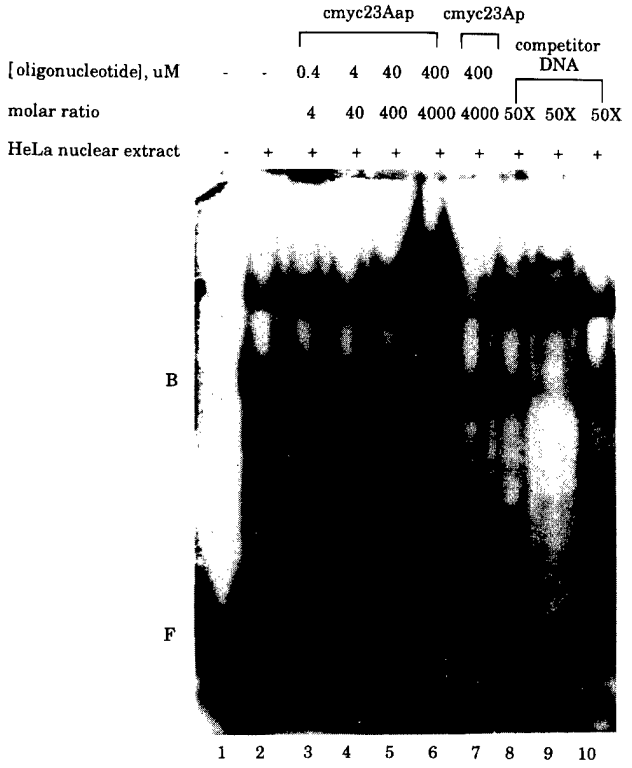

EMSA demonstrating sequence-specific nuclear protein binding to the human c-*myc* duplex target and its inhibition by triplex-forming oligonucleotide. ^{32}P-Labeled 23-bp human c-*myc* fragment was incubated with competitor duplex or oligonucleotides as described, and then HeLa nuclear extract was added. Nonspecific competitor, MAZ consensus, and E2F consensus DNA were added to lanes 8–10, respectively. Nonspecific competitor sequence: 5′-AAAGATCCTCTCTCGCTAATCTC-3′. MAZ consensus sequence: 5′-GGGGGAGGGGG-3′. E2F consensus sequence: 5′-ATTTAAGTTTCGCGCCCTTTCTCAA-3′. Abbreviations: B = protein–DNA complex; F = unbound DNA probe.

Figure 5

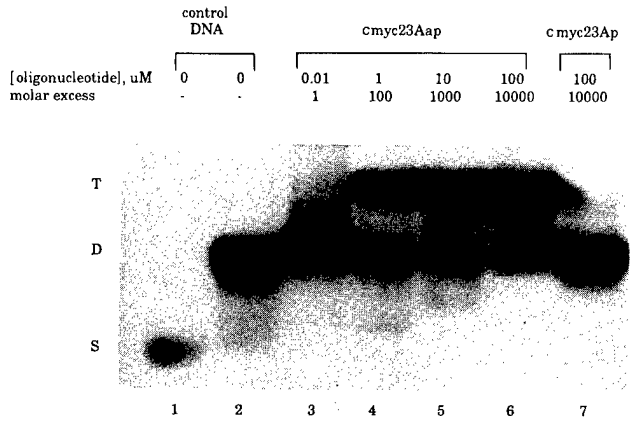

EMSA of oligonucleotide-directed triplex formation in the c-*myc* P2 promoter target. The pyrimidine-rich strand of the 23-mer target was labeled (lane 1) and annealed with the unlabeled purine-rich strand (lane 2). The 23-bp duplex target was then incubated with increasing concentrations of triplex-forming oligonucleotide π (lanes 3–6) or control oligonucleotide (lane 7). The concentration of triplex-forming oligonucleotide or control oligonucleotide added to the 10 nM ^{32}P-labeled 23-bp duplex and their molar ratio to the target duplex DNA are indicated above each lane. Abbreviations: S = single-strand DNA; D = duplex DNA; T = triplex DNA.

Figure 4

sequence**(Figure 5)**. DNAse I footprinting was performed to confirm the exact location of triplex formation. Triplex formation by this oligonucleotide prevents binding of a HeLa nuclear protein (presumably MAZ) to the target site. We have also shown that the P2-targeted TFO is a potent and specific inhibitor of c-myc transcription in vitro **(Figure 6)**. These data demonstrate that this novel TFO inhibits transcription of the c-myc P2 promoter. We propose that the P2-targeted TFO has its effect by blocking the binding of the regulatory factor MAZ.

3. <u>Inhibition of nuclear protein binding to two sites in the murine c-myc promoter by intermolecular triplex formation (Biochemistry 34:7659-7667, 1995).</u>

The c-myc gene is overexpressed in a variety of tumor types and appears to play an important role in the abnormal growth of a number of cell types. In an effort to determine the ability of sequence- and species-specific triplex-forming oligonucleotides to inhibit expression of a targeted gene in animals, we have identified two novel triplex-forming sites in the murine c-myc promoter. One is homologous to the triplex-forming human PuF binding element located upstream of the P1

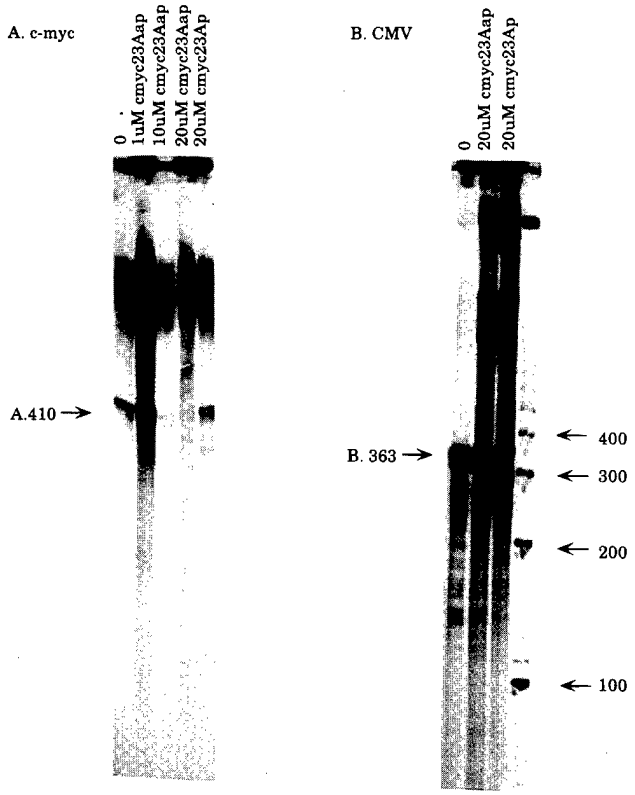

: *In vitro* transcription assay demonstrating specific inhibition of c-*myc* transcription: (A) *in vitro* transcription from a plasmid containing the c-*myc* promoter region; (B) *in vitro* transcription from a purified CMV early promoter region. Oligonucleotides were added to the template DNA as described at concentrations indicated above each lane. *In vitro* transcription of the plasmid containing c-*myc* promoter yields a 412-base RNA transcript indicated by arrow A. The transcription is inhibited by triplex-forming oligonucleotide whereas the purine-rich control oligonucleotide has no effect on *in vitro* transcription. *In vitro* transcription using CMV promoter template yields a single 363-base transcript indicated by arrow B. Neither the c-*myc* TFO nor the control oligonucleotide has any effect on transcription from the CMV promoter. The 100-bp ladder was end-labeled with T4 PNK and used as the molecular weight marker.

Figure 6.

transcription start site. The other triplex-forming site is found in a region between P1 and P2 that encompasses the ME1a1 binding site and part of the E2F binding site and is highly homologous to the human sequence. Synthetic oligodeoxyribonucleotides designed to target these essential regulatory elements form sequence-specific triple helices as demonstrated by gel mobility shift analysis and DNASE I footprinting. Polypurine: polypyrimidine regions in the P1 and P2 promoters form specific protein-DNA complexes upon incubation with a murine YC8 nuclear extract. Preincubation of each of the promoter fragments with its respective triplex-forming oligonucleotide results in the inhibition of nuclear protein binding. Non-triplex-forming oligonucleotides do not significantly affect protein binding. The data presented are a preliminary step toward generating an animal model for the phenotypic effects of triplex formation within the c-myc promoter.

4. Triplex formation by the human c-Ki-ras promoter prevents regulatory protein binding. (Biochemistry). The human Ki-ras promoter contains a 22 base pair homopurine:homopurine (pur:pyr) motif within a region that is nuclease hypersensitive in both native chromatin and supercoiled plasmids. Gel mobility shift analysis and competition experiments show that this pur:pyr motif binds a nuclear protein(s) which is an important regulatory factor. Gel mobility shift analysis and DNase I footprinting demonstrate that oligonucleotides can form triplex DNA with this sequence [purine*purine:pyrimidine (pur*pur:pyr) or mixed purine/pyrimidine*purine:pyrimidine (pur/pyr*pur:pyr) intermolecular triple helices through guanine (G) recognition of guanine:cytosine (G:C) base pairs and either adenine (A) or thymine (T) recognition of adenine:thymine (A:T) base pairs in the target sequence]. Triple helices containing either T*A:T or A*A:T triplets are formed exclusively with oligonucleotides antiparallel to the homopurine target strand. The affinity of the oligonucleotide which forms T*A:T triplets is approximately equal to or, slightly greater than, the affinity of an oligonucleotide which forms A*A:T triplets. Oligonucleotide-directed triplex formation inhibits sequence specific nuclear protein binding to the Ki-ras promoter. These observations suggest that triplex formation by the oligonucleotides described here may provide a means to specifically inhibit transcription of the Ki-ras oncogene.

transcription of this oncogene.

5. Triplex formation by the human c-Ki-ras promoter prevents regulatory protein binding. (J. Biol. Chem. 269:18232-18238,1994). The human Ki-ras promoter contains a 22 base pair homopurine:homopurine (pur:pyr) motif within a region that is nuclease hypersensitive in both native chromatin and supercoiled plasmids. Gel mobility shift analysis and competition experiments show that this pur:pyr motif binds a nuclear protein(s) which is an important regulatory factor. Gel mobility shift analysis and DNase I footprinting demonstrate that oligonucleotides can form triplex DNA with this sequence [purine*purine:pyrimidine (pur*pur:pyr) or mixed purine/pyrimidine*purine:pyrimidine (pur/pyr*pur:pyr) intermolecular triple helices through guanine (G) recognition of guanine:cytosine (G:C) base pairs and either adenine (A) or thymine (T) recognition of adenine:thymine (A:T) base pairs in the target sequence]. Triple helices containing either T*A:T or A*A:T triplets are formed exclusively with oligonucleotides antiparallel to the homopurine target strand. The affinity of the oligonucleotide which forms T*A:T triplets is approximately equal to or, slightly greater than, the affinity of an oligonucleotide which forms A*A:T triplets. Oligonucleotide-directed triplex formation inhibits sequence specific nuclear protein binding to the Ki-ras promoter. These observations suggest that triplex formation by the oligonucleotides described here may provide a means to specifically inhibit transcription of the Ki-ras oncogene.

Specific Aim 2. To characterize the antiproliferative effects of the neu, c-myc, and c-Ha-ras targeted acridine-oligonucleotide conjugates, individually and in combination, in breast carcinoma cells.

1. Triplex formation by a c-myc targeted triplex forming acridine-oligonucleotide conjugate prevents Puf (nm23) binding to the c-myc P1 promoter. (Gyn. Onc., 49:339-343, 1993) and inhibits expression of the c-myc gene and cellular proliferation by HL-60 cells. (Manuscript submitted.). We have synthesized an acridine-oligonucleotide conjugate targeted to the 5' flanking region of the c-myc gene (-115 to -142) which is largely polypurine/polypyrimidine and has been shown to form triplex (Figure 7). The triplex forming sequence binds the Puf protein which is necessary for the transcriptional activity of c-myc. The c-myc targeted conjugate is comprised of acridine, a six methylene linking molecule, and a 27 bp G-rich triplex forming oligonucleotide. The G-rich 27 bp oligonucleotide conjugate forms triplex DNA, while the C-rich complementary conjugate

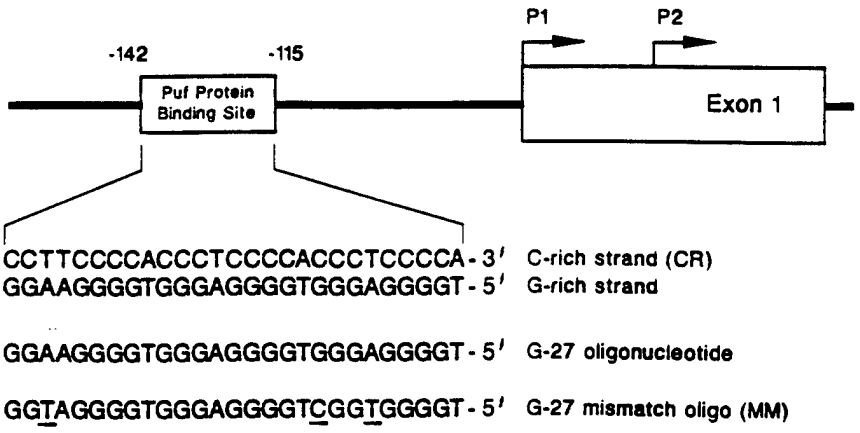

FIG. 1. c-myc promoter region showing target sequence and oligonucleotides.

Figure 7. Sequence of the c-myc P1 triplex forming region and triplex forming oligonucleotides.

does not. The binding of both the oligonucleotide and the conjugate are sequence specific. Synthesis of a conjugate with 2 bp substitutions completely abrogates triplex formation as evidenced by gel shift and DNAse footprint analysis.

We have used polyacrylamide gel analysis of triplex formation to demonstrate that the triplex forming oligonucleotides can form both duplex and triplex DNA structures and DNAse 1 footprinting analysis to determine the relative sequence specificity of this binding. Both duplex and triplex formation by the c-myc targeted conjugate occur at relatively low conjugate:target ratios. This documents the formation of duplex and triplex DNA structures in the presence of increasing concentrations of acridine-oligonucleotide conjugate. The c-myc targeted acridine-oligonucleotide conjugate demonstrates sequence specific interaction with its target sequence, as shown by the DNAse I footprint pattern which is identical to the binding pattern of the G-27 oligonucleotide. Experiments performed at lower oligonucleotide and conjugate concentrations demonstrate an identical or slightly reduced binding affinity, but a 15 to 30 fold decreased "off rate" of the conjugate. On the other hand, no binding is seen by the complementary C-rich oligonucleotide or conjugate (data not shown). We can demonstrate that triplex formation prevents protein binding to the target sequence and in vitro transcription by the c-myc promoter.

In order to document the effect of the targeted compound on c-myc expression, RNA was isolated from HL-60 cells at various times following acridine-oligonucleotide addition. As shown in **Figure 8**, there is a dramatic and early inhibition of c-myc expression by the G-rich, but not by the C-rich conjugate, associated with a decrease in the number of viable cells which were treated with the triplex forming conjugate. Similar results were obtained in an experiment with the SKOV-3

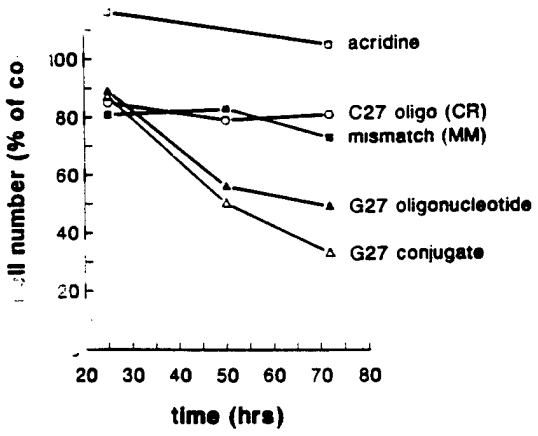

HeLa cells. Viable cell number as percentage of control (untreated) cells.

Figure 8.

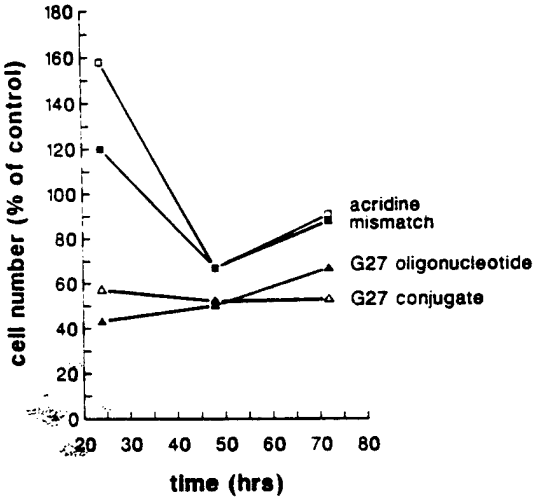

SKOV-3 cells. Viable cell number as percentage of control (untreated) cells.

Figure 9.

ovarian cell line **(Figure 9)**. There is no inhibition of c-myc expression by the 2 bp substituted conjugate. This preliminary data suggests that the c-myc promoter targeted compound is able to specifically inhibit expression of the c-myc protooncogene. This compound has no effect on

expression of the actin and DHFR gene in these cells. Initial experiments were designed to determine whether the targeted acridine conjugate had a greater antiproliferative effect or cellular toxicity than did either acridine or oligonucleotide alone. Neither 5 uM acridine, or the oligonucleotide have a significant effect on thymidine incorporation by HL-60 cells after 48 hours of exposure. The acridine conjugate, on the other hand, (5 uM) resulted in 94% inhibition of DNA synthesis. This observation indicates that this c-myc targeted compound is an effective antiproliferative agent. These results were confirmed by studying the effect of this compound on cell number. The c-myc targeted compound however, demonstrated a concentration dependent inhibition of cellular proliferation. This indicates that the effect of targeted acridine compound may be specific for c-myc expression. Neither 5 uM acridine, or the oligonucleotide have a significant effect on thymidine incorporation by HL-60 cells after 48 hours of exposure. The acridine conjugate, on the other hand, (5 uM) resulted in 94% inhibition of DNA synthesis. This observation indicates that this c-myc targeted compound is an effective antiproliferative agent. These results were confirmed by studying the effect of this compound on cell number. The c-myc targeted compound however, demonstrated a concentration dependent inhibition of cellular proliferation. This indicates that the effect of targeted acridine compound may be specific for c-myc expression.

Specific Aim 3: To characterize the ability of the neu, c-myc, and c-Ha-?ras targeted acridine-oligonucleotide conjugates to bind their target sequences in vivo and to correlate in vivo conjugate binding with the transcriptional activity of the target gene.

1. Delivery of triplex forming oligonucleotides to breast cancer cell nuclei by adenovirus-polylysine complexes (Gene Therapy 3:287-297, 1996).

Table 1 Oligonucleotide delivery to cancer cells: recovery of *ODN from nuclei

Cell line	*Species*	*Tissue of origin*	*AdpL–ODN pmol (μM)*	*Free ODN pmol (μM)*
SK-BR-3	Human	Breast Ca	8.0 (32.0)	0.23 (0.92)
SK-MEL-28	Human	Melanoma	17.7 (70.7)	0.22 (0.89)
G-401	Human	Wilm's tumor	8.8 (35.2)	0.15 (0.59)
HeLa	Human	Cervical Ca	12.3 (49.0)	4.6 (18.5)
NBT-II	Rat	Bladder Ca	4.4 (17.6)	0.34 (1.4)
SK-OV-3	Human	Ovarian Ca	5.0 (20.0)	Not done
HT-29	Human	Colon Ca	6.0 (24.1)	Not done
SK-OV-3	Human	Ovarian Ca	5.0 (20.0)	Not done
T-24	Human	Bladder Ca	12.5 (50.0)	Not done

Nine cancer cell lines were treated with internally labeled HN28ap in AdpL–ODN complexes. For comparison, internally labeled free ODN was added to five of these cell lines. The tumors of origin are listed. Scintillation counting on isolated nuclei was used to determine the amount of labeled ODN (*ODN) in the nuclei after 24 h. The 24-h intranuclear concentration of HN28ap was calculated based on an estimated nuclear volume of 500 fl/nucleus × 500 000 cells treated. High concentrations of ODN are recovered from the nuclei of all cell lines after AdpL–ODN treatment.

Although triplex forming oligonucleotides show great promise in their ability to specifically inhibit single gene expression, they must cross the cell membrane, escape the endosomal versicle, and

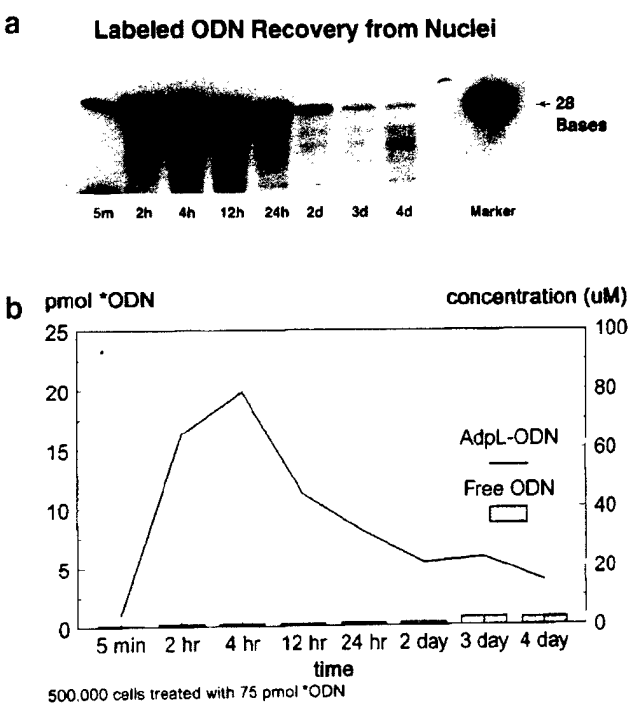

Figure 3 The rapid uptake and persistence of internally labeled HN28ap in SK-BR-3 cells after treatment with AdpL–ODN complexes is illustrated. 5×10^5 cells (at each time-point) were treated and nuclei were prepared and divided for autoradiography (a) or scintillation counting (b). ODN uptake in the nucleus begins rapidly and peaks at 4 h. The ODN persists mostly as intact HN28ap for at least 24 h, and is still readily detectable in the nucleus for 4 days. From the known specific activity of the labeled ODN, the amount of ODN (in pmol) in the nucleus was measured (treatment was with 75 pmol of ODN at each time-point). Intranuclear concentrations of the ODN were calculated from estimated nuclear volumes of 500 fl/nucleus × 500 000 cells treated. Free ODN treatments for each time-point were included for comparison.

Figure 10.

possibly traverse the nuclear membrane to arrive at their intracellular target molecules. In an attempt to improve the delivery of phosphodiester triplex forming ODNs to malignant cells, we have constructed adenovirus-polylysine (AdpL)-ODN complexes designed to take advantage of the receptor mediated endocytosis and endosomolysis of adenoviruses to transfer the ODNs to the cell nucleus. Treatment of several different types of tumor cells in culture by AdpL-ODN complex resulted in superior uptake and persistence of the ODNs compared to both free ODN and cationic lipid-ODN complexes **(Table 1)**. Nuclear uptake peaks at 4h and intact ODN persists in the nucleus with a half-life of 12 hours **(Figure 10)** . ODN concentrations of 20-70 uM are achieved at 24 hours in all monolayer cell lines evaluated to date. ODNs are detected in 50-100% of the total cell population by immunohistochemistry with apparent uptake into vesicles and nuclear localization. Luciferase expression of a codelivered reporter plasmid suggests that these ODNs are free in the nucleus. AdpL-ODN complexes will provide a valuable tool for delivering unmodified ODNs to the nucleus of malignant cells.

Specific Aim 4. To determine the sequence specificity of binding and transcriptional inhibition by the neu, c-mytc, and c-Ha-ras targeted acridine-oligonucleotide conjugates, utilizing vectors containing variant promoter target sequences.

1. DNA binding drugs abrogate triplex formation by the human Ki-ras promoter (Biochemistry 35:1106-1114, 1996). We have used DNASE I footprinting and gel shift assays to characterize the interaction of DNA binding drugs mithramycin, distamycin, and berenil with an intermolecular triplex formed by the human c-Ki-ras promoter. A purine-rich triplex-forming oligonucleotide (ODN) forms a stable intermolecular triple helix (triplex) with a homopurine (PR):homopyrimidine (PY) motif in the human c-Ki-ras promoter which contains a 22bp PR:PY region (-328 to -307). This triplex structure is comprised of 15 G.G:C triplets interspersed with 7 T.A:T triplets. Mithramycin binding sites in the human c-Ki-ras promoter encompass most of the triplex target site and three G-C-rich sequences downstream

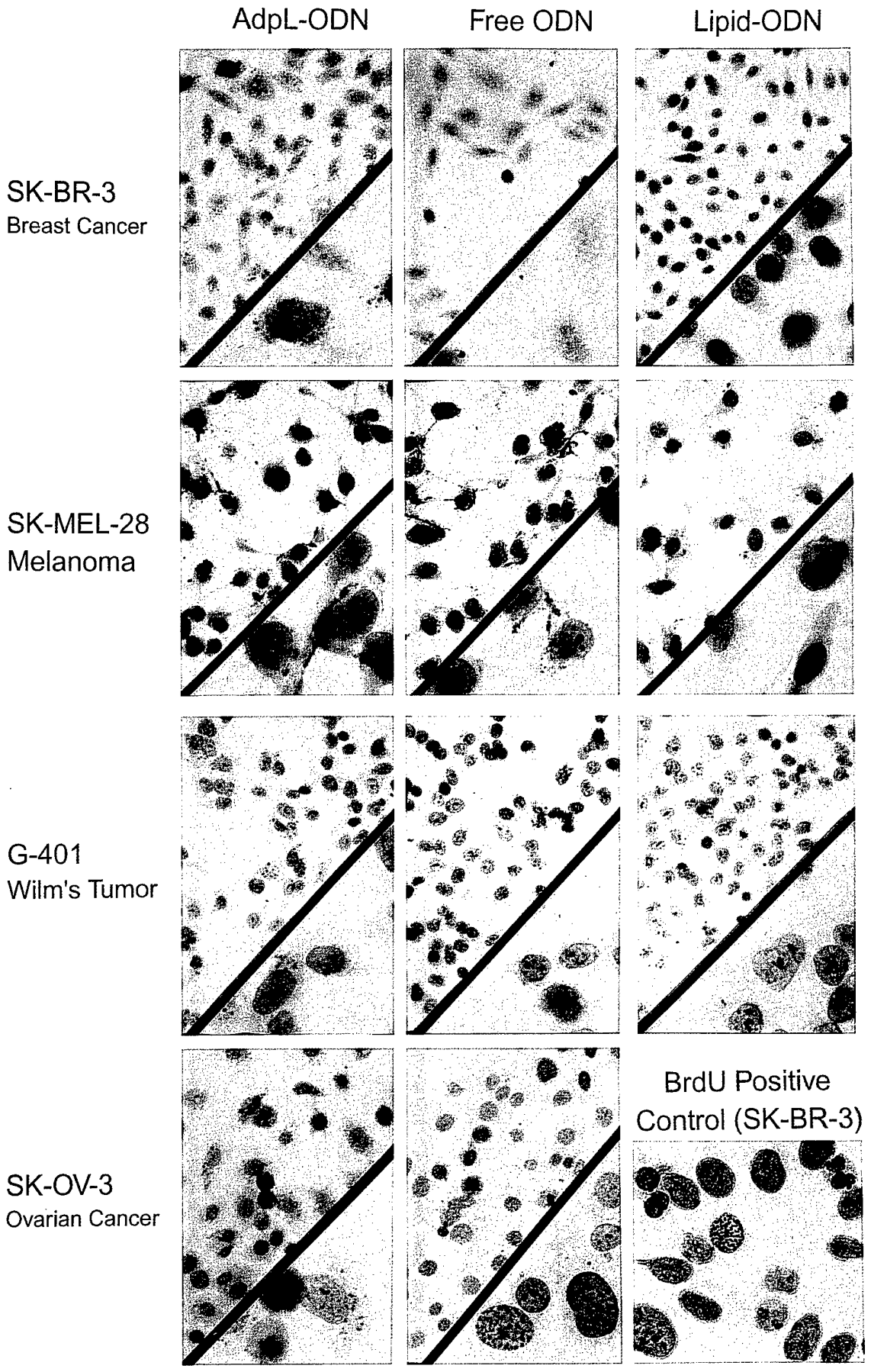
AdpL-ODN
Free ODN
Lipid-ODN
SK-BR-3
Breast Cancer
SK-MEL-28
Melanoma
G-401
Wilm's Tumor
SK-OV-3
Ovarian Cancer
BrdU Positive
Control (SK-BR-3)

Figure 11

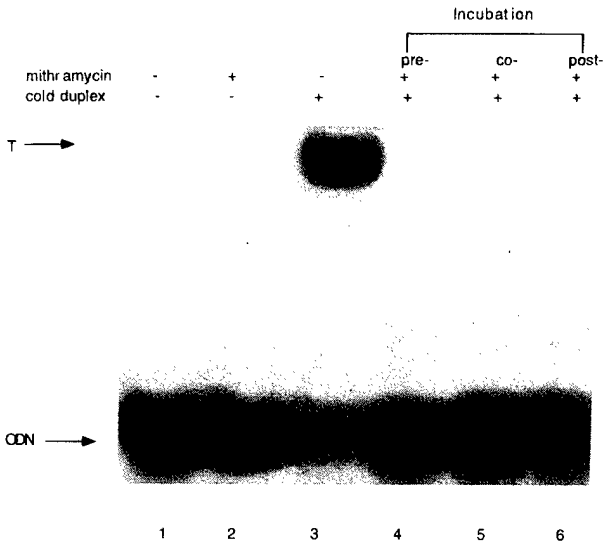

Gel mobility shift analysis showing the inhibition of triplex formation by mithramycin. Mithramycin (100 μM) was incubated with unlabeled synthetic target DNA (50 nM) prior to (pre-), during (co-) the addition of ^{32}P-labeled triplex ODN (100 nM), or after overnight triplex formation (post-). ODN = radio-labeled oligodeoxynucleotide; T = triplex DNA.

Figure 12.

of this triplex-forming region. Mithramycin binding within the c-Ki-ras promoter completely abrogates triplex formation **(Figure 12)**. Furthermore, the addition of mithramycin to pre-formed triplex by c-Ki-ras promoter displaces the major groove bound ODN. Five prominent distamycin binding sites are noted within the c-Ki-ras promoter including the triplex-forming site as well as A-T-rich regions upstream and downstream of the triplex site. Berenil does not bind within the triplex target sequence, and only one berenil binding sequence downstream of the triplex motif was present within the c-Ki-ras promoter fragment. Neither distamycin nor berenil prevents triplex formation, and, furthermore, the addition of either distamycin or berenil to the pre-formed triplex structure did not displace the major-groove-bound third strand. This study demonstrates that GC-specific and AT-specific minor groove ligands differentially affect the intermolecular pur.pur:pyr triplex. A possible biological significance of mithramycin interaction with intramolecular triplex is discussed.

2. Acridine conjugation increases intracellular and intravascular stability of triplex forming oligonucleotides in vitro and in vivo. (manuscript submitted). When MCF-7 breast carcinoma cells are treated with radiolabelled c-myc targeted oligonucleotide, 57-68% of intracellular oligonucleotide is found in the nuclei in cells treated with oligonucleotide for periods as short as five minutes, or as long as 48 hours. Importantly, there is very little degradation of the oligonucleotide over this period. Interestingly, much of the oligonucleotide which is taken up (75-85%) is retained by these cells after the cells are placed into fresh medium, which does not contain oligonucleotide. Acridine conjugation improves the ability of triplex forming oligonucleotides to enter the cell. When the NALM/6 preB cell line is incubated ^{32}P radiolabelled conjugate or oligonucleotide for 24 hours it is clear that the addition of an acridine conjugate significantly increases the ability of the oligonucleotide to enter the cell. In fact, the concentration of intracellular conjugate is almost double that of the oligonucleotide. Later time points (24 and 48 hours) demonstrated that both the oligonucleotide and conjugate reach equilibrium and are present at similar intracellular concentrations. We have also determined the effect of acridine conjugation on intracellular stability of the c-myc targeted oligonucleotide. When the conjugate and oligonucleotide are added to NALM/6 cells and the intracellular compound isolated at 24 and 48 hours, both are relatively intact. However, the relative retention of the acridine-conjugate is significantly higher than that of the unconjugated oligonucleotide.

We have also determined the stability of a triplex forming acridine-oligonucleotide conjugate in whole animals. When the conjugate is administered intravenously to mice it has a serum half-life of approximately ten minutes. However, we noted that radioactive conjugate was present in the animal at relatively high levels at 24 and 48 hours after administration, in contrast to radiolabelled oligonucleotide which is largely excreted in urine during the first hour after IV administration. Further investigation revealed that the "whole animal half-life' is between 24 and 36 hours in contrast to the serum half-life of 5 to 10 minutes. Both the intestine and liver demonstrate extremely high levels of conjugate uptake. In fact, 25% of the administered dose can be found in the intestine at 24 hours following administration, compared to none of the oligonucleotide. Likewise, 8% of the total administered dose is found in the liver of treated animals, with significant but lower levels found in the bone marrow and kidney. Gel electrophoretic analysis of the conjugate at 24 and 48 hours reveals that the majority of radiolabelled conjugate remains intact at these time points. These data suggest that the addition of acridine to the 5' and of the oligonucleotide results in substantial stabilization of this molecule and it is now feasible to begin to consider the administration of these agents in therapeutic settings.

3. Triplex DNA formation is dependent on divalent cation concentration.(Nucleic Acids Res., in press). In order to characterize intracellular conditions which may affect the therapeutic usefulness of triplex forming oligonucleotides, we have characterized the effects of monovalent metal cations on triplex formation by the DHFR promoter. Quantitative DNAse I protection analysis demonstrated that potassium has a potent, concentration dependent inhibitory effect on triplex formation by this sequence. However, potassium does not alter the rate of triplex disassociation. Sodium also has an inhibitory effect on triplex formation, but only at concentrations which are three times as high as those required for maximal inhibition by potassium. Since potassium represents the major intracellular cation, this inhibition of triplex formation by K^+ at concentrations well below the physiologic range, may represent an impediment to the utilization of triplex forming molecules for transcriptional inhibitors. Therefore, we have also characterized the relationship between divalent and monovalent cations on triplex formation. We have demonstrated a positive effect of Mn^{2+} or Co^{2+} in promoting triplex formation, event as the K+ concentration approaches physiologic levels. We have constructed a model to account for the effects of these monovalent and divalent cations on the reactivity of the components of triplex DNA formation.

4. Liposome delivery of triplex forming oligonucleotides enhances transcriptional inhibition of target genes. Liposomes represent an attractive way to increase the delivery of adequate concentrations of TFO to the nucleus to form triplex structures with a large proportion of target sequences and to inhibit expression of the target gene (95). We have established a collaboration with Applied Immune Sciences, Santa Clara, CA in order to develop a liposome delivery system for triplex based gene therapy for breast cancer (see letter of Collaboration). Our preliminary experiments have demonstrated that liposome delivery of neu targeted triplex forming oligonucleotide results in a dramatic increase in the ability of this oligonucleotide to inhibit expression of the gene and proliferation of MCF-7 cells. This suggests that liposome delivery may substantially increase the intranuclear concentration of TFO, perhaps allowing the complete inhibition of neu expression.

Specific Aim 5. To determine the effect of the neu, c-myc, and c-Ha-ras targeted conjugates on expression of the murine and human target genes in intact animals.

1. Expression of the beta-galactosidase gene under the control of the human c-myc promoter is inhibited by mithramycin (Oncogene 10:2323-2330, 1995).

In order to assess the functional contribution of the human c-myc promoter region in the expression of the c-myc gene, transgenic mouse lines containing a bacterial lac Z gene encoding beta-galactosidase under the control of the human c-myc protooncogene promoter were generated. Transgenic mouse embryos heterozygous for the human c-myc Z transgene demonstrate high amounts of beta-galactosidase activity as early as day 11 of embryogenesis by histochemical staining of whole embryos using 5-bromo-4-chloro-3-indolyl-beta-D- galactopyranoside (X-Gal) as substrate, localizing specifically to early spinal cord tissue. beta-galactosidase activity can be demonstrated by histochemical staining in brain tissue of day 14 embryos, localizing mainly to the prefrontal cortex region, while relative amounts of beta-galactosidase in spinal cord tissue are reduced. Determination of specific activity of beta-galactosidase using resorufin-beta-galactopyranoside as substrate in homogenates of whole embryos heterozygous for the human c-myc/lac Z transgene demonstrates significantly elevated beta-galactosidase activity over control embryos in day 11 and day 14 embryos **(Figure 13).**. Surprisingly, cell homogenates of brain tissue from adult G1 generation mice heterozygous for the human c-myc/lac Z transgene demonstrate greater than 10-fold higher specific activity of beta-galactosidase over normal control brain tissue. Specific inhibition of the c-myc/lac Z transgene was also demonstrated in developing embryos using mithramycin given at a dose of 150 micrograms kg-1 d-1 intraperitoneal to pregnant females on days 7-13 of gestation. Both histochemical staining of beta-galactosidase and specific activity assays of day 14 embryos demonstrated significantly lower levels of beta-galactosidase than untreated controls. These results are unique since we are able to detect expression of beta-galactosidase in developing embryonic central nervous system tissue along with adult brain tissue of animals carrying the human c-myc Z

β-galactosidase activity of day 11, day 14 and day 18 embryos of transgenic mice

Animal Number	*Day 11*	*DNA Blot*	*Specific activity*[a] *Day 14*	*DNA*[b] *Blot*	*Day 18*	*DNA Blot*
1	277	N.D.[c]	792	+	110	+
2	168	N.D.	636	+	72	+
3	165	N.D.	364	+	61	+
4	140	N.D.	104	+	59	+
5	92	N.D.	205	–	47	+
6	39	N.D.	149	–	39	–
7	29	N.D.	118	–	21	–
8	13	N.D.	86	–	21	–
9					20	–
10					17	–
	Control[d] 75.8 (0-336)		*Control* 22 (7-33)		*Control* 10.8 (2-21)	
			Average Positive 474.0		*Average Positive* 69.8	
			Average Negative 139.5		*Average Negative* 23.6	

[a]Specific activity of β-galactosidase measured as the change in OD_{572} over 2 h at 37°C using resorufin-β-galactosidase as substrate/protein concentration (g/ml by the micro-Biuret method). [b]The presence of the human c-*myc* /lacZ transgene was determined by DNA blot analysis in day 14 and day 18 embryos. + : presence of the transgene; – : absence of the transgene. [c]N.D. not determined. [d]Control denotes the average β-galactosidase specific activity of day 11, day 14 and day 18 embryos from the mating of normal, non-transgenic mice (ranges are given in parentheses)

Table 2

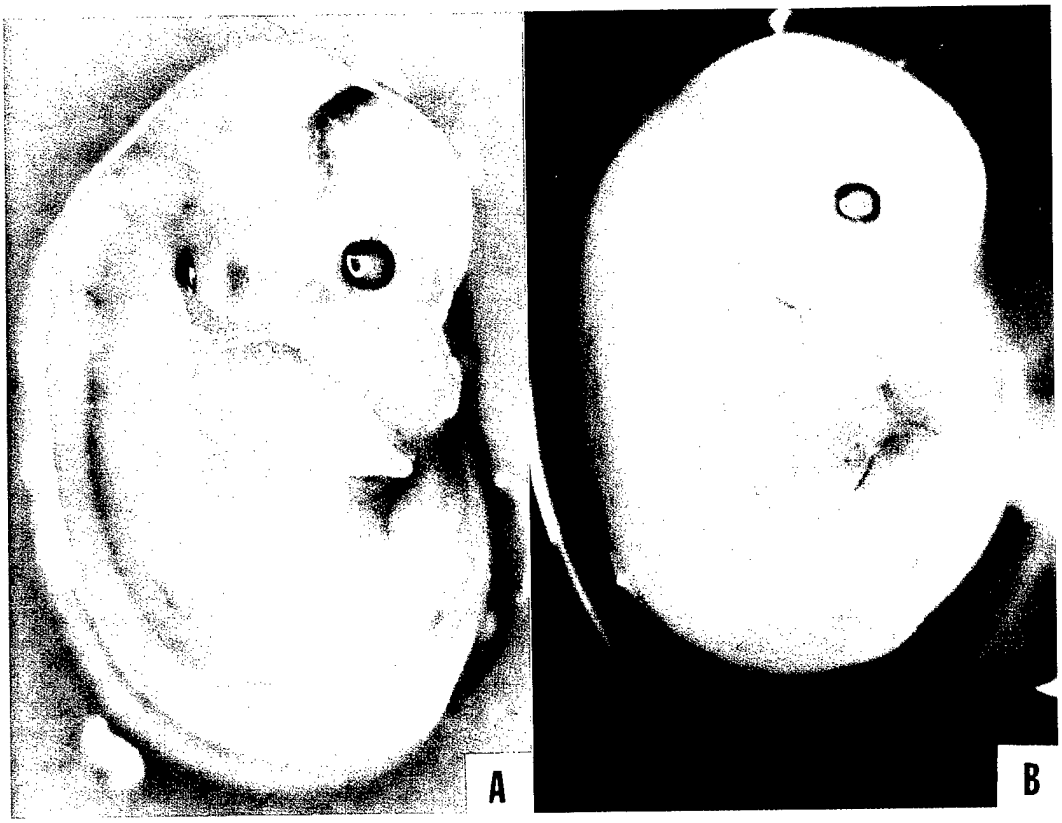

Figure 2 Day 11 embryo of a transgenic mouse line possessing 10–20 copies of the c-*myc*/lac Z transgene. Embryos were stained for β-galactosidase as described in the Materials and methods section. (**A**) day 11 embryo staining positive for β-galactosidase; (**B**) day 11 litter mate staining negative for β-galactosidase activity. Note β-galactosidase activity localizes to developing spinal cord tissue

Figure 3 Day 14 embryos of a transgenic mouse line possessing 10–20 copies of the c-*myc*/lac Z transgene. Embryos were stained for β-galactosidase as described in the Materials and methods section. (**A**) Day 14 embryo staining positive for β-galactosidase; (**B**) day 14 litter mate staining negative for β-galactosidase. Note that β-galactosidase activity now appears in the prefrontal cortex region and spinal cord stains less intense than day 11 embryos (**A**)

transgene and we are able to specifically inhibit expression of the transgene using mithramycin administered in utero.

12. Effective treatment of murine lymphoma. We have utilized the murine c-myc TFO to perform preliminary animal studies with murine tumors. Since the murine TFO inhibits murine c-myc expression, we studied the effect of pretreatment of the YC8 murine lymphoma cell line (112) prior to inoculation of mice with 5 X 10^6 cells. These cells were exposed to 10 and 100 uM concentrations of acridine-oligonucleotide conjugate or 3'-amine blocked oligonucleotides. Following a two hour exposure to TFO, the cells were inoculated into the flank of BalbC mice. The mice were observed for tumor growth. After 10 days the mice were sacrificed and tumor size and weight determined. The tumors treated with 10 uM acridine conjugate demonstrated 35% inhibition of growth, while those treated with 100 uM acridine conjugate were inhibited by 63%. The amine-blocked oligonucleotide demonstrated an even greater inhibition of cell growth. These experiments are currently being repeated, but strongly suggest that these oligonucleotides will be capable of inhibiting cell growth.

CONCLUSIONS

During the three year period funding of this grant we have shown that triplex formation represents a viable means of transcriptional inhibition, although there are several problems which remain before this approach can be used in clinical trials. Triplex DNA provides a sequence specific mechanism which may allow the targeting of DNA binding compounds to specific sequences. It has been well documented that triplex forming oligonucleotides can bind specifically to their target sequences, prevent regulatory protein binding, and inhibit transcriptional activity. We have developed a set of "gene specific" triplex forming molecules which prevent regulatory protein binding and inhibit expression of the Ki-ras, c-myc, and neu genes in vitro. We hypothesize that the inhibition of expression of these genes, which play important roles in the malignant transformation of breast cancer cells, will reverse the malignant phenotype. Triplex formation results in very effective and very specific inhibition of in vitro transcription. However, there are several problems with this approach in in vivo settings. These include to ability to deliver adequate concentrations of triplex forming molecules to the nucleus to drive triplex formation; the ability to design stable molecules which are readily taken up by tumor cells; and the ability to identify additional target sequences in the promoters of these genes. The published work resulting from this grant has addressed each of these problems. We have made substantial progress towards the design and execution of successful clinical trials. With the rapid development of gene therapy technology, we have begun to develop vectors which express "triplex forming transcripts" which have considerable promise as therapeutic agents.

Individuals Paid From Army Grant

Full-time

Cheryl Carden	1993-94
Sara Barker	1993-95
Vincenzo Guarcello	1993-95
Kedar Shrestha	1993-95
Charles Mayfield	1993-95
Donald Miller	1993-95
Brad Rodu	1993-95
Aruna Subramanian	1993-95

Part-time

Sara Naren	1995 (2 months)
Sandy Subramanian	1995 (3 months)
Arcola Williams	1995 (2 months)

Gene Therapy (1996) 3, 287–297

Efficient delivery of triplex forming oligonucleotides to tumor cells by adenovirus-polylysine complexes

SW Ebbinghaus[1], N Vigneswaran[1], CR Miller[1], RA Chee-Awai[1], CA Mayfield[1], DT Curiel[1] and DM Miller[1,2]

[1]*The University of Alabama at Birmingham, and* [2]*Birmingham Veterans Affairs Medical Center, AL, USA*

Oligonucleotides (ODNs) show great promise in their ability to specifically inhibit single gene expression but must cross the cell membrane, escape the endosomal vesicle, and possibly traverse the nuclear membrane to arrive at their intracellular target molecules. In an attempt to improve the delivery of phosphodiester triplex forming ODNs to malignant cells, we have constructed adenovirus-polylysine (AdpL)-ODN complexes designed to take advantage of the receptor mediated endocytosis and endosomolysis of adenoviruses to transfer the ODNs to the cell nucleus. Treatment of several different types of tumor cells in culture by AdpL–ODN complex resulted in superior uptake and persistence of the ODNs compared to both free ODN and cationic lipid-ODN complexes. Nuclear uptake peaks at 4 h and intact ODN persists in the nucleus with a half-life of 12 h. ODN concentrations of 20–70 μM are achieved at 24 h in all monolayer cell lines evaluated to date. ODNs are detected in 50–100% of the total cell population by immunohistochemistry with apparent uptake into vesicles and nuclear localization. Luciferase expression of a co-delivered reporter plasmid suggests that these ODNs are free in the nucleus. AdpL–ODN complexes will provide a valuable tool for delivering unmodified ODNs to the nucleus of malignant cells.

Keywords: *gene therapy; HER-2/neu oncogene; k-ras oncogene; receptor mediated endocytosis; liposomes*

Introduction

Oligonucleotides (ODNs) have great potential as therapeutic agents and biological probes because of their ability to bind to intracellular nucleic acid targets in a site-specific manner. By binding to the DNA (through triple helix formation) or RNA (through antisense or ribozyme activity) of a particular target gene, ODNs can specifically inhibit gene expression. Because of their ability to inhibit the expression of critical oncogenes or viral genes, ODNs may represent the next generation of rationally designed antineoplastic and antiviral drugs. These agents will also be useful to biologists in determining the function of an individual gene and its interaction with other genes in basic cellular functions as well as malignant transformation. However, ODNs designed for antisense, ribozyme, or triplex applications must traverse significant cellular barriers to arrive at their molecular targets. They must cross the cell membrane and escape the endosome; in addition, ODNs designed for triplex formation must travel to the nucleus to arrive at their sites of action in the genomic DNA. The mechanism(s) by which ODNs enter the cell are not fully understood. ODNs are thought to enter the cell by adsorptive endocytosis or fluid phase pinocytosis; however, investigators have also demonstrated cell surface proteins that bind ODNs in a receptor-like manner.[1–5] In either case, data presented here and by others[6] have shown that ODN uptake varies widely by cell type and may not be sufficient for the desired biological effects of the ODN. The intranuclear concentration of ODN required for intermolecular triplex formation in human chromatin is unknown; however, triplex mediated repression of *in vitro* transcription has generally been described at ODN concentrations of 10–20 μM (although these concentration requirements also depend on the template concentration).[7–10] Several reports of cell culture treatments with up to 5 μM of triplex forming phosphodiester ODNs in the media have resulted in intracellular ODN concentrations no greater than 7 μM ODN.[10–12] An additional problem with the cellular bioavailability of therapeutic ODNs is the sensitivity of unmodified oligonucleotides to intracellular and serum nucleases. In fact, the half-life of phosphodiester ODNs microinjected into the cytoplasm of several eukaryotic cell lines can be measured in minutes.[13] Phosphorothioate backbone modifications have in part circumvented this nuclease sensitivity,[13–18] but at the expense of a decrease in affinity for the target nucleic acid species,[14,16,19–21] an increase in both specific[20] and non-specific protein binding,[16,22] an increase in non-sequence specific cellular effects,[23,24] and an alteration in catalytic ribozyme activity.[25] For these reasons, it is desirable to find methods of achieving high concentrations of unmodified ODNs in the cell. In particular for ODNs designed to form intermolecular triplex DNA with human promoter sequences, high concentrations of preferably phosphodiester ODN in the nucleus are required. Several investigators have described the delivery of ODNs into various cell lines with liposomes, generally enhancing the stability and uptake of these ODNs several-fold.[25–27] To date, these liposomal delivery systems

Correspondence: DM Miller, 1824 6th Avenue South, Birmingham, AL 35294, USA
Received 27 June 1995; accepted 6 September 1995

probably represent the most effective means of ODN transfer into cells.[6]

Adenovirus–polylysine(AdpL)–DNA complexes have been well described as highly effective vectors for the delivery of plasmid DNA to a wide variety of cells and tissues.[28–31] These vectors consist of defective adenovirus particles that can deliver nucleic acids carried on their capsid exterior through a polylysine bridge. Gene delivery is enhanced in a wide variety of cell types by receptor-mediated endocytosis of the adenovirus. After uptake, endosomal acidification induces a conformational change in the viral particle, leading to exposure of hydrophobic amino acids which disrupt the endosomal vesicle. Adenovirus particles are highly efficient at both endocytosis and endosomolysis.[32–34] By unknown mechanisms, the adenoviruses naturally translocate their genetic material to the cell nucleus. Thus, AdpL–DNA complexes exploit the adenovirus' cellular entry mechanisms to deliver nucleic acids non-covalently linked to the viral capsid. AdpL–DNA delivery offers the additional advantage of utilizing replication-defective adenovirus particles which do not express recombinant genes or integrate into the genome; they act only as carriers for the DNA of interest. This DNA can be produced by conventional methods at high efficiency and to the desired level of purity. Surprisingly, the use of these vectors for ODN delivery has not been described.

In this report, we offer the first description of AdpL–ODN delivery of potentially therapeutic ODNs to malignant cells in culture. We have used three complementary methods to demonstrate the highly efficient delivery of two previously described triplex forming ODNs directed against the HER-2/neu and k-ras promoters.[8,35] We have used traditional cell fractionation techniques which, despite their known limitations[13] are the only means of approximating the concentration of ODNs in the cell and in the nucleus. This information is of critical importance for evaluating the cellular pharmacodynamics of therapeutic ODNs. For confirmatory data, we have employed immunohistochemistry using an antibody to a bromodeoxyuridine (BrdU) containing ODN. This technique, of directly visualizing ODNs in cells and tissues, was developed in our laboratory and offers several potential advantages over traditional fluorescence labeling of ODNs: it is easy and convenient, modifies the ODN with a nucleoside analog rather than a large planar fluorophor, yields data on the uptake of ODN by individual cells, and is applicable to tumor and tissue specimens. Finally, we have co-transduced the ODN with a luciferase expressing plasmid to demonstrate that the DNA transferred from the AdpL–DNA complexes is functional. Taken together, these data show the highly efficient nature of ODN delivery using the AdpL delivery system.

Results

We wished to measure the uptake or delivery of ODNs into malignant cells by three complementary techniques. First, cell fractionation provides a way to estimate the concentration of ODN in the cell or nucleus. The immunohistochemical technique reported here provides data on the percentage of the cell population that contains ODN. Finally, the luciferase activity of a co-delivered plasmid indirectly measures the bioavailability of the ODN in the cell. For these studies, we measured the uptake of two ODNs shown to bind specifically to target gene promoters through DNA triplex formation.[8,35] The ODN HN28ap binds to the promoter of the HER-2/neu oncogene and inhibits nuclear protein binding and *in vitro* transcription. The ODN KR32TBU is a modification of the ODN KR22Tap that binds to the k-ras promoter and inhibits nuclear protein binding. We have found that the BrdU modified ODN KR32TBU retains the ability to form triplex DNA while rendering the ODN immunoreactive to anti-BrdU antibodies (Vigneswaran N *et al*, unpublished). The ODN sequences used in these studies are illustrated in Figure 1. The position of the internal ^{32}P label in HN28ap and of the BrdU modifications in KR32TBU are also shown.

Figure 2 illustrates the highly efficient uptake of unlabeled HN28ap in AdpL–ODN complexes by SK-BR-3 breast cancer cells. Subconfluent cultures of 10^6 cells were treated with 360 pmol of unlabeled HN28ap as free ODN or in AdpL–ODN complexes. The cells were harvested after 24 h and the nuclei, crude cell lysate, and media were purified and end-labeled. The extracts were then separated on a 16% denaturing polyacrylamide gel to determine the uptake and localization of the ODN. An untreated control cell population was used to determine the background labeling. The HN28ap ODN is readily visualized as a specific 28-base band not present in the untreated control cells (arrowheads). In the cells treated with free ODN, the ODN is visualized only in the media. In the AdpL–ODN treated cells, the ODN is taken into the cells and into the nucleus. (The ODN is not visualized in the media in the AdpL–ODN treated cells because intact AdpL–ODN complexes in the media were not disrupted before purification in Sep-Pak columns; polylysine bound ODN is not isolated by this technique.) These results indicate that SK-BR-3 cells do not readily take up detectable (by this method) quantities of free ODN from the media, while AdpL complexes deliver the ODN to the cell and nucleus very efficiently.

The time-course and persistence of HN28ap delivered by AdpL–ODN complex was determined by treating SK-BR-3 breast cancer cells with internally labeled ODN

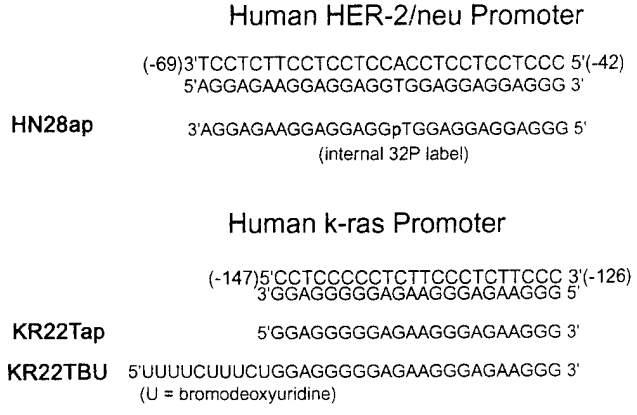

Figure 1 Two triplex forming ODNs were used to evaluate ODN uptake and delivery. The ODNs are designed to form antiparallel urine triple helices with their respective target sequences in the HER-2/neu and k-ras promoters. The ODN designated as HN28ap was labeled internally at the 13th internucleotide phosphate in some experiments. The ODN designated as KR32TBU was modified with eight BrdU nucleotides (designated as U) from the original triplex forming KR22Tap sequence to render it immunoreactive with anti-BrdU antibodies.

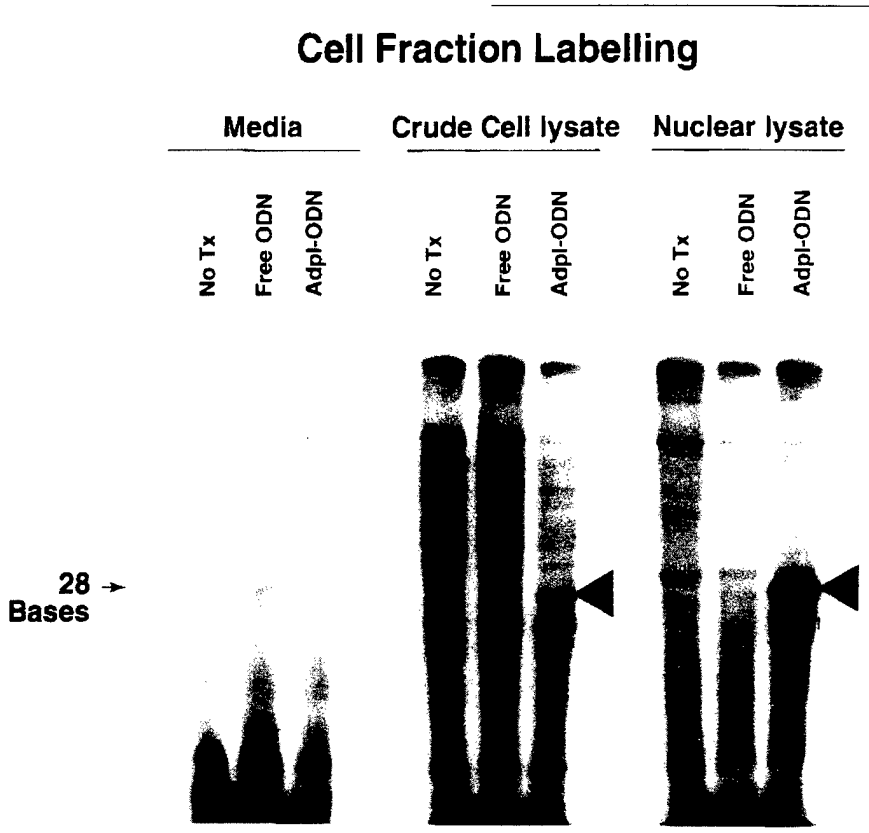

Figure 2 *The uptake of free or AdpL complexed ODN by SK-BR-3 cells is shown. The cells were treated with unlabeled HN28ap for 24 h, and the media, crude cell lysate, and nuclear lysate were purified and end-labeled. The no-treatment (No Tx) cells serve as a control for background labelling. In the AdpL–ODN treated cells, a strong 28-base band in the crude cell lysate and nuclear lysate is apparent (arrowheads) representing intact HN28ap. In the free ODN treated cells, this band is apparent only in the media. This figure clearly demonstrates the uptake and nuclear localization of the ODN after delivery by AdpL complex. Intact ODN from Free ODN treated cells is not detectable at 24 h in the cells or nucleus.*

(Figure 3). We used internally labeled ODN to avoid possible exchange or cleavage of the terminal 5′ phosphate moiety of end-labeled ODN. 5×10^5 Cells were treated with a mixture of internally ^{32}P labeled HN28ap and unlabeled HN28ap in AdpL–ODN complexes for a total of 75 pmol of ODN (representing an ODN concentration of 0.0375 μM in the media) at each time point. A 24-h free ODN treatment was also performed for comparison. Nuclei were prepared as described and divided for scintillation counting of total nuclear radioactivity and for lysis, extraction, and gel electrophoresis of the labeled material. The autoradiograph in Figure 3a shows the rapid uptake of AdpL–ODN peaking at 4 h. The ODN remains largely undegraded for at least 24 h, and detectable quantities of intact ODN are present in the nucleus of the cell for 4 days. The total nucleus-associated radioactivity was measured by liquid scintillation counting and the intranuclear ODN concentration was estimated from the determined total ODN and the estimated nuclear volume of 500 fl/nucleus. The concentrations achieved in the nucleus represent a marked 1000-fold increase over the starting concentration of the ODN in the media (0.0375 μM) consistent with an active uptake mechanism for the AdpL–ODN complex. The approximate intranuclear half-life of ODN is 12 h. Uptake of the free ODN is also suggested by the presence of low concentrations of the nucleus-associated ^{32}P label at the various time-points; however, detectable intact ODN was not present on autoradiography of the purified nucleic acids at the 24 h time-point (not shown). These data suggest that the free ODN is degraded either in the medium or after uptake into the SK-BR-3 cells with subsequent uptake of free radiolabel (either as free ^{32}P-phosphate or mononucleotide) into the nucleus at 24 h. The AdpL complex appears to provide protection against degradation of the ODN as well as enhance its delivery to the nucleus.

Similar experiments were performed in a wide variety of monolayer cancer cell lines from several different tumor types. The cell treatments and data collection were identical to the conditions used for the SK-BR-3 cells as described above except that only a 24-h time-point was obtained. Table 1 lists the cell lines examined and the 24-h intranuclear concentration determined as described. The AdpL–ODN treatments consistently achieved a 20–70 μM concentration of ODN in the nucleus at 24 h in all cell lines tested. Free ODN uptake was also evaluated in several of the cell lines. The data demonstrate modest free ODN uptake into the nucleus of HeLa cells, with a 24-h intranuclear concentration of 18.5 μM. In all other cell lines tested, free ODN uptake into the nucleus at 24 h was very low (concentrations of approximately 1 μM). As discussed below, we found the uptake of free ODN measured by immunohistochemistry to be highly variable between different cell lines. The uptake of internally labeled ODN shows generally good concordance with the light microscopic analysis of BrdU-ODN uptake, except that HeLa cells appear to demonstrate some degree of nuclear localization of the internally labeled ODN that

Table 1 Oligonucleotide delivery to cancer cells: recovery of *ODN from nuclei

Cell line	*Species*	*Tissue of origin*	*AdpL–ODN pmol (μM)*	*Free ODN pmol (μM)*
SK-BR-3	Human	Breast Ca	8.0 (32.0)	0.23 (0.92)
SK-MEL-28	Human	Melanoma	17.7 (70.7)	0.22 (0.89)
G-401	Human	Wilm's tumor	8.8 (35.2)	0.15 (0.59)
HeLa	Human	Cervical Ca	12.3 (49.0)	4.6 (18.5)
NBT-II	Rat	Bladder Ca	4.4 (17.6)	0.34 (1.4)
SK-OV-3	Human	Ovarian Ca	5.0 (20.0)	Not done
HT-29	Human	Colon Ca	6.0 (24.1)	Not done
SK-OV-3	Human	Ovarian Ca	5.0 (20.0)	Not done
T-24	Human	Bladder Ca	12.5 (50.0)	Not done

Nine cancer cell lines were treated with internally labeled HN28ap in AdpL–ODN complexes. For comparison, internally labeled free ODN was added to five of these cell lines. The tumors of origin are listed. Scintillation counting on isolated nuclei was used to determine the amount of labeled ODN (*ODN) in the nuclei after 24 h. The 24-h intranuclear concentration of HN28ap was calculated based on an estimated nuclear volume of 500 fl/nucleus × 500 000 cells treated. High concentrations of ODN are recovered from the nuclei of all cell lines after AdpL–ODN treatment.

would not be predicted by the amount of intracellular BrdU-ODN visualized in this cell line.

In order to confirm the cell fractionation data and to provide an estimate of the percentage of cells that take up ODN, we performed immunohistochemistry on cells after treatment with KR32TBU. This technique has the advantage of being both rapid and convenient. In addition, modification of the ODN with BrdU, a nucleoside analog, should alter the uptake and stability of the ODN to a minimal extent. In order to facilitate comparison of free ODN uptake and liposome enhanced transfection, free ODN and liposome-mediated ODN delivery were assayed simultaneously. In these experiments, 10^4 cells were seeded on to a four-chamber slide 1 day before treatment with the ODN. The cells were then treated with 10 pmol of KR32TBU in an AdpL–ODN complex, as free ODN, or in a liposome–ODN complex with DOTAP/DOPE. After an overnight incubation, the cells were fixed to the slide and immunostained for the presence of ODN with an anti-BrdU antibody. The cells were examined by light microscopy and representative photomicrographs from four of the six cell lines are shown in Figure 4. We have summarized the results in Table 2 by scoring the percentage of cells reacting positively and the intensity of the reactivity on a three-point scale of low (+) to high (+++).

The data demonstrate several interesting features. First, the AdpL–ODN-treated cells consistently demonstrate a

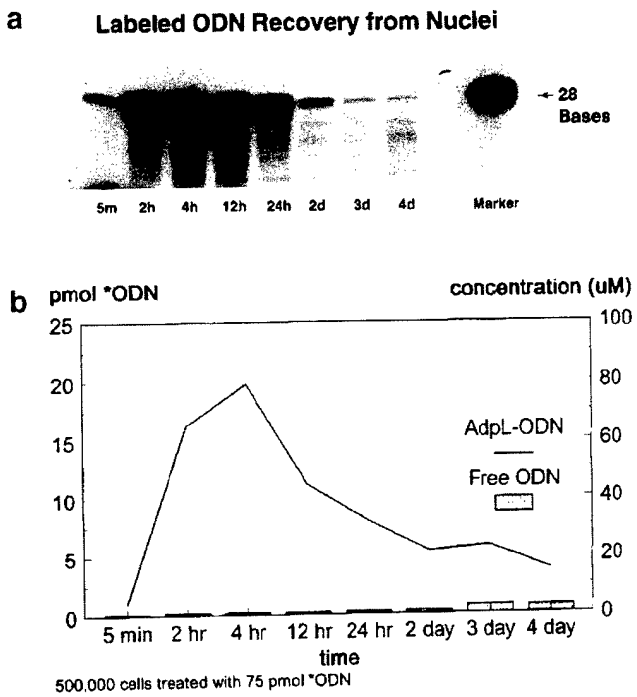

Figure 3 *The rapid uptake and persistence of internally labeled HN28ap in SK-BR-3 cells after treatment with AdpL–ODN complexes is illustrated. 5 × 10^5 cells (at each time-point) were treated and nuclei were prepared and divided for autoradiography (a) or scintillation counting (b). ODN uptake in the nucleus begins rapidly and peaks at 4 h. The ODN persists mostly as intact HN28ap for at least 24 h, and is still readily detectable in the nucleus for 4 days. From the known specific activity of the labeled ODN, the amount of ODN (in pmol) in the nucleus was measured (treatment was with 75 pmol of ODN at each time-point). Intranuclear concentrations of the ODN were calculated from estimated nuclear volumes of 500 fl/nucleus × 500 000 cells treated. Free ODN treatments for each time-point were included for comparison.*

Figure 4 *Representative photomicrographs from four of the cancer cell lines treated with the BrdU modified ODN (KR32TBU) as AdpL–ODN, free ODN, or liposome–ODN. The ODN is detected as brown against a faint hematoxylin (blue) counterstain after immunohistochemistry for BrdU is performed. High power 400 × and 1000 × (bottom right corner inset) magnifications are shown for each cell line. Cell lines are included showing high (SK-BR-3, SK-MEL-28, and SK-OV-3) and intermediate (G-401) immunoreactivity after AdpL–ODN complex treatment. These cells are designated +++ and ++ respectively in Table 2. Examples of high (SK-MEL-28) and low (SK-BR-3, G-401, SK-0V-3) immunoreactivity are shown for the free ODN treated cells, designated as +++ and + respectively. Intermediate (SK-BR-3) and low (SK-MEL-28 and G-401) intensity reactivity are seen in the liposome–ODN treated cells (++ and + respectively). The liposome–ODN treatment is not shown for the SK-OV-3 cell line. Instead, a BrdU positive control (in which free BrdU monomers at 5 μM were added to the medium of SK-BR-3 cells) is shown which illustrates the typical pattern of BrdU incorporation into the chromatin. The pattern of nuclear reactivity of the free ODN treated SK-OV-3 cells is identical to this free BrdU pattern which implies degradation of the ODN and incorporation of the nucleotides into the chromatin. In contrast, the nuclear reactivity of the AdpL–ODN treated cells is distinct, with small granules that are not present in the mitoses when the nuclear membrane is not present (illustrated in the SK-OV-3 cells). The results of immunohistochemical reactivity for all six cell lines are summarized in Table 2.*

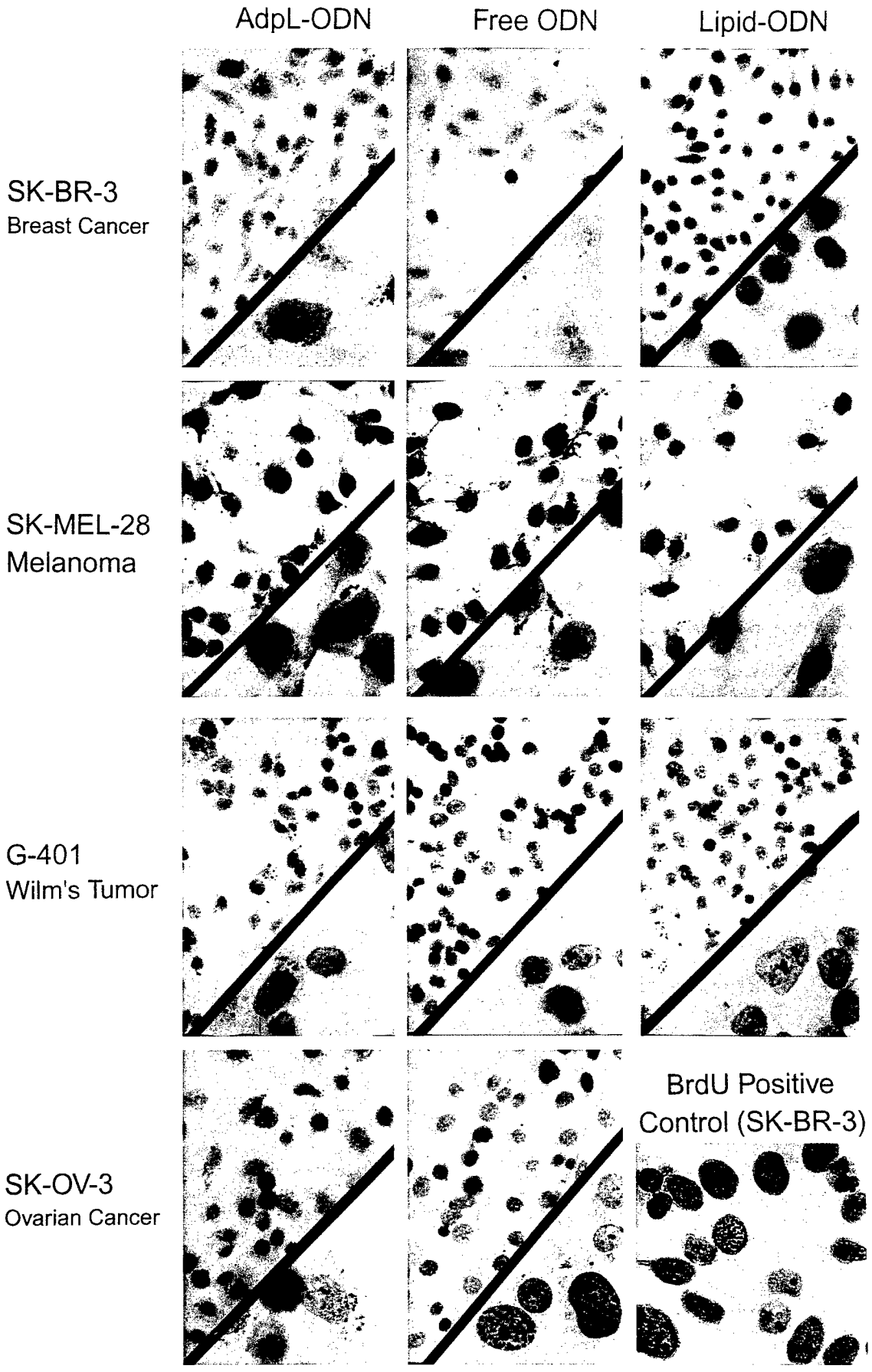
AdpL-ODN
Free ODN
Lipid-ODN
SK-BR-3
Breast Cancer
SK-MEL-28
Melanoma
G-401
Wilm's Tumor
SK-OV-3
Ovarian Cancer
BrdU Positive
Control (SK-BR-3)

Table 2 Oligonucleotide delivery to cancer cells: immunohistochemistry

Delivery mode	*SKBR3*		*SKOV3*		*HeLa*		*Mel-28*		*G-401*		*NBT-II*	
	%	*Int*	*%*	*Int*	*%*	*Int*	*%*	*Int*	*%*	*Int*	*%*	*Int*
Adpl-TFO	75	+++	90	+++	50	++	100	+++	50	++	80	+++
Liposome-TFO	40	++	90	++	40	+	40	+	30	+	80	+
Free-TFO	10	+	40	+	30	+	90	+++	5	+	30	+

%, % of reactive cells; Int, intensity of reactivity: + (low); ++ (intermediate); +++ (high).
Immunohistochemistry was performed on six cell lines after treatment with the BrdU modified ODN. Representative photomicrographs are shown in Figure 4. The results are summarized here as the percentage (%) of reactive cells after examining 10 high-power fields and the intensity (Int) of immunoreactivity on a three-point scale (+++ = high; ++ = intermediate; + = low).

higher percentage and intensity of immunoreactivity than free ODN or liposome–ODN treated cells. Morphologically in the AdpL–ODN treated cells, the majority of the ODN appears to be in large, densely stained cytoplasmic granules in a perinuclear location, consistent with uptake through the endocytic pathway. In most cells, the nucleus is reactive; however, in several mitotic cells with absent nuclear membranes, the chromosomes were not reactive (see SK-OV-3 cells treated with AdpL–ODN in Figure 4). These results are consistent with intact ODN present in the nucleus, since free BrdU is efficiently incorporated into the chromosomes during DNA synthesis and yields a distinctive chromatin and chromosomal reactivity pattern (see BrdU Positive Control in Figure 4). The pattern observed in the AdpL–ODN treated cells is clearly different than free BrdU monomer incorporation. In this regard, we have recovered intact 32-mer from the nuclear lysates of these cells on gel electrophoresis (not shown).

To prove that the nuclei were immunoreactive, a separate culture flask of SK-BR-3 cells was treated with the AdpL–ODN complex, and the nuclei were isolated and fixed to a glass slide. Figure 5 shows the resulting photomicrographs from nuclear preparations stained with hematoxylin and eosin (H&E) and immunoreacted for BrdU (BrdU Stain). These photomicrographs clearly demonstrate the nuclear localization of the KR32TBU and provide a reasonable check on the quality of the nuclear preparations.

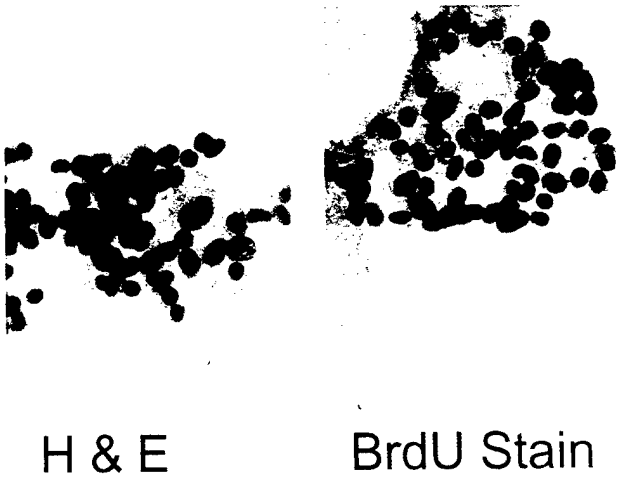

Figure 5 Isolated SK-BR-3 nuclei were stained with hematoxylin and eosin (H&E) or immunoreacted for BrdU (BrdU Stain) after treatment of intact SK-BR-3 cells with AdpL–ODN for 24 h. The figure serves to verify the uptake of the ODN into the nucleus of these cells as detected by the intense reactivity of the nuclei. The H&E stain demonstrates that the nuclear preparations were of good quality with very little detectable cytoplasm and no intact cells.

A second interesting feature of this data is the highly variable nature of free ODN uptake by various cell lines. The uptake ranged from 5% in the G-401 cell line to 90% in the SK-MEL-28 cell line (Figure 4 and Table 2). These results provide a graphic illustration of cell line to cell line variability of ODN uptake. In addition, the pattern of immunoreactivity of the free ODN treated cells differs from the AdpL–ODN pattern: in these cells, a diffuse cytoplasmic reactivity is seen with little or no nuclear positivity. This pattern is consistent with the uptake of smaller amounts of ODN with degradation in the endosome or cytoplasm. In some cell lines, nuclear positivity is noted after free ODN treatment (see SK-OV-3 cells treated with free ODN in Figure 4); however, the pattern in these cells is nearly identical to the reactivity pattern of free BrdU monomers after uptake into chromatin (see BrdU Positive Control in Figure 4). This pattern strongly suggests degradation of the ODN and incorporation of the BrdU monomers into the chromatin. These data are consistent with the data observed in the labeled ODN experiments and serve to confirm our hypothesis that the uptake of radiolabel into the nucleus of free ODN treated cells represents degradation of the ODN and uptake of the free label.

Finally, the results of liposome-mediated ODN delivery to these cell lines with DOTAP/DOPE was markedly inferior to the results obtained with the AdpL–ODN complexes. The amount of uptake was lower, and the pattern of reactivity was distinct from the free ODN and the AdpL–ODN patterns. The ODN was detected in a single or few large, globular cytoplasmic vesicles, in contrast to the usually small multiple vesicles of the AdpL–ODN treated cells. There was neither the diffuse cytoplasmic staining pattern observed from the free ODN treatments nor the nuclear localization seen in the AdpL–ODN treatments. This pattern is consistent with endocytic uptake and trapping of the liposome–ODN complex.

The intracellular bioavailability of the HN28ap delivered by AdpL–ODN was indirectly measured by the luciferase activity of a co-delivered luciferase reporter plasmid. We assume that for the plasmid to express the reporter gene it must be intact and free in the nucleus. We further assume that dissociation of the plasmid from the AdpL–DNA complex into the nucleus will be

accompanied by dissociation of the ODN from the AdpL–DNA complex. Therefore we measured the luciferase activity of the pGL control plasmid as an indicator of the intracellular bioavailability of the ODN. For these studies, a 1:1 (w/w) ratio of pGL control plasmid and ODN (HN28ap or HN20tata) was used for the assembly of the AdpL–DNA complexes. Two breast cancer cell lines (SK-BR-3 and MCF-7) were treated with 2 μg of total DNA in this AdpL–DNA complex, and the light production of cell extracts from 10^6 cells at 48 h was measured. Figure 6 illustrates the luciferase activity of cells treated with no plasmid (background), pGL control plasmid (pGL), or pGL–ODN containing complexes (HN28ap/pGL or HN20tata/pGL). Significantly higher total luciferase activity was observed in the SK-BR-3 cells, but both cell lines demonstrate high levels of luciferase activity, consistent with the transduction/expression levels in previous reports of AdpL–DNA complexes.[31] These data provide additional evidence for the delivery and release of the ODN in the nucleus of cultured cells by AdpL–DNA complex.

Discussion

In this report, we have demonstrated the uptake of two triplex forming ODNs into diverse malignant tissue cultures. By using three complementary techniques of detection, we have been able to estimate the efficiency of ODN uptake, the intranuclear concentrations of ODN, and the intracellular bioavailability of the ODN after delivery to several different cell lines by AdpL–ODN complex. The AdpL delivery system was compared to the uptake of free ODN and the liposome DOTAP/DOPE. One of the most important observations of this study is the variable nature of free ODN uptake by different cell lines. This variability must be taken into account when comparing the biological effects of antisense, triplex, or ribozyme ODNs from different reports. The cell lines used in this study, for example, may show markedly different effects by the same ODN ranging from the SK-MEL-28 line

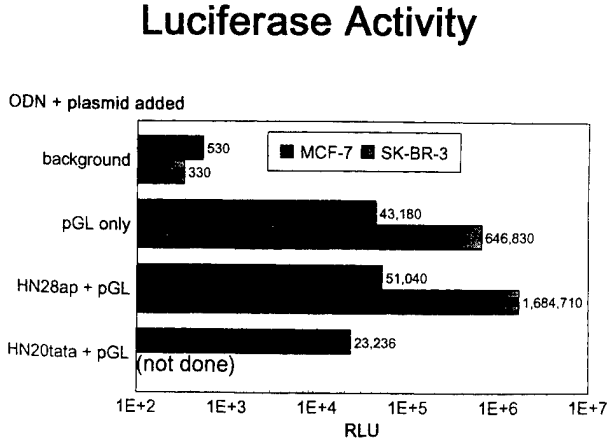

Figure 6 SK-BR-3 and MCF-7 breast cancer cells were treated with AdpL complexes containing the pGL control luciferase reporter plasmid alone or in combination with the ODNs HN28ap or HN20tata. The luciferase activity of the reporter plasmid suggests that both the reporter plasmid and the ODN are released from the complex and free in the nucleus. RLU = relative light units measured in 30 s from 1% of the extract from 10^6 cells (approximately 10 μg total protein).

which efficiently takes up free ODN in over 90% of the cells to the G-401 cells which take up negligible amounts of free ODN. Data on the cellular uptake and stability of ODN is an important component of any report of the biological activity of ODNs.

Although the cellular uptake of free ODN is quite variable, marked improvement in ODN uptake and stability was observed in all cell lines by adenovirus enhanced ODN delivery. Although numerous studies have demonstrated the uptake of ODNs in cell culture,[1–6,10–13,15,16,22–24,26,27] few studies have evaluated the intranuclear uptake of ODNs by different cell lines and delivery systems. AdpL–ODN complexes are capable of delivering high concentrations of intranuclear ODN to a diverse array of malignant cells from many different tissues of origin. Our results with AdpL–ODN delivery compared favorably to the ODN uptake observed from liposome–ODN complexes. The AdpL–ODN complexes take advantage of the endosomolytic and nuclear localization properties of adenoviruses and are particularly advantageous for ODN whose targets are in the cell nucleus such as triplex-forming ODN. The polylysine–ODN interaction appears to provide protection from intracellular and serum nucleases; the measured ODN half-life of 12 h in the nucleus of SK-BR-3 cells is quite striking in light of the fact that the ODNs used in this report are phosphodiester ODN without stabilizing backbone modifications.

While phosphorothioate ODN are the most common therapeutically designed ODNs, this backbone modification has been shown to decrease the affinity of purine-rich ODN for its duplex target by 62–75% and completely abrogate the ability of pyrimidine rich ODN to form triplex.[19] Although the direct therapeutic utility of adenoviruses is compromised by their immunogenicity,[36] AdpL–ODN complexes will provide an important tool for evaluating the biological activity of triplex forming ODNs that require high intranuclear concentrations of preferably phosphodiester ODN localized in the nucleus.

This study relied on the isolation of nuclei to determine intranuclear ODN concentrations. Cell fractionation is liable to contamination of nuclei with whole cells or other subcellular fractions,[37] and it has been stated that this contamination may be as much as 50%.[13] For this reason, we have verified the purity of our isolated nuclei microscopically. We have also attempted to err on the side of conservatism in both our techniques and calculations (conditions for isolation of nuclei described here would be more likely to lose nuclei than gain subcellular contaminants and 500 fl is an intentional overestimate of the intranuclear volume). In addition, scintillation counting cannot distinguish intact from degraded ODN. For this reason, we verified the integrity of the ODN by gel electrophoresis of internally labeled ODN. The data presented here regarding greater than 20 μM intranuclear ODN concentrations should represent a minimum concentration achievable with this AdpL delivery system under these conditions.

We have developed a rapid and convenient assay for the uptake of ODN in cell culture. The BrdU-ODN immunohistochemical assay has several advantages and disadvantages compared to other methods of detecting ODN in cells. The BrdU modification may be advantageous compared with fluorescently labeled ODN since BrdU is a nucleoside analog rather than a large, planar fluorophor (such as acridine or fluorescein); the intra-

cellular trafficking of BrdU modified ODN should closely mimic the native ODN. Although the use of BrdU-ODNs facilitates immunohistochemical detection, these ODNs have not been studied in detail. The 5-halide modification of the pyrimidine ring may enhance cellular uptake or inhibit nuclease degradation of the ODN, thereby altering the apparent intracellular kinetics. (The ability of fluorinated pyrimidines (5-fluorouracil and congeners) to inhibit thymidylate synthetase is due to the 5-halide modification of the uracil ring.) In addition, since BrdU monomers are efficiently incorporated into DNA and detected by immunohistochemistry, positive reactivity may detect either intact or degraded ODN. We have observed a distinct reactivity pattern for chromosomally incorporated BrdU monomers and intact ODN (as shown in Figure 4). Another drawback is that the immunohistochemistry for BrdU modified ODN can only provide subjective and qualitative data on intracellular ODN trafficking. Given these limitations, the technique of studying tissues with BrdU monomers is well established and easily performed in most laboratories using immunohistochemistry and light microscopy. For studying ODN uptake, the BrdU modified ODN immunohistochemistry is readily applicable to cells in culture as described here; the technique is also applicable to studying ODN delivery to tumors and tissues in whole animals with standard histological processing techniques. Application of this technique can thus serve as a convenient method for evaluating ODN uptake by a panel of cell lines and in whole animal tissues. Finally, by using dual immunohistochemical reactions, the uptake and biological activity of the ODN can be correlated in individual cells. For example, treatment of k-*ras* expressing cells with the BrdU modified k-*ras* triplex forming ODN (KR32TBU) would be expected to repress k-*ras* expression. By using antibodies to both BrdU and k-ras, it would be possible to detect the presence of the ODN and the absence of k-*ras* reactivity (indicating repression of k-*ras* expression) in the individual cells of a treated cell population.

Oligonucleotides show great promise as specific inhibitors of gene expression for therapeutic and scientific purposes. However, all ODNs must resist nuclease degradation and traverse the barriers of the cell membrane, endosomal vesicle, and possibly the nuclear membrane before they can interact with their intracellular targets. Adenovirus–polylysine–oligonucleotide complexes circumvent these difficulties and represent an efficient and reliable method of transferring high quantities of intact ODN inside the cell.

Materials and methods

Oligonucleotide synthesis

We studied the uptake of two ODNs previously shown to be capable of triplex formation (Figure 1). The ODN 'HN28ap' (for human neu 28-mer antiparallel) contains the sequence: 5'ggg Agg Agg Agg Tgg Agg Agg AAg Agg A 3'. This ODN (described in detail in Ref. 8) was synthesized on a Milligen Cyclone Plus DNA Synthesizer (Millipore, Burlington, MA, USA) and purified by polyacrylamide gel electrophoresis. End-labeling was performed by standard methods using the T4 polynucleotide kinase reaction with gamma-^{32}P-ATP. Internal labeling was performed as described by McShan *et al*[10] by first synthesizing the proximal 13 bases, distal 15 bases, and a complementary 34-mer separately. The distal 15-mer was end-labeled, and the proximal 13-mer plus labeled distal 15-mer were annealed to the complementary 34-mer, yielding a 'nicked' duplex. The nick was repaired with T4 DNA ligase, and the 28-base internally labeled oligomer was separated from the complementary 34-mer by 20% denaturing polyacrylamide gel electrophoresis. The ODN 'HN20tata' (for human neu 20-mer with TATA) contains the sequence: 5'gAA gTA AgA ATA TgA Agg Ag 3'. It is antiparallel to a purine-rich sequence containing the TATA box in the HER-2/neu promoter but is incapable of triplex formation. It was used in some co-delivery luciferase assays and was synthesized and purified as described for HN28ap. The ODN 'KR32TBU' (for k-*ras* 32-mer with thymidines and bromodeoxyuridines) contains the sequence: 5'UUU UCU UUC Ugg Tgg ggg TgT Tgg gTg TTg gg 3' where U is BrdU. This ODN is a modification of the ODN KR22Tap (described in Ref. 35); this ODN was purchased from Oligos Etc (Wilsonville, OR, USA) and used without further purification based on the electrophoretic profile provided by the manufacturer.

Cell lines and growth conditions

Cell lines were purchased from the American Tissue Culture Collection (ATCC, Rockville, MD, USA) or grown from frozen stocks of cells previously purchased from the ATCC. Cell lines were grown in a monolayer under the ATCC recommended medium containing 10% fetal bovine serum (FBS) and 1% penicillin-streptomycin (PCN-strep) in a 37°C incubator with 5% CO_2. Unless otherwise stated, tissue culture flasks, plates, media, additives, and reagents were from Gibco BRL (Gaithersburg, MD, USA). Data derived from cell treatments are from cells passaged serially between 2 and 20 times after initial thawing. The various cell lines used and their tissues of origin are listed in Table 1.

Adenovirus preparation and AdpL–DNA complex assembly

The adenovirus strain p259A is an E1A/B deleted version of the human type 5 strain p202-Ad5.[31] In addition to the genomic deletion, the virus has a mutant hexon protein reactive to the monoclonal antibody MP301.[31] Virus amplification and purification was performed by slight modifications of standard procedures.[38,39] Briefly, 30 175 cm^2 flasks of HEK 293 cells were grown to 50% confluence and infected with 5×10^{10} adenoviral particles in Dulbecco's modified Eagle's medium (DMEM) with 2% FBS. After an initial 2–4 h incubation at 37°C, an equal volume of DMEM with 18% FBS and 2% PCN-strep was added to each culture. After 48–72 h, a prominent cytopathic effect was observed in the cells, and they became loosely adherent to the flask. The cells were detached with gentle mechanical agitation and pooled by centrifugation at 1000 r.p.m. for 10 min at 4°C in a Sorvall RT-6000 centrifuge (Dupont, Atlanta, GA, USA). The cells were resuspended in DMEM and lysed with four rapid freeze–thaw cycles (with dry ice-ethanol alternating with a 37°C circulating water bath). The cellular debris was pelleted and discarded by centrifugation at 4000 r.p.m. for 20 min in a Sorvall RT-6000. The supernatant was collected and the adenovirus particles were purified by two serial CsCl density gradient separations. The final opal-

escent adenoviral band was harvested, diluted in five volumes of viral preservation medium (containing 50% glycerol, 10 mM Tris-HCl, pH 8.0, 100 mM NaCl, and 0.1% bovine serum albumin), aliquoted, and stored in single-use vials at –80°C. The concentration and purity of viral particles was estimated by measuring the optical density at 260/280 nm. (1 A_{260} unit = 10^{12} viral particles.)

AdpL–DNA complexes were assembled as described[31] by the serial addition of 2.5×10^{10} adenoviral particles in the appropriate cell culture medium with 2% FBS; the antibody–polylysine conjugate MP-301pL in HEPES buffered saline (HBS), pH 7.3; 6 μg of total DNA (ODN or 1:1 (w/w) plasmid-ODN mixtures of pGL control:HN28ap where indicated) in HBS; and poly-L-lysine (average molecular weight 295 kDa, Sigma, St Louis, MO, USA) in HBS. The AdpL–DNA complexes were used immediately without further storage for cell treatments. All reagents were sterilized by passage through a 0.2-micron filter and handled with strict aseptic technique. Since the stoichiometry of the AdpL–DNA complexes is constant throughout this report; the quantity of AdpL–ODN or AdpL-DNA used for cell treatments is given as the quantity of ODN (in pmol) or plasmid DNA (in μg) used in the complex. This allows for easy comparison of AdpL–ODN, free ODN, and liposome–ODN treatments.

Liposomes

DOTAP and DOPE were purchased from Avanti Lipids (Anniston, AL, USA) and prepared according to the manufacturer's recommendations. A 1:1 (w/w) mixture of DOTAP/DOPE was lyophilized, resuspended in deionized water, and sterilized through a 0.2-micron syringe filter. Liposome–ODN complexes were formed by allowing a 4:1 (w/w) mixture of the aqueous suspension of DOTAP/DOPE to condense with the ODN KR32TBU in sterile deionized water for 30 min at room temperature.

Cell treatments with oligonucleotides

For cell fractionation, cell cultures were treated in log growth phase by aspirating the culture medium and adding equivalent amounts of the ODN or the AdpL–ODN complexes in a minimal volume of culture medium containing 2% FBS (2 ml for 25 cm^2 flasks, 5 ml for 75 cm^2 flasks, and 10 ml for 150 cm^2 flasks). The cultures were incubated for 2–4 h at 37°C in the tissue culture incubator, and then an equal volume of culture medium containing 18% FBS and 2% PCN-strep was added. Cell cultures were incubated at 37°C for 24 h or as indicated after the initial addition of the ODN. The number of cells treated and amount of ODN were as indicated. Cell fractionation techniques are described below.

Cell treatments for immunohistochemistry were performed on microscope slides with four 2 cm^2 cell culture chambers (Nunc, Naperville, IL, USA). In each of these experiments, 10^4 cells were seeded into the chamber and allowed to grow for 1 day prior to treatment. The medium was aspirated and 10 pmol of KR32TBU (as free ODN, AdpL–ODN complex, or liposome–ODN complex) was added in 500 μl of medium with 2% FBS. The cells were incubated for 2–4 h at 37°C, and 500 μl of medium with 18% FBS and 2% PCN-strep was added. The cells were incubated at 37°C overnight and fixed for immunohistochemistry 20–24 h after the initial addition of the ODN. Immunohistochemical reactions are described below.

Cell treatments for the luciferase assay were performed by plating 10^6 SK-BR-3 or MCF-7 breast cancer cells 1 day prior to treatment. In these experiments, the AdpL–DNA complexes were assembled with either 6 μg of pGL control (Promega, Madison, WI, USA) plasmid DNA or 3 μg each of the plasmid DNA and ODN (the ODNS HN28ap and HN20tata were used in these experiments). Again, the cell treatment consisted of adding the AdpL–DNA complex in serum poor (2%) medium for 2–4 h prior to adding serum-rich medium for the remainder of the 37°C, 48-h incubation period as detailed above. Cell lysis and luciferase assay conditions are described below.

Cell fractionation techniques

Cell fractionation was performed with modifications of standard procedures.[10,37,40] Cells were harvested from growth in a monolayer by treatment with trypsin–EDTA (Gibco BRL) at 37°C for 1–20 min until the cells appeared rounded and were easily detached from the flask by gentle tapping. The cells were washed twice in phosphate buffered saline (PBS) and resuspended in 500 μl NP-40 lysis buffer (containing 10 mM Tris-HCl, pH 7.5; 3 mM $MgCl_2$; 10 mM NaCl; and 0.5% Nonidet P-40). The cells were vortexed gently for 10 s and incubated on ice for 2 min. The cell lysate was then added to an equal volume of ice cold nuclear preparation solution 2 (containing 20 mM HEPES, pH 7.9; 600 mM NaCl; 1.5 mM $MgCl_2$; 0.2 mM EDTA; 0.5 mM DTT; 20% glycerol (v/v)) and layered over 10 volumes of ice cold nuclear preparation solution 3 (containing 20 mM HEPES, pH 7.9; 5 mM $MgCl_2$; 0.1 mM EDTA; 2 mM, DTT; 2.5 mM KCl; 20% glycerol (v/v)) in a round-bottom centrifuge tube. The mixture was subjected to a horizontal centrifugation at 1000 *g* for 10 min at 4°C. The pellet represents 'pure nuclei' and microscopically appeared to contain very few intact cells or other cellular debris (see Figure 5 'H&E Stain'). Uptake of the radiolabeled ODN was measured by suspending the nuclei in liquid scintillant and counting on a Beckman LS3800 scintillation counter (Beckman Instruments, Fulterton, CA, USA). For experiments in which the nucleic acid fraction was harvested from the nuclei, the nuclei were resuspended in PBS made 1% with respect to sodium lauryl sulfate (SLS) and boiled at 95°C for 5 min. The resulting nuclear lysate was extracted once with phenol and once with phenol/chloroform/isoamyl alcohol (25:24:1). The aqueous phase was either analyzed directly by polyacrylamide gel electrophoresis or short genomic DNA fragments and ODNs were further purified by reverse phase chromatography with Sep-Pak C-18 columns after 20-fold dilution in C-18 loading buffer (containing 100 mM Tris-HCl, pH 8.0; 500 mM NaCl; and 5 mM EDTA). The nucleic acid fraction thus purified was a suitable substrate for end-labeling the entire fraction with the T4 polynucleotide kinase reaction. The cell culture media were purified for labeling by 20-fold dilution in C-18 loading buffer and reverse phase column chromatography. In one set of experiments, a crude cell lysate was purified and end-labeled as described for the nuclei, except that cells were lysed directly by boiling in 1% SLS before extraction.

The cell volume of monolayer tissue culture cells was estimated at 1 picoliter (the volume of a 10-micron cube), and nuclear volumes were estimated at 500 femptoliters.

These numbers are in the range of previously determined cell and nuclear volumes. For example, peripheral blood monocytes have a volume of 200 fl and MT4 cells have a volume of 450 fl.[10] The amount of labeled ODN (in pmol) in the cell or nucleus was determined from the total c.p.m. of these fractions and the specific activity of the ODN. The concentration of ODN was calculated by dividing the amount of ODN (in pmol) by the product of the nuclear volume and the total number of cells analyzed.

Immunohistochemistry

Immunohistochemistry for BrdU in cells is a modification of the procedures described by Gratzner.[41] Cell cultures were treated on chamber slides as described above. Following the treatment, the cells were washed with PBS and fixed with cold acetone/methanol/37% formalin (19:19:2 v/v/v). (Fixation has previously been shown not to affect ODN distribution).[42] After fixation, the slides were air dried, washed in PBS, and treated with 3% H_2O_2 for 5 min to remove the endogenous peroxidase. The intracellular localization of the BrdU-ODN was detected with a murine IgG_1 monoclonal antibody specific for 5-bromo-2′-deoxyuridine-5′-monophosphate (Boehringer Mannheim, Indianapolis, IN, USA). Slides were incubated in a 1 μg/ml solution of this antibody at 4°C overnight. The secondary antibody was a biotin-labeled goat anti-murine-IgG (Dako, Carpinteria, CA, USA). The slides were incubated in a 1:200 dilution of the secondary antibody for 60 min prior to incubation in a 1:500 dilution of avidin–peroxidase conjugate (Dako) for 60 min. The final chromogenic reaction was performed by adding 3,3′-diaminobenzidine (Sigma) to produce brown-colored deposits corresponding to the BrdU localization. The tissue culture cells were counterstained with hematoxylin to demonstrate the cellular and nuclear morphology. Positive (5 μM free BrdU, Sigma) and negative (PBS) control treatments were included for each cell line on the same slide. As another negative control, SK-BR-3 cells treated with AdpL–HN28ap complex (that does not contain BrdU) were subjected to the same reactions. Lack of immunoreactivity in these cells confirms the specificity of the anti-BrdU antibody and excludes the possibility of cross-reactivity between the secondary antibody (a biotin labeled goat antimurine IgG) with the antibody–polylysine conjugate (MP301pL). The slides were examined by one of us (NV) in an unblinded fashion and scored subjectively for the approximate percentage of cells containing any visible stain after examining at least ten 400× magnification fields. The intensity of brown stain was scored on a three-point scale (+–+++: + = low; ++ = intermediate; +++ = high). The histochemical slides were submitted in a blinded fashion to an experienced pathologist not associated with this study. The semiquantitative analysis presented in Table 2 was confirmed by this blinded review.

Luciferase assay

The plasmid pGL control (Promega) contains the firefly luciferase gene under control of the SV40 early promoter and enhancer. The plasmid was transformed into competent *E. coli* (DH5-alpha); large-scale plasmid preparation from ampicillin resistant colonies was performed by alkaline lysis and anion exchange columns with the Qiagen Maxi Plasmid Kit (Qiagen, Chatsworth, CA, USA) according to the manufacturer's recommendations. This plasmid was assembled into AdpL–DNA columns as described above.

SK-BR-3 and MCF-7 cells were treated as described for 48 h. The cells were washed twice with PBS and 1 ml of 1× Lysis Reagent (Promega) was added to the plate for 15 min at room temperature. The lysed cells were scraped free of the plate and collected into a microfuge tube. The cellular debris was pelleted by centrifugation in a microfuge for 10 s. The lysate was assayed immediately for luciferase activity by adding 10 μl (1%) of the lysate to 100 μl of beetle luciferin in Luciferase Assay Reagent (Promega). The luciferase activity was measured at 30 s on a Lumat LB9501 luminometer (Wallac, Gaithersburg, MA, USA). Data are reported as relative light units (RLU) in 30 s per 10^6 cells. We have previously determined that lysate from SK-BR-3 and MCF-7 cells prepared as described contains approximately 1 mg/ml of total protein. Luciferase activities from the MCF-7 treatments represent the means of three separate experiments.

Acknowledgements

This work was supported by grants from the American Cancer Society (PRTF 153 to SWE), National Institutes of Health (RO1 CA42664 and RO1 CA42337 to DMM; R29 CA61964 to CAM), Share Foundation (to DMM), Council for Tobacco Research (Scholar Award to CAM), and Veterans Administration (Merit Review Grant to DMM). The authors gratefully acknowledge the assistance of Brad Rodu for serving as a blinded reviewer of our histochemical slides.

References

1 Zamecnik P *et al*. Electron micrographic studies of transport of oligodeoxynucleotides across eukaryotic cell membranes. *Proc Natl Acad Sci USA* 1994; **91**: 3156–3160.
2 Yakubov LA *et al*. Mechanism of oligonucleotide uptake by cells: involvement of specific receptors? *Proc Natl Acad Sci USA* 1989; **86**: 6454–6458.
3 Stein CA *et al*. Dynamics of the internalization of phosphodiester oligodeoxynucleotides in hl60 cells. *Biochemistry* 1993; **32**: 4855–4861.
4 Budker VG, Knorre DG, Vlassov VV. Cell membranes as barriers for antisense constructions. *Antisense Res Dev* 1992; **2**: 177–184 (review).
5 Akhtar S, Juliano RL. Cellular uptake and intracellular fate of antisense oligonucleotides. *Trends Cell Biol* 1992; **2**: 139–144.
6 Temsamani J *et al*. Cellular uptake of oligodeoxynucleotide phosphorothioates and their analogs. *Antisense Res Dev* 1994; **4**: 35–42.
7 Mayfield C *et al*. Triplex formation by the human ha-ras promoter inhibits sp1 binding and *in vitro* transcription. *J Biol Chem* 1994; **269**: 18232–18238.
8 Ebbinghaus SW *et al*. Triplex formation inhibits her-2/neu transcription *in vitro*. *J Clin Invest* 1993; **92**: 2433–2439.
9 Young SL, Krawczyk SH, Matteucci MD, Toole JJ. Triple helix formation inhibits transcription elongation *in vitro*. *Proc Natl Acad Sci USA* 1991; **88**: 10023–10026.
10 McShan WM *et al*. Inhibition of transcription of HIV-1 in infected human cells by oligodeoxynucleotides designed to form DNA triple helices. *J Biol Chem* 1992; **267**: 5712–5721.
11 Postel EH, Flint SJ, Kessler DJ, Hogan ME. Evidence that a triplex-forming oligodeoxyribonucleotide binds to the c-myc promoter in Hela cells, thereby reducing c-myc mRNA levels. *Proc Natl Acad Sci USA* 1991; **88**: 8227–8231.
12 Orson FM *et al*. Oligonucleotide inhibition of IL2r alpha mRNA

transcription by promoter region collinear triplex formation in lymphocytes. *Nucleic Acids Res* 1991; **19**: 3435–3441.

13 Fisher TL, Terhorst T, Cao X, Wagner RW. Intracellular disposition and metabolism of fluorescently-labeled unmodified and modified oligonucleotides microinjected into mammalian cells. *Nucleic Acids Res* 1993; **21**: 3857–3865.

14 Ghosh MK, Ghosh K, Dahl O, Cohen JS. Evaluation of some properties of a phosphorodithioate oligodeoxyribonucleotide for antisense application. *Nucleic Acids Res* 1993; **21**: 5761–5766.

15 Agrawal S, Temsamani J, Tang JY. Pharmacokinetics, biodistribution, and stability of oligodeoxynucleotide phosphorothioates in mice. *Proc Natl Acad Sci USA* 1991; **88**: 7595–7599.

16 Ghosh MK, Ghosh K, Cohen JS. Phosphorothioate-phosphodiester oligonucleotide co-polymers: assessment for antisense application. *Anticancer Drug Des* 1993; **8**: 15–32.

17 Akhtar S, Kole R, Juliano RL. Stability of antisense DNA oligodeoxynucleotide analogs in cellular extracts and sera. *Life Sci* 1991; **49**: 1793–1801.

18 Campbell JM, Bacon TA, Wickstrom E. Oligodeoxynucleoside phosphorothioate stability in subcellular extracts, culture media, sera and cerebrospinal fluid. *J Biochem Biophys Meth* 1990; **20**: 259–267.

19 Hacia JG, Wold BJ, Dervan PB. Phosphorothioate oligonucleotide-directed triple helix formation. *Biochemistry* 1994; **33**: 5367–5369.

20 Maury G *et al*. Rapid determination of the affinity of 28- and 14-mer phosphorothioate oligonucleotides for HIV-1 reverse transcriptase by fluorescence spectroscopy. *Biochim Biophys Acta* 1993; **19**: 1–8.

21 Kibler-Herzog L *et al*. Duplex stabilities of phosphorothioate, methylphosphonate, and RNA analogs of two DNA 14-mers. *Nucleic Acids Res* 1991; **19**: 2979–2986.

22 Murakami A *et al*. Interaction of antisense DNA with nucleic acids/proteins. *Nucleic Acids Symp Ser* 1992; **27**: 123–124.

23 Morvan F *et al*. Comparative evaluation of seven oligonucleotide analogues as potential antisense agents. *J Med Chem* 1993; **36**: 280–287.

24 Ho PT, Ishiguro K, Wickstrom E, Sartorelli AC. Non-sequence-specific inhibition of transferrin receptor expression in hl-60 leukemia cells by phosphorothioate oligodeoxynucleotides. *Antisense Res Dev* 1991; **1**: 329–342.

25 Dahm SC, Uhlenbeck OC. Role of divalent metal ions in the hammerhead RNA cleavage reaction. *Biochemistry* 1991; **30**: 9464–9469.

26 Capaccioli S *et al*. Cationic lipids improve antisense oligonucleotide uptake and prevent degradation in cultured cells and in human serum. *Biochem Biophys Res Commun* 1993; **197**: 818–825, and erratum 1994; **200**: 1769.

27 Juliano RL, Akhtar S. Liposomes as a drug delivery system for antisense oligonucleotides. *Antisense Res Dev* 1992; **2**: 165–176 (review).

28 Zatloukal K *et al*. *In vivo* production of human factor VII in mice after intrasplenic implantation of primary fibroblasts transfected by receptor-mediated, adenovirus-augmented gene delivery. *Proc Natl Acad Sci USA* 1994; **91**: 5148–5152.

29 Gao L *et al*. Direct *in vivo* gene transfer to airway epithelium employing adenovirus–polylysine–DNA complexes. *Hum Gene Ther* 1993; **4**: 17–24.

30 Wagner E *et al*. Coupling of adenovirus to transferrin-polylysine/DNA complexes greatly enhances receptor-mediated gene delivery and expression of transfected genes. *Proc Natl Acad Sci USA* 1992; **89**: 6099–6103.

31 Curiel DT *et al*. High-efficiency gene transfer mediated by adenovirus coupled to DNA–polylysine complexes. *Hum Gene Ther* 1992; **3**: 147–154.

32 Seth P, Rosenfeld M, Higginbotham J, Crystal RG. Mechanism of enhancement of DNA expression consequent to cointernalization of a replication-deficient adenovirus and unmodified plasmid DNA. *J Virol* 1994; **68**: 933–940.

33 Michael SI *et al*. Binding-incompetent adenovirus facilitates molecular conjugate-mediated gene transfer by the receptor-mediated endocytosis pathway. *J Biol Chem* 1993; **268**: 6866–6869.

34 Defer C, Belin MT, Caillet-Boudin ML, Boulanger P. Human adenovirus–host cell interactions: comparative study with members of subgroups b and c. *J Virol* 1990; **64**: 3661–3673.

35 Mayfield C, Squibb M, Miller D. Inhibition of nuclear protein binding to the human ki-ras promoter by triplex-forming oligonucleotides. *Biochemistry* 1994; **33**: 3358–3363.

36 Yang Y *et al*. Cellular immunity to viral antigens limits E1-deleted adenoviruses for gene therapy. *Proc Natl Acad Sci USA* 1994; **91**: 4407–4411.

37 Howell KE, Devaney E, Gruenberg J. Subcellular fractionation of tissue culture cells. *Trends Biochem Sci* 1989; **14**: 44–47.

38 Jones N, Shenk T. Isolation of adenovirus type 5 host range deletion mutants defective for transformation of rat embryo cells. *Cell* 1979; **17**: 683–689.

39 Chardonnet Y, Dales S. Early events in the interaction of adenoviruses with Hela cells. I. Penetration of type 5 and intracellular release of the DNA genome. *Virology* 1970; **40**: 462–477.

40 Dignam JD, Lebovitz RM, Roeder RG. Accurate transcription initiation by RNA polymerase II in a soluble extract from isolated mammalian nuclei. *Nucleic Acids Res* 1983; **11**: 1475–1489.

41 Gratzner HG. Monoclonal antibody to 5-bromo- and 5-iododeoxyuridine: a new reagent for detection of DNA replication. *Science* 1982; **218**: 474–475.

42 Noonberg SB, Garovoy MR, Hunt CA. Characteristics of oligonucleotide uptake in human keratinocyte cultures. *J Invest Dermatol* 1993; **101**: 727–731.

Reprinted from Biochemistry, 1996, 35.

Influence of GC and AT Specific DNA Minor Groove Binding Drugs on Intermolecular Triplex Formation in the Human c-Ki-ras Promoter†

Nadarajah Vigneswaran,‡ Charles A. Mayfield,§ Brad Rodu,‡ Roger James,‡ H.-G. Kim,§ and Donald M. Miller*,§,||

Department of Oral Pathology, Bolden Laboratory, Department of Medicine, Department of Biochemistry and Molecular Genetics, Comprehensive Cancer Center, University of Alabama at Birmingham, Alabama 35294-3300 and the Birmingham Veterans Affairs Medical Center, Birmingham, Alabama 35294-0001

Received July 10, 1995; Revised Manuscript Received November 20, 1995⊗

ABSTRACT: We have used DNase I footprinting and gel shift assays to characterize the interaction of DNA binding drugs mithramycin, distamycin, and berenil with an intermolecular triplex formed by the human c-Ki-ras promoter. A purine-rich triplex-forming oligonucleotide (ODN) forms a stable intermolecular triple helix (triplex) with a homopurine (PR):homopyrimidine (PY) motif in the human c-Ki-ras promoter which contains a 22bp PR:PY region (−328 to −307). This triplex structure is comprised of 15 G·G:C triplets interspersed with 7 T·A:T triplets. Mithramycin binding sites in the human c-Ki-ras promoter encompass most of the triplex target site and three G-C-rich sequences downstream of this triplex-forming region. Mithramycin binding within the c-Ki-ras promoter completely abrogates triplex formation. Furthermore, the addition of mithramycin to pre-formed triplex by c-Ki-ras promoter displaces the major groove bound ODN. Five prominent distamycin binding sites are noted within the c-Ki-ras promoter including the triplex-forming site as well as A-T-rich regions upstream and downstream of the triplex site. Berenil does not bind within the triplex target sequence, and only one berenil binding sequence downstream of the triplex motif was present within the c-Ki-ras promoter fragment. Neither distamycin nor berenil prevents triplex formation, and, furthermore, the addition of either distamycin or berenil to the pre-formed triplex structure did not displace the major-groove-bound third strand. This study demonstrates that GC-specific and AT-specific minor groove ligands differentially affect the intermolecular pur·pur:pyr triplex. A possible biological significance of mithramycin interaction with intramolecular triplex is discussed.

Homopurine−homopyrimidine sequences occur disproportionately in the regulatory regions of eukaryotic genes and represent approximately 1% of the total genome (Birnboim et al., 1979; Wells et al., 1988). These sequences are DNase hypersensitive, both in chromatin and in superhelical plasmids (Wells et al., 1988). Recent studies suggest that these regions can form H-DNA which represents intramolecular triple-helical DNA (triplex DNA) (Mirkin & Frank-Kamenetskii, 1994). The *in vivo* existence of intramolecular triplex DNA has been suggested in various cell types by the reaction of multiple chromatin sites with an antibody specific for triplex DNA (Agazie et al., 1994). Transient formation of intramolecular triplex by these tandemly repeated homopyrimidine:homopurine tracts may play an important role in regulating gene expression (Wells et al., 1988).

The polypurine:polypyrimidine sequences are often important positive cis-acting elements which are necessary for activated transcription (Firulli et al., 1994; Raghu et al., 1994). In recent years, a number of groups have successfully exploited these regions as targets for the formation of intermolecular triple-helical DNA using synthetic oligonucleotides (ODN)[1] (Beal & Dervan, 1991; Gee et al., 1992; Ebbinghaus et al., 1993; Mayfield et al., 1994a,b). Two types of intermolecular triplex DNA have been described; pyr·pur:pyr triplex and pur·pur:pyr triplex. They differ in their sequence composition and relative orientation of the third strand. In pyr·pur:pyr triplex a pyrimidine-rich ODN binds in a parallel orientation relative to the purine-rich tract of the double-stranded DNA (DS DNA) via the formation of T·A:T and pH-dependent C^+·G:C triplets (Moser & Dervan, 1987). In the pur·pur:pyr type, purine-rich or mixed purine/pyrimidine ODNs bind in an antiparallel orientation to the purine-rich strand of the DS DNA (Moser & Dervan, 1987; Beal & Dervan, 1991. The resulting triplex DNA consists of predominantly of G·G:C triplets interspersed with A·A:T or T·A:T triplets (Moser & Dervan, 1987; Beal & Dervan, 1991). In triple-helical DNA, the pyrimidine- or purine-rich ODN is bound in the major groove of the DS DNA and interacts with specific purine bases of the target DNA by forming either Hoogsteen or reverse Hoogsteen hydrogen bonds, respectively (Moser & Dervan, 1987; Beal & Dervan, 1991). Intermolecular triplex formation by the binding sites of transcription factors has been shown to inhibit the transcription of a number of eukaryotic promoters (Postel et al., 1991; Orsen et al., 1991; Ebbinghaus et al.,

† Supported by Grants CA61964-01A1 (to C.M.), CA42664, and CA42337 (to D.M.M.), from the National Institutes of Health, by the Share Foundation (to D.M.M.), by Veterans Administration Merit Review Grant (to D.M.M.), and by Council for Tobacco Research Scholar Award SA020 (to C.M.).

* To whom correspondence should be addressed, 1824 6th Avenue South, Wallace Tumor Institute, Room 520, Birmingham, AL 35294. Phone: (205) 934-1977. Fax: (205) 975-6911.

‡ Department of Oral Pathology.

§ Bolden Laboratory, Department of Medicine.

|| Department of Biochemistry and Molecular Genetics.

⊗ Abstract published in *Advance ACS Abstracts*, January 15, 1996.

[1] Abbrevations: ODN, oligonucleotide; bp, base pair; DS, double strand.

0006-2960/96/0435-1106$12.00/0

1993; Mayfield et al., 1994b). The c-Ki-ras protooncogene is a member of a highly conserved ras gene family whose protein products are important in signal transduction and regulation of cell proliferation (Barbacid, 1987). Although the c-Ki-ras gene is expressed constitutively at basal levels in all cells, its expression is increased transiently during tissue growth and cell division (Muller et al., 1983; Goyette et al., 1984). Because of the pivotal role of c-Ki-ras expression in the control of cell growth and differentiation, it is reasonable to expect that its transcription would be tightly regulated by multiple pathways.

Although regulation of c-Ki-ras transcription in normal and neoplastic cells is not well understood, it is clear that expression of the c-Ki-ras gene is controlled by both proximal and distal elements, generally located in the 5′ upstream region of the gene (Jordano & Perucho, 1986; Yamamoto & Perucho, 1988). As with other housekeeping genes, both the human and mouse c-Ki-ras promoters lack an obvious TATA or CCAAT box but contain four GC-boxes which act as putative binding sites for the transcription factor Sp1 (McGrath et al., 1986; Yamamoto & Perucho, 1988; Hoffman et al., 1987). These GC box sequences are found in a region which corresponds to the essential elements of the c-Ki-ras promoter (Jordano & Perucho, 1986). A homopurine−homopyrimidine region that is sensitive to endogenous nuclease and S1 nuclease in supercoiled plasmids is located in the region between −250 and −400 bp upstream of the exon 0/intron 1 boundary (Jordano & Perucho, 1986). This region contains a 22 bp homopurine:homopyrimidine motif located from −126 to −147 with respect to the the major transcription start site (−307 to −328 from exon 0/intron 1) (Jordano & Perucho, 1986; Mayfield et al., 1994a). Sequence-specific binding of a nuclear protein to this motif has been reported (Mayfield et al., 1994a). This sequence also forms an intermolecular triple helix with a synthetic ODN abrogating the binding of nuclear protein (Mayfield et al., 1994a). A similar region in the mouse c-Ki-ras promoter contains a 27 bp S1 hypersensitive homopurine:homopyrimidine motif which adopts an intramolecular triple-helical H-DNA conformation in mildly acidic conditions (Pestov et al., 1991).

The antiproliferative effects of DNA binding drugs are thought to be primarily due to the interaction of these drugs with double-stranded DNA and their resultant inhibition of DNA and RNA synthesis as well as DNA repair. Although DNA bindings drugs may show some degree of sequence preference, the degeneracy of their potential binding sequences is quite high and their binding affects the expression of multiple genes. Mithramycin is a GC-specific DNA binding drug which binds as a dimer within the minor groove, in the presence of Mg^{2+} (Behr & Hartmann, 1965; Sastry & Patel, 1993). Mithramycin selectively inhibits the transcription of genes with GC-rich promoters such as c-myc, H-ras, and dihydrofolate reductase (dhfr) (Snyder et al., 1991; Blume et al., 1991). This effect has been attributed to its interference with Sp1 binding sequences in these promoters (Snyder et al., 1991). On the other hand, distamycin and berenil bind in the minor groove of AT-rich DNA although there are subtle differences in their preferential binding sequences (Portugal & Waring, 1987).

The effect of DNA binding drugs on pur·pur:pyr triplex is not known. A number of recent studies have addressed the ability of nonintercalative minor groove binders to interact with triplex DNA (Chalikian et al., 1994; Park & Breslauer, 1992; Thomas & Thomas, 1993; Pilch & Breslauer, 1994; Durand et al., 1994). These studies have been limited to short pyrimidine·purine:pyrimidine triple helices (less than 20 bp long) comprised of primarily poly[$d(T)_n$·$d(A)_n$:$d(T)_n$] triplex sequences. Most of these studies have also utilized artificial triplex-forming sequences as opposed to naturally occurring gene specific triplex-forming sequences. The specific interaction of DNA binding drugs with naturally occurring triplex target sequences is important for a number of reasons. First, a DNA binding drug might interact preferentially with triplex DNA, as opposed to DS DNA, enhancing the stability of the triplex structure. Secondly, the combined exposure to ODN and "triplex-specific" DNA binding drugs may increase their ability to inhibit specific genes. Finally, the identification of a drug which can cause the disassociation of triplex DNA may have applications in the study of function and structure of intramolecular triplex (H-DNA) *in vivo*.

In this study we have examined the interaction of mithramycin, distamycin, and berenil with the intermolecular pur·pur:pyr triplex structure formed by the human c-Ki-ras promoter. These three DNA minor groove binding ligands demonstrate well characterized differences in their recognition sequences (Sastry & Patel, 1993; Carpenter et al., 1993; Portugal & Waring, 1987). We have utilized the human c-Ki-ras promoter region as a prototypic triplex-forming sequence since this region, comprised of poly(dG-dA) stretches, provides potential binding sites for both GC- and AT-specific minor groove binding compounds (Jordano & Perucho, 1986; Yamamoto & Perucho, 1988; Mayfield et al., 1994a).

EXPERIMENTAL PROCEDURES

Drugs and Enzymes. Mithramycin, distamycin, and berenil (Diminiazine aceturate) were obtained from Sigma Chemical Co. These drugs were stored as a 10^{-2} M stock solution in distilled water at −20 °C. Restriction endonucleases *Eco*R1 and *Bam*H1, T_4 polynucleotide kinase, Klenow fragment of DNA polymerase, and DNase I were purchased from Gibco BRL.

Oligonucleotide Synthesis. Phosphodiester oligonucleotides were synthesized with standard DNA bases on the Milligen Cyclone DNA synthesizer using phosphoramidite chemistry. Oligonucleotides were purified using reverse-phase oligonucleotide purification-elution cartridges (CLONTECH) followed by gel electrophoresis. The structural integrity and purity of these oligonucleotides were confirmed by 5′-^{32}P labeling using [^{32}P]ATP and T_4 polynucleotide kinase, followed by electrophoresis on a denaturing polyacrylamide gel. Oligonucleotide concentrations were determined from absorbance measurements at 260 nm using calculated molar extinction coefficients for each oligonucleotide.

Isolation of c-Ki-ras Promoter Fragment. The 181 bp (−61 to −234) c-Ki-ras2 promoter fragment was amplified from HL-60 genomic DNA using Vent DNA polymerase. The 5′ PCR primer was designed with an *Eco*R1 recognition site and the 3′ primer with a *Bam*H1 recognition site. The amplified fragment was gel purified, digested with *Eco*R1 and *Bam*H1, and then cloned into a plasmid vector pTZ 18R. ^{32}P-labeled promoter fragments used in DNase I footprinting

experiments were prepared by digestion of the plasmid construct with *Eco*R1 followed by 3′ end labeling with [^{32}P]dATP using the Klenow fragment of DNA polymerase. The fragment was then digested with *Bam*H1, and the resulting 181 bp promoter fragment was purified by gel electrophoresis through nondenaturing polyacrylamide gels. Sequence analysis of this fragment by Maxam−Gilbert method confirmed the correct sequence.

Electrophoretic-Gel Mobility Shift Analysis of Drug Binding and Triplex Formation. The DS DNA probe used in this study is a 22 bp synthetic c-Ki-ras triplex target sequence. To prepare the ^{32}P-labeled DS DNA, the synthetic coding strand was 5′-^{32}P-end-labeled with [^{32}P]ATP and T_4 polynucleotide kinase and annealed to its complement. Labeled target duplex and ODN were coincubated overnight in a buffer consisting of 90 mM Tris, 90 mM borate, and 10 mM $MgCl_2$ (TBM, pH 8.0) at 37 °C. Samples were electrophoresed at 100 V approximately for 15 h, through 16% nondenaturing polyacrylamide gel buffered with 90 mM Tris-borate (pH 8)/10 mM $MgCl_2$. Gels were then exposed at −70 °C for autoradiography. For drug interference gel shift studies, the 5′-^{32}P-end-labeled ODN was used to shift the cold duplex probe under the experimental conditions which remained the same as mentioned above. Mithramycin and distamycin were added in appropriate concentrations to the sample containing target DS DNA in three different circumstances: I, 30 min before the addition of ODN; II, simultaneously with addition of the ODN; III, approximately 30 min before loading the pre-formed triplex. Controls included the incubation of individual drugs in appropriate concentration with either labeled DS DNA probe alone or labeled ODN alone.

DNase I Footprinting. The 181 bp ^{32}P-labeled c-Ki-ras promoter fragment was incubated overnight with the oligonucleotide in the presence and absence of the appropriate concentrations of either mithramycin or distamycin or berenil in a buffer consisting of 90 mM Tris-HCl (pH 7.4) and 10 mM $MgCl_2$ at 37 °C. Samples were precooled on ice and then digested with DNase I for 2−3 min, and the reaction was terminated by the addition of 10 mM ethylenediaminetetraacetic acid (EDTA) followed by heating to 95 °C for 5 min. Samples were cooled on ice, and the digested DNA product was extracted once with phenol/chloroform and then ethanol precipitated. The cleaved DNA product was resuspended in 50% formamide containing bromophenol blue and xylene cyanol and denatured by heating at 95 °C for 5 min. The samples were quickly cooled on ice and then analyzed on an 8% polyacrylamide sequencing gel in the presence of 8 M urea, at 42 W for 2 h. The gels were visualized by autoradiography. To identify the drug binding sites, the ^{32}P-labeled promoter fragment was coincubated individually with appropriate concentrations of mithramycin, distamycin, or berenil in a buffer identical to the one used for oligonucleotide binding. Maxam−Gilbert sequencing reactions (A+T) and (G+C) of the promoter fragment were performed and analyzed on the same gel as the DNase I digest for sequence determination (Maxam & Gilbert, 1980). Approximately 15 000 cpm of labeled plasmid fragment was used for all DNase I protection assays resulting the final target concentration of 10 nM.

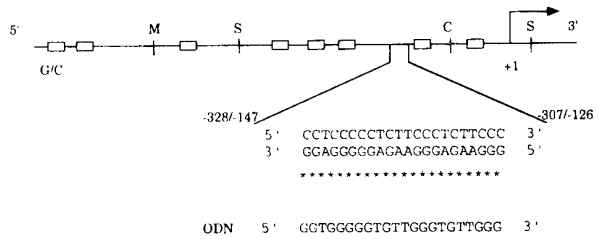

FIGURE 1: Map of the human c-Ki-ras promoter showing the 22 bp triplex target sequence. The alignment and the sequence of the triplex-forming oligodeoxynucleotide (ODN) is also shown.

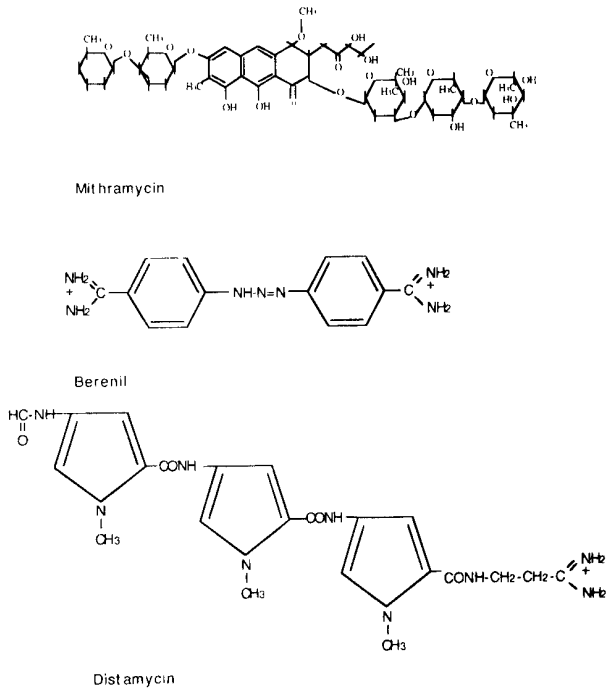

FIGURE 2: Structures of mithramycin, berenil, and distamycin.

RESULTS

The sequence of the target site and its relative position within the c-Ki-ras promoter is shown in Figure 1. The specific alignment and the sequence of the ODN which forms triplex at this site triplex is also shown in Figure 1. Mithramycin, distamycin, and berenil represent DNA binding drugs of different chemical structural families (Figure 2) that bind in the minor groove of the DS DNA.

Electrophoretic Mobility Shift Analysis of Triplex Formation. Triplex formation was initially documented by electrophoretic mobility shift analysis. The synthetic coding strand of the 22 bp c-Ki-ras duplex DNA target was used as a probe for gel shift analysis. The addition of ODN at 1 μM final concentration (1000-fold excess relative to duplex) leads to the complete shift of the 5′-^{32}P- labeled double-stranded DNA target (DS) to a distinct triplex band (Figure 3, lane 5). Alternatively, when the ODN (100 nM) was 5′-end-labeled and added to unlabeled DS target DNA (50 nM) to give a 2-fold excess of ODN, the labeled ODN involved in triplex formation appears as a distinct more slowly migrating band separated from the excess unbound ODN (Figure 4, lane 3).

Specificity of Triplex Formation. As shown in Figure 5, lane 3, DNase I cleavage of the 181 bp human c-Ki-ras promoter fragment in the presence of ODN gives rise to protection of the entire 22 bp polypurine−polypyrimidine

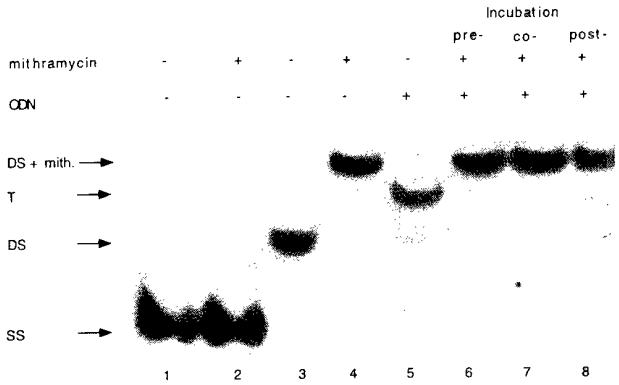

FIGURE 3: Gel mobility shift analysis demonstrating the binding of triplex-forming ODN and mithramycin to triplex target site. The ^{32}P-labeled synthetic target DNA (10 nM) was incubated in the absence or presence of ODN (1 μM) or mithramycin (100 μM) or both. Mithramycin was added prior (pre-), during (co-), and after (post-) the formation triplex. SS = single 22 bp pyrimidine strand; DS = double-stranded target DNA; T = triplex DNA; mith. = mithramycin.

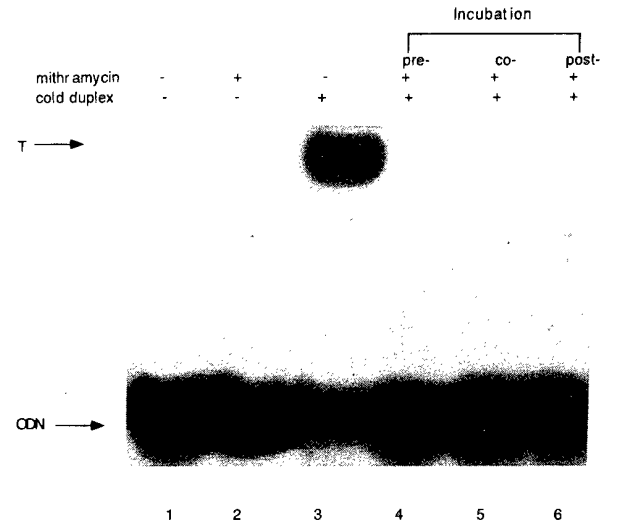

FIGURE 4: Gel mobility shift analysis showing the inhibition of triplex formation by mithramycin. Mithramycin (100 μM) was incubated with unlabeled synthetic target DNA (50 nM) prior to (pre-), during (co-) the addition of ^{32}P-labeled triplex ODN (100 nM), or after overnight triplex formation (post-). ODN = radiolabeled oligodeoxynucleotide; T = triplex DNA.

target sequence which confirms the complete formation of triple-helical DNA under these conditions. The specific sequence of this protection site is determined by alignment of Maxam−Gilbert sequencing of this promoter fragment in conjunction with the DNase I footprints (Figure 5). Complete protection of the target sequence is achieved at 5 μM concentration of ODN (approximately 5000-fold in excess compared to target site concentration) consistent with our previous data (Mayfield et al. 1994a).

Mithramycin Binding to Human c-Ki-ras Promoter Region and Its Effect on Intermolecular Triplex Formation. We also determined the pattern of mithramycin binding to the c-Ki-ras promoter by DNase I footprint analysis. The reaction conditions used for mithramycin binding were identical to those described for triplex formation. Typical DNase I digestion patterns of the 181 bp fragment of the c-Ki-ras promoter in the presence and absence of mithramycin are shown in Figure 5, lanes 1 and 2. The DNase I digestion pattern of this fragment is modified by mithramycin binding,

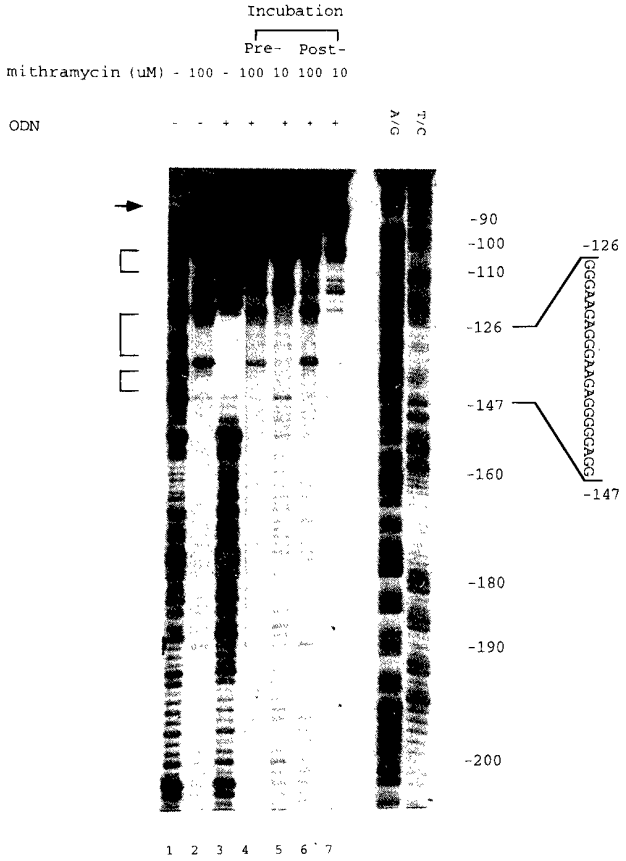

FIGURE 5: DNase I protection assay demonstrating mithramycin binding (lane 2) and triplex formation (lane 3) to the c-Ki-ras promoter. A 181 bp ^{32}P-labeled c-Ki-ras promoter fragment (10 nM) was incubated in the absence or presence of ODN (5 μM), mithramycin (100 and 10 μM), or both. The abrogation of triplex formation by mithramycin binding prior (pre-, lanes 4 and 5) and after (post-, lanes 6 and 7) the formation of triplex is also demonstrated. Maxam−Gilbert sequencing reactions A+G and C+T are seen in the last two lanes.

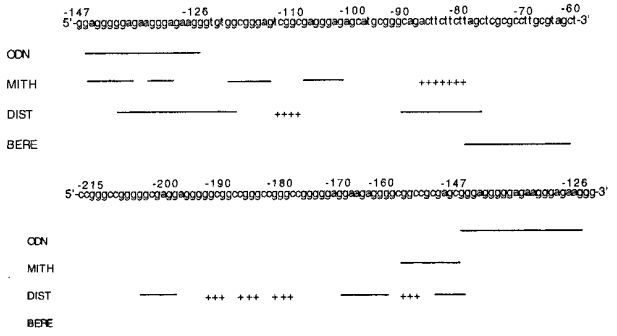

FIGURE 6: DNase I protection map showing the effects of triplex formation, mithramycin, distamycin, and berenil binding to the human c-Ki-ras promoter. Bars indicate regions which are protected from cleavage; + represents the hypersensitive region.

as evidenced by at least three regions (as shown in brackets) of DNase I protection (lane 2) observed only in the presence of mithramycin (Figure 5). In addition, the extent of DNase I cleavage at certain sites (arrows) is strongly enhanced in the presence of mithramycin relative to that in control DNA (Figure 5, lane 2). Alignment of the DNase I digestion patterns with the Maxam−Gilbert sequencing data demonstrates that each of these mithramycin induced protected sites center around G+C-rich regions (Figures 5 and 6). On the other hand, DNase I hypersensitivity sites correspond to the

A+T-rich regions which flank large mithramycin binding sites (Figures 5 and 6). DNase I protection by mithramycin binding is primarily confined to the region between −145 and −90 where −1 represents the 3′ boundary of the major transcription start site of c-Ki-ras (Figures 5 and 6). Specifically, these DNase I protected sites are seen from −115 to −105, −123 to −118, −135 to −128, and −144 to 140 (Figures 5 and 6). Importantly, two of these protected sites are located within the triplex target sequence (Figures 5 and 6).

Furthermore, incubation of mithramycin (100 and 10 μM) with the c-Ki-ras promoter fragment for 30 min prior to the addition of triplex-forming ODN completely abrogates triplex formation as evidenced by the absence of an ODN-induced pattern of DNase I protection in Figure 5, lanes 4 and 5, and the preservation of all mithramycin-induced DNase I protected sites in these lanes. The pattern of protection in the presence of both ODN and mithramycin is identical to that obtained with mithramycin alone indicating that ODN binding is inhibited as a direct result of mithramycin binding to its target sequences (Figure 5). A similar inhibition of triplex formation was noted when the ODN and mithramycin were incubated with the promoter fragment simultaneously (data not shown). Moreover, the addition of mithramycin to preformed triplex (overnight incubation) still gives rise to a mithramycin-induced pattern with the disappearance of ODN-induced protection (Figure 5, lanes 6 and 7). The DNase I digestion pattern of these reactions, shown in lanes 6 and 7, reveals only the mithramycin-induced modifications, but not the ODN-dependent protection site (Figure 5). Perhaps the strongest footprinting evidence that mithramycin does displace the third strand comes from the strong band in the center of the triplex target site which is not affected by mithramycin (Figure 5, lane 2) but is abolished by the ODN (lane 3). When mithramycin and the ODN are present together, this band is still present resembling the binding of mithramycin alone (lanes 4 and 6).

Mithramycin binding to the c-Ki-ras triplex forming sequence and the inhibition of triplex formation by its binding was also confirmed by electrophroetic gel mobility shift assay. As shown in Figure 3, the binding of mithramycin (100 μM) to the radiolabeled 22 bp target DS DNA fragment (10 nM) resulted in retardation of this fragment's gel mobility (lane 4). Importantly, the gel mobility retardation of this fragment induced by mithramycin binding is slightly greater than that of triplex formation (Figure 3, lanes 4 and 5). Figure 3, lane 6, shows that the gel shift seen when the radiolabeled DS target DNA fragment is incubated with mithramycin followed by triplex formation is identical to the gel shift seen with mithramycin binding alone. Similar results were obtained when mithramycin was added to the target DNA simultaneously with the ODN or after overnight triplex formation (Figure 3, lanes 7 and 8). Since the migration of triplex DNA is only slightly greater than the mithramycin-bound DS c-Ki-ras target DNA, it is difficult to determine whether the gel retardation of the target DS DNA was caused by mithramycin binding alone or by both mithramycin and ODN binding. This problem was solved by forming triplex with radiolabeled ODN to shift the cold DS DNA as a way of demonstrating triplex formation. Figure 4 shows that the addition of mithramycin prevents triplex formation by the labeled ODN whether it was added prior to the ODN binding (lane 4), or simultaneously (lane 5), or to the pre-formed triplex DNA (lane 6). Importantly, no interaction between mithramycin and labeled ODN alone was noted (Figure 4, lane 2).

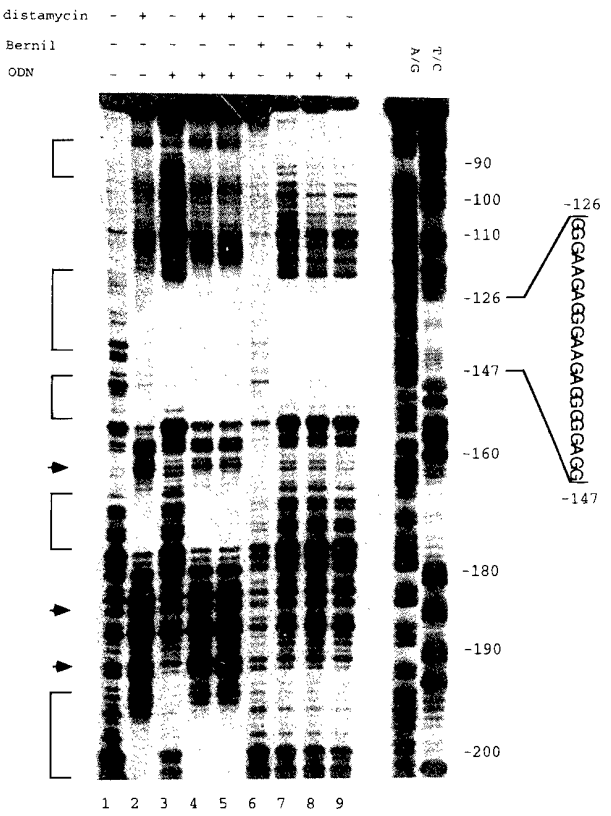

FIGURE 7: DNase I protection assay demonstrating the binding of distamycin (100 μM; lane 2), berenil (100 μM; lane 6), and triplex-forming ODN (5 μM; lane 3) to the c-Ki-ras promoter. A 181 bp ^{32}P-labeled c-Ki-ras promoter fragment was incubated with either distamycin or berenil before (lanes 4 and 8) and after (lanes 5 and 9) the formation of triplex. Maxam−Gilbert sequencing reactions A+G and C+T are seen in the last two lanes.

The concentration dependence of mithramycin inhibition on triplex formation was also tested. c-Ki-ras target DNA (10 nM) was pre-treated with 100, 10, and 1 μM concentration of mithramycin, and triplex formation was tested by DNAse I footprint and gel retardation assays (data not shown). These experiments showed significant inhibition of triplex formation at 100 and 10 μM mithramycin concentrations but not in the presence of 1 μM concentration of mithramycin.

Distamycin and Berenil Binding to Human c-Ki-ras Promoter Region and Their Effects on Intermolecular Triplex Formation. We also characterized the DNase I digestion patterns of the 181 bp human c-Ki-ras promoter fragment in the presence and absence of distamycin and berenil which are shown in Figure 7. The DNase I digestion patterns in the presence of 100 and 10 μM (data not shown) concentrations of either distamycin (lane 2) or berenil (lane 6) were altered when compared to control digest in lane 1 (Figure 7). Distamycin binding to the c-Ki-ras promoter fragment produces at least five regions of DNase I protection distributed within the whole length of this fragment (Figure 7, lane 2). On the other hand, berenil produces relatively small changes in the DNase I digestion pattern of this promoter fragment (Figure 7, lane 6). A single DNase I protection site was attributable to berenil binding to the c-Ki-ras fragment extending from −92 to −65 bp (Figure 7, lane

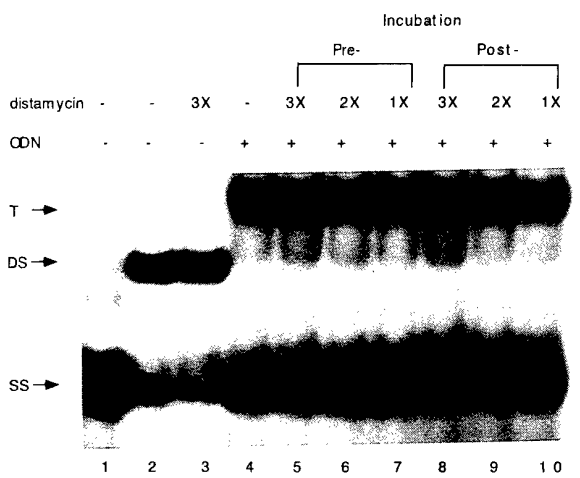

FIGURE 8: Gel mobility shift analysis demonstrating the binding of triplex-forming ODN and distamycin to the triplex target site. The ^{32}P-labeled synthetic target DNA (10 nM) was incubated with in the absence or presence of ODN (1 μM), distamycin (100 μM = 3×; 50 μM = 2×; 10 μM = 1×), or both. SS = single 22bp pyrimidine strand; DS = double-stranded target DNA; T = triplex DNA.

6). This sequence contains two alternating A/T sequences (TTGCGTA, −70 to −64 and TTCTTAGCT, −89 to −82) which are known to be preferred binding sequences for berenil (Portugal & Waring, 1987; Barceló & Portugal, 1993). Berenil does not bind within the triplex target site which does not contain its preferred binding sequence.

Nucleotides which were protected from DNase I cleavage due to distamycin binding included −92 to −79, −139 to −123, −153 to −149, −176 to −165, and −201 to −198 (Figures 6 and 7). Moreover, distamycin also produces changes in the digestion efficiency of the DNA sequences flanking its binding sites. For example, enhanced cleavage is noted in the vicinity of bases −110, −160, −180, and −190 which generally correspond to longer stretches of alternating G/C sequences flanking its binding sites (Figures 6 and 7). Figure 7 demonstrates that preincubation of the c-Ki-ras promoter fragment with either distamycin (lane 4) or berenil (lane 8) prior to the addition of TFO did not prevent triplex formation. The DNase I digestion pattern shown in Figure 7, lane 4, demonstrates that the observed protection sites are the result of both distamycin and ODN binding to their respective target sites. Although berenil does not bind within the triplex target sequence, its binding proximal to the triplex target sequence does not affect the formation of triplex as seen by the presence of both berenil- and ODN-induced footprints simultaneously in Figure 7, lane 8. Addition of either distamycin or berenil to the promoter fragment following triplex formation results in the digestion patterns seen in lane 5 (distamycin) and lane 9 (berenil) (Figure 7). DNase I digestion patterns seen in lane 5 and lane 9 are identical to those seen in lane 4 and 8, respectively, and suggest that these modifications are the result of simultaneous binding of drug molecules (distamycin or berenil) and triplex-forming ODN to their respective binding sites (Figure 7).

Data obtained by gel mobility shifts confirm the DNase I footprinting studies of the effect of berenil and distamycin binding on triplex formation (Figure 8). Figure 8 shows that the presence of distamycin in concentrations of 100, 50, and 10 μM has no effect on triplex formation. Unlike mithramycin, distamycin binding to the duplex target DNA does not retard its mobility in 16% native gel as demonstrated by the identical gel mobility of bands in lane 2 and 3 (Figure 8). This may be due to rapid dissociation of duplex (or triplex) bound distamycin during the electrophoresis, in contrast to mithramycin which is known to dissociate slowly from DNA. Thus gel retardation of the DS DNA can only be due to triplex formation. Again, in agreement with DNase I protection data, the presence of berenil in either 100, 50, or 10 μM concentrations did not alter the binding of ODN to its 22 bp duplex target fragment as evidenced by a complete shift of the labeled duplex probe to a distinct triplex band (data not shown). No changes were noted in the gel mobility of either ODN or duplex target fragment when they were preincubated with 100 μM berenil (data not shown). These findings confirm the observation that berenil does not bind within the triplex-forming target sequence and thus neither prevents the triplex formation nor destabilizes preformed triple-helical DNA in the c-Ki-ras promoter. In Figure 8, lanes 5, 6, and 7, the target DS DNA was preincubated with distamycin for 30 min prior to the addition of ODN. These experiments confirm that distamycin binding to the triplex target sequence does not interfere with triple-helical DNA formation. Similarly, addition of distamycin to preformed triplex DNA (Figure 8 lanes 8, 9, and 10) has no effect on the stability of triplex.

DISCUSSION

Our data demonstrate that mithramycin binds within the triplex target site of the c-Ki-ras promoter and strongly inhibits the formation of triplex DNA. Moreover, binding of mithramycin in the minor groove results in complete displacement of a preformed the major groove-bound triplex ODN. In comparison, AT-specific minor groove binders distamycin and berenil interact with the c-Ki-ras promoter without disrupting the triplex. Furthermore, occupancy of the major groove by a third strand did not prevent the binding of distamycin. In agreement with previous studies, distamycin and berenil demonstrate marked differences with regard to their binding sites within the c-Ki-ras promoter sequence (Portugal & Waring, 1987; Barceló & Portugal, 1993). The c-Ki-ras triplex forming motif provides binding sites for distamycin but not for berenil.

The results presented here confirm a previous report that a 22 bp homopurine:homopyrimidine motif within the human c-Ki-ras promoter forms intermolecular triple helix (Mayfield et al., 1994a). The binding affinity of oligonucleotides which form T·A:T triplets is slightly greater than the affinity of an oligonucleotide which forms A·A:T triplets (Mayfield et al., 1994a), so the ODN used in this study was designed to bind antiparallel to the purine-rich strand of the duplex forming G·G:C and T·A:T triplets. The triplex formed at physiological pH in the presence of 10 mM Mg^{2+} at 37 °C, and the effect of drug binding was characterized both before and after the formation of triplex. The resulting data provide a detailed comparison of the effects of GC-specific and AT-specific minor groove binding drugs on a gene-specific, intermolecular purine·purine:pyrimidine triplex structure. These findings may aid in important practical understanding of how these DNA binding drugs affect intramolecular triplex DNA (H-DNA) structures *in vivo*.

The minor groove in G+C-rich regions of double-stranded DNA is wider and shallower than in A+T-rich regions and

contains the amino group of guanine which makes it less favorable for groove binding ligands. Thus, most of non-intercalating groove binders prefer the more narrow and deep minor groove of the A+T-rich region. The exception is mithramycin, which interacts specifically with the 2-amino group of the guanine in GC-rich areas of DS DNA (Cons & Fox, 1989; Carpenter et al., 1993). It is evident from previous studies that incubation in the presence of 10 mM Mg^{2+} for 30 min is adequate to attain >95% saturation of mithramycin binding to the target sites in the DNA (Sarker & Chen, 1989). Under these experimental conditions, mithramycin binds to at least four well defined sites within the c-Ki-ras promoter region which lie between −60 to −215 relative to the major transcription initiation site. As expected, all of these binding sites cluster around regions of high GC content (Figure 6). Close examination of each of these regions reveals that mithramycin binding requires a minimum of two contiguous GG or GC dinucleotides with a binding site of 3 bp (Figure 6), which is in agreement with previous studies (Van Dyke & Dervan, 1983; Con & Fox, 1989). It is also apparent from the DNase I protection pattern that mithramycin does not bind to all GC-rich regions of the c-Ki-ras promoter fragment (Figure 6). This may be due to the fact that mithramycin's ability to recognize a particular sequence is influenced by the structural environment in which the sequence is located (Carpenter et al., 1993). The presence of adjacent GC base pairs is not mandatory for mithramycin binding since it is able to bind as a dimer with any of the following sequences: TCCC, GGGG, CCGC, GGCA, and CCCT (Carpenter et al., 1993). In fact, most of the mithramycin binding regions in the c-Ki-ras promoter are restricted to the long stretches of $A(G)_n{\cdot}(C)_nT$ sequences (Figure 6). Consequently, mithramycin binding to the c-Ki-ras promoter encompasses most of the triplex target site and sequences downstream of this site (Figure 6).

The DNA adjacent to mithramycin binding sites is distorted and exhibits sequence-dependent variations in the helical twist and rise parameters (Sastry & Patel, 1993). Furthermore, mithramycin-induced alterations involving local DNA structure render the adjacent $(AT)_n$ and $A_n{\cdot}T_n$ regions hypersensitive to DNase I (Cons & Fox, 1991; Carpenter et al., 1993; Fox & Cons, 1993). This is reflected by the enhanced DNase I cleavage of an AT-rich cluster, at −80 to −90 of the c-Ki-ras promoter fragment (Figure 6). These findings lend credence to the argument that mithramycin binding within and near the triplex-forming region of the c-Ki-ras promoter distorts the local DNA structure, making it more A-DNA-like without unwinding or lengthening the DNA helix as reported in previous studies (Fox & Cons, 1993). Thus, mithramycin's inhibitory effect on triple-helical assembly is very likely attributable to conformational changes of duplex target DNA and not to other structural changes. Although it was initially suggested that the triplex DNA has an A-form conformation (Arnott & Selsing, 1974), recent reports dispute this concept and indicate that the underlying DS DNA remains B-form with a sugar pucker near C2′-endogeometry (Howard et al., 1992). Our data agree with this finding, since mithramycin-induced structural changes in the triplex-forming region (B-form to A-form) do not enhance the triplex formation but inhibit its formation. Similar inhibitory effects of mithramycin on pyrimidine·purine:pyrimidine triplex formation have been reported recently (Stonehouse & Fox, 1994). In contrast to mithramycin, most AT-specific minor groove binders have no influence on DNA conformation and no consequential inhibitory effects on triplex formation. The DNA binding ability of mithramycin is not affected by spermine or spermidine bound in the major groove (Sarker & Chen, 1989). Our study demonstrates that mithramycin binds its target in pre-formed triplex DNA. Indeed, the major groove bound ODN is displaced from its target site by mithramycin.

Previous studies have shown that mithramycin inhibits the transcription of genes with GC-rich regulatory sequences, such as the c-myc, dhfr, and collagen 1 genes. The drug prevents binding of the transcription factor Sp1 (Snyder et al., 1991; Blume et al., 1991; Nehls et al., 1993), which forms protein−DNA complexes in the major groove of the DNA. Although Sp1 binding sites in c-Ki-ras regulatory regions are not well characterized, the triplex-forming site of this gene also binds one or more nuclear proteins (Mayfield et al., 1994a). Our evidence that mithramycin binding sites in c-Ki-ras promoter overlap triplex-forming and protein-binding sequences suggests that the triplex site represents an essential element for transcriptional initiation. Although mithramycin blocks Sp1 binding to the major groove by altering local DNA structure, it does not displace previously bound Sp1 (Snyder et al., 1991). In contrast mithramycin binding results in complete displacement of a triplex-forming ODN from the major groove.

We found that recognition sequences of distamycin and berenil within the c-Ki-ras promoter are distinctly different which is in agreement with a previous study comparing their binding sites in the double stranded tyrT DNA fragment (Portugal & Waring, 1987). Two binding sites for distamycin are found in the triplex forming region of the c-Ki-ras promoter, with additional sites present in upstream and downstream sequences. On the basis of this footprint analysis, distamycin appears to bind to longer sequences, including several lying outside the presumed A+T-rich primary binding sites (Figure 6). This finding is in agreement with a previous study which reported that distamycin can bind to sequences containing clusters of G/C interruptions, particularly when they are present at the ends of the binding sequences (Portugal & Waring, 1987). It appears that distamycin binds to poly-dA:poly-dT sequences with isolated G:C interruptions. It has been suggested that the absence of a cationic terminus on distamycin allows this molecule to unravel from the bottom of the minor groove, in compensation for the intrusion of a guanine's 2-amino group (Kopka et al., 1985). This may further explain the ability of distamycin to bind to the minor groove of the triplex region without any destabilizing effect. Our results agree with NMR data which suggest that the interaction of distamycin did not change the chemical shift of a triplex composed of $d(T)_6{\cdot}d(T)_6{:}d(A)_6$, except for some broadening effect in the imino protons of the triplex structure (Umemoto et al., 1990). Netropsin and Hoechst 33258 dye, which are AT-specific minor groove binding drugs similar to distamycin, have been shown to interact with short sequences of $d(T)_n{\cdot}d(T)_n{:}d(A)_n$ triple helix without displacing the major-groove-bound third strand (Park & Breslauer, 1992; Durland et al., 1994). However, distamycin binding to the DS DNA target reduces the affinity of ODN to this site. Furthermore, it has been shown that distamycin binds within the minor groove of the DS DNA only in the B-form and not in the A-form (Zimmer & Wahnert, 1986). Distamycin binding

to the minor groove of the triplex DNA in the c-Ki-ras promoter supports the view that this triplex structure has a B-form conformation.

There is only one berenil binding sequence downstream of the triplex forming region of the c-Ki-ras promoter. Unlike distamycin, berenil preferentially binds to alternating AT sequences (TpA or ApT steps) which do not contain G:C interruptions (Barceló & Portugal, 1993). Berenil produces relatively small changes in DNA structure in regions distal from the binding site. This explains why berenil has no effect on c-Ki-ras triplex DNA. It is noteworthy that berenil can induce the formation of unusual triple helical structures [DNA (pyrimidine)·RNA (purine)·DNA (pyrimidine); RNA (purine)·RNA (purine)·DNA (pyrimidine)] that otherwise would not form (Pilch & Breslauer, 1994).

The affinity and specificity of various DNA binding drugs with DS DNA and pyr·pur:pyr triplex DNA have been studied extensively in recent years. Ethidium, an intercalator, binds more strongly to the T·A:T triplets than to duplex A:T, whereas it destabilizes triplex DNA containing predominantly C^+·G:C sequences (Scaria & Shafer, 1991). A derivative of benzo[e]pyridoindole consisting of four planar rings binds preferentially with and stabilizes the pyrimidine·purine: pyrimidine triplex DNA that contains both T·A:T and C^+·G:C triplets (Mergny et al., 1992). Another DNA intercalating drug, coralyne, has also been reported to show higher affinity for triple helix composed of T·A:T and C^+·G:C over DS DNA (Lee et al., 1993).

The influence of minor groove binders on triplex formation by the naturally occurring c-Ki-ras triplex forming motif may have important implications for the proposed transcriptional regulatory role of intramolecular triplex DNA formation by this promoter (Hoffman et al., 1990; Pestov et al., 1991; Raghu et al., 1994). As yet, intramolecular triplex formation in the human c-Ki-ras regulatory regions has not been demonstrated, although sequence motifs involved in H-DNA formation by the murine Ki-ras promoter are conserved in the human c-Ki-ras gene. The highly conserved human and murine Ki-ras genes share 82% nucleotide homology (McGrath et al., 1983). The 22 bp homopurine.homopyrimidine triplex motif in the human c-Ki-ras promoter consists of 10 bp overlapping repeats of CCCTCTTCCC (or 7 bp tandem repeats of CCCTTCT) and another 10 bp mirror repeat of CCTTCTCCCC immediately upstream of this motif (Jordano & Perucho, 1986; Yamamoto & Perucho, 1988; Mayfield et al., 1994a). In a similar location (−290 to −318 from exon 0/intron 1), the murine Ki-ras promoter contains a 27 bp homopurine·homopyrimidine mirror repeat which shows strong S1 hypersensitivity and forms an intramolecular triplex DNA (H-DNA) in a supercoiled plasmid (Hoffman et al., 1990; Pestov et al., 1991). Moreover, this motif demonstrates considerable sequence homology with the human sequence, forms intermolecular triplex DNA, and competes for binding of a HeLa nuclear factor with the purine: pyrimidine motif in the human promoter (Mayfield et al., 1994a). A recent study has shown that this motif is responsible for approximately half of the murine Ki-ras promoter activity (Hoffman et al., 1990; Raghu et al., 1994). In addition, it was noted that H-DNA forming ability of this motif as well as its sequence integrity are essential for the promoter activity (Raghu et al., 1994). There is a similar polypurine·polypyrimidine region in the c-myc promoter which has been proposed to form an intramolecular triple helix which is transcriptionally important (Firulli et al. 1994). Interestingly, a common protein called NSEP-1 binds to the H-motifs of both c-Ki-ras and c-myc genes (Kolluri et al., 1992). This suggests that interaction of this protein with promoter DNA may be regulated by intramolecular triplex DNA formation.

DNA binding drugs, including mithramycin, inhibit the binding of the transcription factors to their target sequences by either overlapping their binding sites or inducing conformational changes in their binding regions. If the effects of mithramycin on intermolecular triplex can be extended to intramolecular triplex, it suggests another possible mechanism for inhibition of transcriptional initiation by mithramycin of genes containing G+C-rich regulatory regions. It is possible that interference of mithramycin with intramolecular triplex assembly may block the interactions of proteins which would bind to the intramolecular-triplex structure in a transcriptionally active locus. However, our initial results require further investigation on the effect of mithramycin on supercoil dependent intramolecular triplex formation in order to substantiate this novel mechanism of transcriptional inhibition.

REFERENCES

Agazie, Y. M., Lee, J. S., & Burkholder, G. D. (1994) *J. Biol. Chem. 269*, 7019−7023.

Arnott, S., & Selsing, E. (1974) *J. Mol. Biol. 88*, 509−521.

Barbacid, M. (1987) *Annu. Rev. Biochem. 56*, 779−827.

Barceló, F., & Portugal, J. (1993) *Biophys. Chem. 47*, 251−260.

Beal, P. A., & Dervan, P. B. (1991) *Science 251*, 1360−1363.

Behr, W., & Hartmann, G. (1965) *Biochem. Z. 343*, 519−527.

Birnboim, H. C., Sederoff, R. R., & Patterson, M. C. (1979) *Eur. J. Biochem. 98*, 301−307.

Blume, S. W., Snyder, R. C., Ray, R., Thomas, S., Koller, C. A., & Miller, D. M. (1991) *J. Clin. Invest. 88*, 1613−1621.

Carpenter, M. L., Marks, J. N., & Fox, K. R. (1993) *Eur. J. Biochem. 215*, 561−566.

Chalikian, T. V., Plum, G. E., Sarvazyan, A. P., & Breslauer, K. J. (1994) *Biochemistry 33*, 8629−8640.

Cons, B. M. G., & Fox, K. R. (1989) *Nucleic Acids Res. 17*, 5447−5459.

Cons, B. M. G., & Fox, K. R. (1991) *Biochemistry 30*, 6314−6321.

Durand, M., Thuong, N. T., & Maurizot, J. C. (1994) *Biochimie 76*, 181−186.

Ebbinghaus, S. W., Gee, J. E., Rodu, B., Mayfeld, C. A., Sanders, G., & Miller, D. M. (1993) *J. Clin. Invest. 92*, 2433−2439

Firulli, A. B., Maibenco, D. C., & Kinniburgh, A. J. (1994) *Arch. Biochem. Biophys. 310*, 236−276.

Fox, K. R., & Cons, B. M. G. (1993) *Biochemistry 32*, 7162−7171.

Gee, J. E., Blume, S., Snyder, R. C., Ray, R., & Miller, D. M. (1992) *J. Biol. Chem. 267*, 11163−11167.

Goyette, M., Petropoulos, C. J., Shank, P. S., & Fausto, N. (1984) *Mol. Cell. Biol. 4*, 1493−1498.

Hoffman, E. K., Trusko, S. P., Freeman, N. A., & George, D. L. (1987) *Mol. Cell. Biol. 7*, 2592−2596.

Hoffman, E. K., Trusko, S. P., Murphy, M., & George, D. L. (1990) *Proc. Natl. Acad. Sci. U.S.A. 87*, 2705−2709.

Howard, F. B., Miles, H. T., Liu, K., Frazier, J., Raghunathan, G., & Sasisekharan, V. (1992) *Biochemistry 31*, 10671−10677.

Jordano, J., & Perucho, M. (1986) *Nucleic Acids Res. 14*, 7361−7378.

Kolluri, R., Torrey, T. A., & Kinniburgh, A. J. (1992) *Nucleic Acids Res. 20*, 111−116.

Kopka, M. L., Yoon, C., Goodsell, D., Pjura, P., & Dickerson, R. E. (1985) *Proc. Natl. Acad. Sci. U.S.A. 82*, 1376−1380.

Lee, J. S., Latimer, L. J. P., & Hampel, K. J. (1993) *Biochemistry 32*, 5591−5597.

Maxam, A. M., & Gilbert, W. (1980) *Methods Enzymol. 65*, 499–500.
Mayfield, C., Squibb, M., & Miller, D. (1994a) *Biochemistry 33*, 3358–3363.
Mayfield, C., Ebbinghaus, S., Gee, J., Jones, D., Rodu, B., Squibb, M., & Miller, D. (1994b) *J. Biol. Chem. 269*, 18232–18238.
McGrath, J. P., Capon, D. J., Smith, D. H., Chen, E. Y., Seeburg, P. H., Goeddel, D. V., & Levinson, A. D. (1983) *Nature 304*, 501–506.
Mergny, J. L., Duval-Valentin, G., Nguyen, C. H., Perrouault, L., Faucon, B., Rougée, M., Montenay-Garesteier, T. M., Bisagani, E., & Helene, C. (1992) *Science 256*, 1681–1684.
Mirkin, S. M., & Frank-Kamenetskii, M. D. (1994) *Annu. Rev. Biophys. Biomol. Struct. 23*, 541–576.
Moser, H. E., & Dervan, P. B. (1987) *Science 238*, 645–650.
Muller, R., Slamon, D. J., Adamson, E. D., Tremblay, J. M., Muller, D., Clina, M. J., & Verma, I. M. (1983) *Mol. Cell. Biol. 3*, 1062–1069.
Nehls, M. C., Brenner, D. A., Gruss, H.-G., Dierbach, H., Mertelsmann, R., & Hermann, F. (1993) *J. Clin. Invest. 92*, 2916–2921.
Orsen, F. M., Thomas, D. W., McShan, W. M., Kessler, D. J., & Hogan, M. E. (1991) *Nucleic Acids Res. 19*, 3435–3441.
Park, Y. W., & Breslauer, K. J. (1992) *Proc. Natl. Acad. Sci. U.S.A. 89*, 6653–6657.
Pestov, D. G., Dayan, A., Siyanova, E. Y., George, D. L., & Mirkin, S. M. (1991) *Nucleic Acids Res. 19*, 6527–6532.
Pilch, D. S., & Breslauer, K. J. (1994) *Proc. Natl. Acad. Sci. U.S.A. 91*, 9332–9336.
Portugal, J., & Waring, M. J. (1987) *Eur. J. Biochem. 167*, 281–289.
Postel, E. H., Flint, S. J., Kessler, D. J., & Hogan, M. E. (1991) *Proc. Natl. Acad. Sci. U.S.A. 88*, 8227–8231.
Raghu, G., Tevosian, S., Shrikant, A., Subramanian, K. N., George, D. L., & Mirkin, S. M. (1994) *Nucleic Acids Res. 22*, 3271–3279.
Sarker, M., & Chen, F. M. (1989) *Biochemistry 28*, 6651–6657.
Sastry, M., & Patel, D. J. (1993) *Biochemistry 32*, 6588–6604.
Scaria, P. V., & Shafer, R. H. (1991) *J. Biol. Chem. 266*, 5417–5423.
Snyder, R. C., Ray, R., Blume, S., & Miller, D. M. (1991) *Biochemistry 30*, 4290–4297.
Stonehouse, T. J., & Fox, K. R. (1994) *Biochim. Biophys. Acta. 1218*, 322–330.
Thomas, T., & Thomas, T. J. (1993) *Biochemistry 32*, 14068–14074.
Umemoto, K., Sarma, M. H., Gupta, G., Luo, J., & Sarma, R. (1990) *J. Am. Chem. Soc. 112*, 4539–4545.
Van Dyke, M. W., & Dervan, P. B. (1983) *Biochemistry 30*, 4290–4297.
Wells, R. D., Collier, D. A., Hanvey, J. C., Shimizu, M., & Wohlrab, F. (1988) *FASEB J. 2*, 2939–2949.
Yamamoto, F., & Perucho, M. (1988) *Oncogene Res. 3*, 125–138.
Zimmer, Ch., & Wähnert, U. (1986) *Prog. Biophys. Mol. Biol. 41*, 31–112.

BI951562B

Reprinted from Biochemistry, 1995, *34*.

Inhibition of *in Vitro* Transcription by a Triplex-Forming Oligonucleotide Targeted to Human c-*myc* P2 Promoter†

Hyung-Gyoon Kim‡ and Donald M. Miller*,‡,§

Department of Biochemistry and Molecular Genetics and Bolden Laboratory, Department of Medicine, University of Alabama at Birmingham, Birmingham, Alabama 35294-0001

Received November 21, 1994; Revised Manuscript Received April 18, 1995⊗

ABSTRACT: Triplex-forming oligonucleotides (TFOs) have been shown to bind in a sequence-specific manner to polypurine/polypyrimidine sequences in several human gene promoters, including the c-*myc* P1 promoter. TFOs have been shown to inhibit transcription *in vitro* and the expression of target genes in cell culture. The human c-*myc* protooncogene contains a 23 base pair purine−pyrimidine-rich motif (−62 to −40) within its predominant promoter, P2, that is a potential target for purine−purine−pyrimidine triplex formation. Using electrophoretic mobility shift analysis (EMSA) and competition experiments, we have demonstrated that a MAZ (myc-associated zinc finger protein) consensus sequence is capable of competing with the purine−pyrimidine motif for the binding of a HeLa nuclear protein. We have shown the formation of an intermolecular triplex using a 23-base purine-rich oligonucleotide antiparallel to the purine-rich target sequence. DNase I footprinting was performed to confirm the exact location of triplex formation. Triplex formation by this oligonucleotide prevents binding of a HeLa nuclear protein (presumably MAZ) to the target site. We have also shown that the P2-targeted TFO is a potent and specific inhibitor of c-*myc* transcription *in vitro*. These data demonstrate that this novel TFO inhibits transcription of the c-*myc* P2 promoter. We propose that the P2-targeted TFO has its effect by blocking the binding of the regulatory factor MAZ.

The c-*myc* protooncogene is the normal cellular homolog of v-*myc*, the viral transforming oncogene from avian myelocytomatosis virus strain MC29 (Colby et al., 1983). It encodes a nuclear phosphoprotein (Persson et al., 1984) whose expression is associated with rapid cellular proliferation in both malignant and nonmalignant cells (Sugiyama et al., 1989). The induced overexpression of c-*myc* appears to be necessary for the rapid proliferation of these cells, while the decreased expression of c-*myc* correlates with a decrease in cellular proliferation. The c-*myc* gene is activated in a wide variety of neoplasms as a consequence of proviral insertion, amplification, and chromosomal translocation (Cole, 1986; Bishop, 1983). Each of these mechanisms increases the expression of normal c-*myc* protein. The c-*myc* gene consists of three exons. The first exon is largely untranslated and contains two promoters with two distinct transcriptional start sites, designated P1 and P2, which are separated by approximately 165 bp[1] (Battey et al., 1983). A third promoter designated P0 is found 550−650 bp upstream of P1 and accounts for only 0−5% of c-*myc* transcription, while P1 generates 10−25% and P2 gives rise to 75−90% c-*myc* mRNA (Bentley et al., 1986).

Cis-acting elements residing in the c-*myc* first exon and intron have been shown to regulate P2 transcription initiation. Two of these regulatory elements, ME1a1 and ME1a2, are positioned between P1 and P2. These sequences are major sites for nuclear factor binding and are highly conserved between the human and mouse c-*myc* genes. Deletion of the ME1a1 binding site results in loss of P2 transcriptional activity (Asselin et al., 1989). In addition, Hall et al. (1990) have shown that ME1a1 is required for transcription initiation from P2 in an *in vitro* transcription system. Recently, a human gene encoding a zinc finger protein that binds ME1a1 was named MAZ (myc-associated zinc finger protein). In addition, a sequence element (GGCGGGAAAA) located between ME1a1 and ME1a2 is conserved between mouse and human and binds the E2F transcription factor (Thalmeier et al., 1989; Hiebert et al., 1989). Since these two sites are essential for transcription of c-*myc* from P2, the inhibition of protein binding by triplex formation presents a method to attenuate c-*myc* transcription.

Purine- and pyrimidine-rich oligonucleotides targeted to purine−pyrimidine-rich sequences form pur*pur·pyr and pyr*pur·pyr intermolecular triple helices (Moser & Dervan, 1987; Fedorova et al., 1988; Lyamichev et al., 1988; Praseuth et al., 1988; Hanvey et al., 1989; Maher et al., 1989) and inhibit binding of protein to target DNA (Hanvey et al., 1989; Maher et al., 1989; Grigoriev et al., 1992; Gee et al., 1992; Mayfield et al., 1994; Ebbinghaus et al., 1993). The oligonucleotide third strand occupies the major groove of the duplex, forming Hoogsteen hydrogen bonds with the purine bases of the duplex (Moser & Dervan,1987; Beal & Dervan, 1991) Both pur*pur·pyr and mixed pur/pyr*pur·pyr triplexes can be formed at physiological pH with predominantly G*G·C triplets along with A*A·T and T*A·T triplets

† This work was supported by NIH Grants RO1 CA42664 and RO1 CA54380, Department of Army Grant DAMD 17-93-J-3018, a Veterans Administration Merit Review Grant, and Share Foundation Grants (to D.M.M.).

* To whom correspondence and reprint requests should be addressed [phone (205) 934-1977, Fax (205) 975-6911].

‡ Department of Biochemistry and Molecular Genetics.

§ Bolden Laboratory, Department of Medicine.

⊗ Abstract published in *Advance ACS Abstracts,* June 1, 1995.

[1] Abbreviations: bp, base pair; TFOs, triplex-forming oligonucleotides; EMSA, electrophoretic mobility shift analysis; MAZ, myc-associated zinc finger protein; PNK, polynucleotide kinase.

0006-2960/95/0434-8165$09.00/0

interspersed (Beal & Dervan, 1991; Postel et al., 1991; Durland et al., 1991). Purine-rich and mixed purine–pyrimidine third strands bind to their target sequences in an antiparallel orientation with respect to the purine-rich strand of duplex target (Beal & Dervan, 1991; Durland et al., 1991).

It has been previously shown that a discrete 27-base oligonucleotide forms a stable triplex within the P1 promoter of the human c-*myc* gene, −116 to −142 base pairs upstream from P1 transcription start site (Cooney et al., 1988). This region contains binding sites for several cellular factors, at least one of which is required for *in vitro* initiation of mRNA synthesis from the c-*myc* promoter (Boles & Hogan, 1987; Postel et al., 1989; Davis et al., 1989). Consistent with those findings, it was found that oligonucleotide binding to the −116 to −142 bp upstream from the P1 start site is capable of inhibiting c-*myc* transcription *in vitro* (Cooney et al., 1988).

We have designed a purine-rich oligonucleotide targeted to the region of the c-*myc* P2 promoter containing the MAZ and E2F binding sites, both of which are important for P2 activity. We have determined the ability of this oligonucleotide to form a sequence-specific interstrand triplex. We also examine the ability of triplex-forming oligonucleotide to block the binding of nuclear protein to the target sequence. Finally, we examined the effect of triplex formation on *in vitro* transcription of the c-*myc* promoter.

MATERIALS AND METHODS

Oligonucleotide Synthesis. Phosphodiester oligonucleotides were synthesized on a Milligen Cyclone Plus DNA synthesizer using standard phosphoramidite chemistry. All oligonucleotides were purified by OPEC (Clontech). The structural integrity and purity were verified by 5′-^{32}P-labeling using [γ-^{32}P]ATP and T4 polynucleotide kinase (PNK) followed by electrophoresis on a polyacrylamide gel. Yields were determined from absorbance measurements at 260 nm using molar extinction coefficients.

Electrophoretic Mobility Shift Analysis (EMSA) of Triplex Formation. For triplex formation, the synthetic pyrimidine-rich strand of the 23-base c-*myc* target was 5′-labeled with [γ-^{32}P]ATP and T4 PNK and annealed to its oligonucleotide complement. The potential triplex-forming oligonuclotide was heated at 65 °C for 10 min to reduce self-aggregation of the G-rich oligonucleotides and then quick-chilled on ice. After the oligonucleotides were incubated with the labeled 23-bp target in a buffer consisting of 90 mM Tris, 90 mM borate (pH 7.4), and 10 mM $MgCl_2$ for 1 h at 37 °C, products were analyzed on a 16% nondenaturing polyacrylamide gel in the same buffer at room temperature (duration of the gel, 3 h), at 150 V.

Promoter Fragment Isolation. pSV2Neo-*myc* containing 12.5 kb of the human c-*myc* gene was digested with *Pvu*II and separated on 1% low melting point agarose gel. The 864-bp fragment containing the human P1 and P2 promoter was purified and ligated into the *Sma*I site of pGL-2 (Promega). The resulting plasmid pMyc-Luc was then digested with *Xho*I and labeled with [α-^{32}P]dATP using the Klenow fragment of DNA polymerase I. The fragment was then digested with *Mlu*I and run on 5% preparative native polyacrylamide gel. The resulting 465-bp promoter fragments were cut out, and the gel slice was passed through a 3-mL syringe to crush it. DNA was eluted in 0.5 M NH_4-OAc, pH 5.2, for overnight at 37 °C with shaking, filtered to remove polyacrylamide, and precipitated with ethanol.

DNase I Footprinting. After being heated at 65 °C for 10 min and then quick-chilled on ice, the oligonucleotides were incubated with the ^{32}P-labeled promoter fragment in 10 mM Tris (pH 7.4) and 10 mM $MgCl_2$ for 1 h at 37 °C. Samples were precooled on ice and 1 μg of poly(dI-dC) was added. DNase I digestion was then performed for 1 min on ice with 0.0001 unit of DNase I, and the reactions were stopped by adding 10 mM EDTA in 90% formamide. Samples were extracted once with phenol–chloroform and twice with chloroform and ethanol precipitated. After precipitation, samples were heated at 95 °C for 5 min, quick-chilled on ice, and analyzed by electrophoresis on a 8 M urea–8% polyacrylamide sequencing gel at 42 W. Bands were visualized by autoradiography, and protected sequences were identified from gels containing both Maxam–Gilbert sequence and DNase I footprints.

Protein Binding Assay. Oligonucleotides were added to the labeled duplex target and incubated in a protein binding buffer consisting of 25 mM Hepes, 12.5 mM $MgCl_2$, 70 mM KCl, 1 μM $ZnSO_4$, 1 mM DTT, 0.1% NP-40, and 10% glycerol (v/v) for 1 h at 37 °C. The samples were cooled on ice; then HeLa nuclear extract and 1 μg of poly(dI-dC) were added and allowed to bind for 30 min on ice. Samples were analyzed by electrophoresis on 5% native polyacrylamide gels at 150 V in 90 mM Tris–borate (pH 8.5) and 2 mM EDTA followed by autoradiography.

In Vitro Transcription. In vitro transcription was performed using a HeLa nuclear extract *in vitro* transcription system (Promega). The template DNA used was generated from *Hin*dIII digestion of the plasmid pMyc-Luc which contains the 864-bp c-*myc* promoter. The concentration of *Hin*dIII-digested DNA was quantitated by UV spectrophotometry. The optimization of transcription reaction was performed with varying concentration of Mg^{2+} and templates. It was found that 3 mM $MgCl_2$ and 1 μg of linearized template gave the most *in vitro* transcription products (data not shown). The template DNA (1 μg) was incubated with varying concentrations of either the TFO or a purine-rich control oligonucleotide in a buffer identical to the one used for triplex gel shift for 12 h at 37 °C. As a control, the cytomegalovirus early promoter (100 ng) yielding a 363-base transcript was treated identically to the c-*myc* promoter template. After incubation with TFO, reactions were cooled to room temperature, and transcription was initiated by the addition of HeLa nuclear extract (79.9 μg of protein, 8 standardized transcription units) to a final volume of 25 μL, containing final concentration of 3 mM $MgCl_2$, 17.6 mM Tris (pH 7.4), 15.6 mM KCl, 31.2 μM EDTA, 78 μM dithiothreitol, 8.8% glycerol, 0.4 mM ATP, 0.4 mM CTP, 0.4 mM UTP, 16 μM GTP, and 0.4 mCi/mL [α-^{32}P]GTP (3000 Ci/mmol). Transcription was allowed to proceed for 1 h at 30 °C then terminated by the addition of a stop solution containing 0.3 M Tris-HCl (pH 7.4), 0.3 M NaOAc, 0.5% SDS, 2 mM EDTA, and 3 μg/mL yeast tRNA. Run-off transcripts were extracted with phenol–chloroform–isoamyl alcohol (25:24:1) and ethanol precipitated. RNA pellets were resuspended in equal volumes of nuclease-free H_2O and loading solution containing 98% formamide, 10 mM EDTA, 0.1% xylene cyanol, and 0.1% bromophenol blue. The run-off transcription products were analyzed by electrophoresis on an 8% polyacrylamide sequencing gel containing 8 M

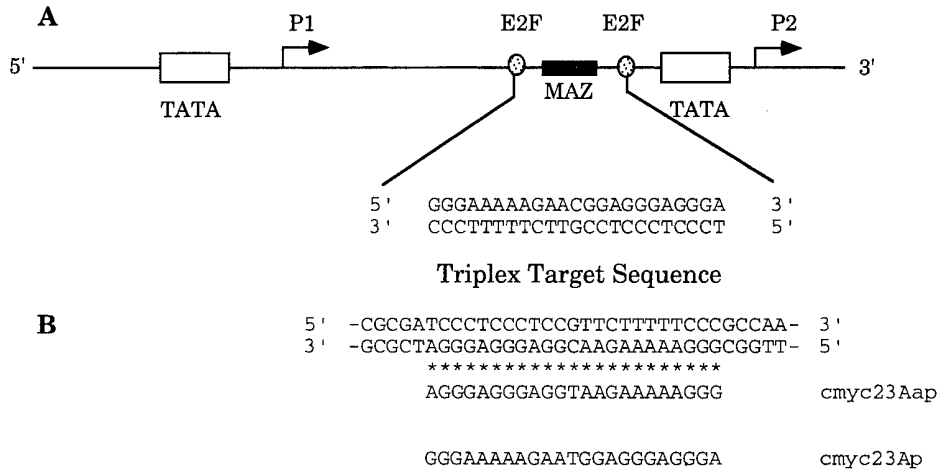

FIGURE 1: (A) Map of the human c-*myc* gene showing two major promoters, P1 and P2, the 23-bp purine−pyrimidine-rich motif, and the triplex target sequence relative to the transcription start site P2 (−62 to −42). Transcription factor, MAZ and E2F, binding sites are also indicated. (B) Oligonucleotide sequences and their alignment with the duplex target. The p and ap nomenclature indicates parallel or antiparallel orientation of the oligonucleotide relative to the purine-rich target strand, respectively.

urea at 42 W for 4 h followed by autoradiography of the gel at −80 °C.

RESULTS

Oligonucleotide Design. The human c-*myc* P2 promoter contains a 23-bp purine−pyrimidine-rich sequence located at −62 to −40 from the P2 transcription start site (Figure 1A). This region is a binding site for MAZ (*myc*-associated zinc finger protein) and E2F, both of which are essential for P2 transcription. The sequence in this region is not strictly homopurine−homopyrimidine but contains only a single C·G interruption. A potential triplex-forming oligonucleotide targeted to the human c-myc P2 purpyr motif was designed in parallel and antiparallel orientation with respect to the purine-rich strand, containing guanine to recognize GC (G*GC triplets) and adenine to recognize AT (A*AT triplets) (Figure 1B). The parallel oligonucleotide was used as a control oligonucleotide that would not form triplex with target sequence.

Triplex Formation by the c-myc P2 Promoter. Triplex formation was demonstrated by EMSA and DNase I footprinting. Triplex DNA, because of its decreased charge density, migrates more slowly than duplex DNA in gel mobility shift assay. As shown in Figure 2, the addition of increasing concentrations of the antiparallel oligonucleotide cmyc23Aap relative to target results in a gradual shift from duplex (D) to a distinct migrating band (T), indicating the formation of triplex DNA (Cooney et al., 1988; Durland et al., 1990, 1991). Some dissociation of the triplex may occur during the course of electrophoresis as indicated by the smear between duplex and triplex bands (Orson et al., 1991; McShan et al., 1992). The concentration-dependent shift of the c-*myc* target duplex to triplex begins at 1 μM oligonucleotide, corresponding to a 100-fold molar excess oligonucleotide to duplex. At 100 μM (10 000-fold excess) most of the duplex is shifted to triplex (Figure 2, lane 6). With the parallel oligonucleotide cmyc23Ap, there is no evidence of triplex formation, even at 100 μM, indicating that the parallel oligonucleotide does not form triplex under these conditions (Figure 2, lane 7).

The data from DNase I footprinting experiments are consistent with those obtained from gel mobility shifts and

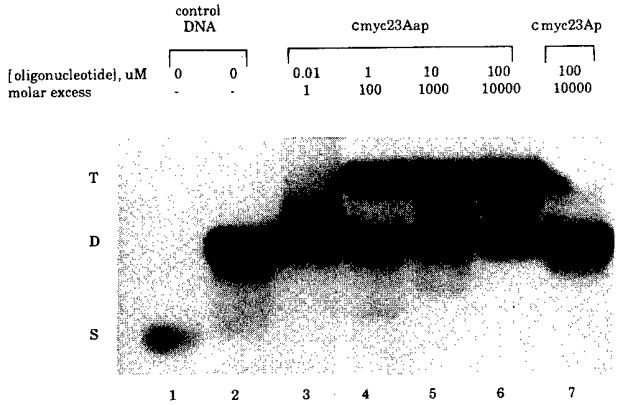

FIGURE 2: EMSA of oligonucleotide-directed triplex formation in the c-*myc* P2 promoter target. The pyrimidine-rich strand of the 23-mer target was labeled (lane 1) and annealed with the unlabeled purine-rich strand (lane 2). The 23-bp duplex target was then incubated with increasing concentrations of triplex-forming oligonucleotide π (lanes 3−6) or control oligonucleotide (lane 7). The concentration of triplex-forming oligonucleotide or control oligonucleotide added to the 10 nM ^{32}P-labeled 23-bp duplex and their molar ratio to the target duplex DNA are indicated above each lane. Abbreviations: S = single-strand DNA; D = duplex DNA; T = triplex DNA.

confirm that triplex formation occurs in a sequence-specific manner when the oligonucleotide third strand is oriented antiparallel relative to the purine-rich strand of target duplex. Protection of the target sequence by the triplex-forming oligonucleotide is concentration-dependent, in a manner consistent with the gel mobility shift analysis. Figure 3 shows that, at an oligonucleotide concentration of 30 μM (3000-fold molar excess with respect to the 465-bp promoter fragment), the antiparallel cmyc23Aap shows complete protection (lane 6) from DNase I digestion. The footprint obtained corresponds to protection of the 23 base pair target sequence (defined by the brackets). These data demonstrate that, within the −62 to −40 region of c-*myc* P2 promoter, cmyc23Aap binds in a sequence-specific manner to its target site. On the other hand, the parallel oligonucleotide cmyc23Ap, at a concentration of 30 μM, shows little protection from digestion by DNase I (lane 7). This may be due to less DNase I digestion or the amount of labeled fragments is less than those of other lanes. These data further

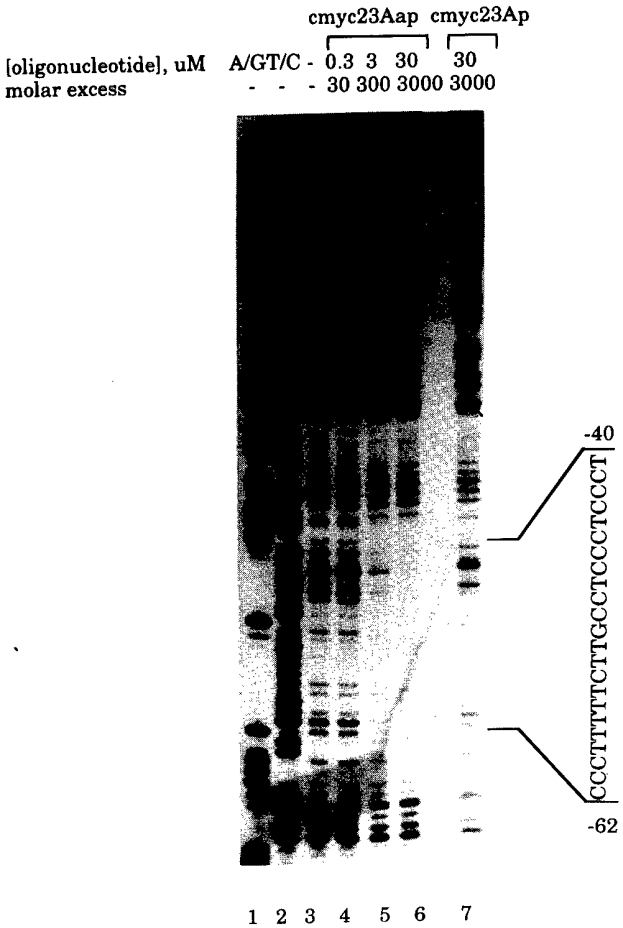

FIGURE 3: DNase I footprinting analysis demonstrating sequence-specific binding of triplex-forming oligonucleotide to the c-*myc* P2 promoter target. Lanes 1 and 2 show Maxam–Gilbert sequencing reactions performed with the same labeled promoter fragments. Lane 3 is the control DNase I digest with no oligonucleotide added. Oligonucleotides were incubated at the concentration indicated above each lane with 100 nM 465-bp ^{32}P-Klenow-labeled promoter fragment followed by limited DNase I digestion. The c-*myc* target sequence indicated by brackets was determined from Maxam–Gilbert sequencing.

suggest that, under these conditions, triplex formation occurs exclusively with the third strand oriented antiparallel to the purine-rich strand of the c-*myc* P2 promoter target.

Effect of Triplex Formation on Nuclear Protein Binding. The effect of triplex formation within the c-*myc* P2 promoter on HeLa nuclear protein binding to the 23-bp promoter target was demonstrated by electrophoretic mobility shift analysis (Figure 4). Lane 2 of Figure 4 shows that the labeled 23-bp duplex target is bound to nuclear proteins as evidenced by retardation of the target upon incubation with HeLa nuclear extract. Incubation of the 23-bp c-*myc* P2 target region with HeLa nuclear extract results in the formation of several shifted bands representing different protein–DNA complexes. Incubation of the target with cmyc23Aap at 10 μM (4000-fold molar excess) followed by incubation with HeLa nuclear extract results in complete abrogation of the lowest retarded band (lane 6), demonstrating that the TFO inhibits nuclear protein binding to the target sequence. The control oligonucleotide cmyc23Ap of identical sequence, but opposite orientation to the target, appears to have little if any effect on protein binding at 10 μM (4000-fold excess) (lane 7).

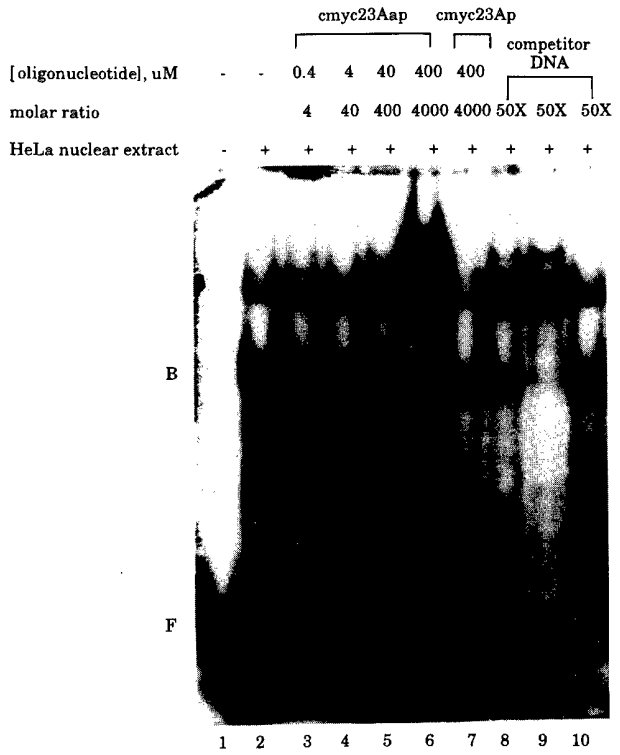

FIGURE 4: EMSA demonstrating sequence-specific nuclear protein binding to the human c-*myc* duplex target and its inhibition by triplex-forming oligonucleotide. ^{32}P-Labeled 23-bp human c-*myc* fragment was incubated with competitor duplex or oligonucleotides as described, and then HeLa nuclear extract was added. Nonspecific competitor, MAZ consensus, and E2F consensus DNA were added to lanes 8–10, respectively. Nonspecific competitor sequence: 5′-AAAGATCCTCTCTCGCTAATCTC-3′. MAZ consensus sequence: 5′-GGGGGAGGGGG-3′. E2F consensus sequence: 5′-ATTTAAGTTTCGCGCCCTTTCTCAA-3′. Abbreviations: B = protein–DNA complex; F = unbound DNA probe.

The sequence specificity of this protein–DNA interaction was examined by competition binding assay. As shown in Figure 4, a 50-fold excess of unlabeled MAZ consensus sequence (Ashfield et al., 1994) effectively competes with the labeled sequence for the binding of protein that disappeared in the presence of triplex-forming oligonucleotide (lane 9), while the same excess of an unlabeled 23-bp nonspecific DNA or E2F consensus sequence (Helin et al., 1992) has no effect on protein binding to the target (lanes 8 and 10). Therefore, this protein–DNA complex is presumably derived from MAZ. These data demonstrate that the nuclear factor binding to this c-*myc* P2 promoter region involves a sequence-specific interaction. Because a low percentage gel (5%) was used to analyze protein binding, the migration of the triplex was indistinguishable from that of duplex and was not detectable in Figure 4. However, when 16% TBM gel was used, it was possible to demonstrate triplex formation by cmyc23Aap but not by cmyc23Ap (Figure 5). These data suggest that significant inhibition of protein binding to the c-*myc* P2 target is a direct result of triplex formation.

Effect of Triplex Formation on c-myc Transcription. The effect of triplex formation on c-*myc* P2 transcription was examined in an *in vitro* "run-off" transcription assay using a HeLa nuclear extract transcription system (Promega). In this assay, the human c-*myc* promoter is incubated with HeLa nuclear extract in the presence of nucleotide triphosphates;

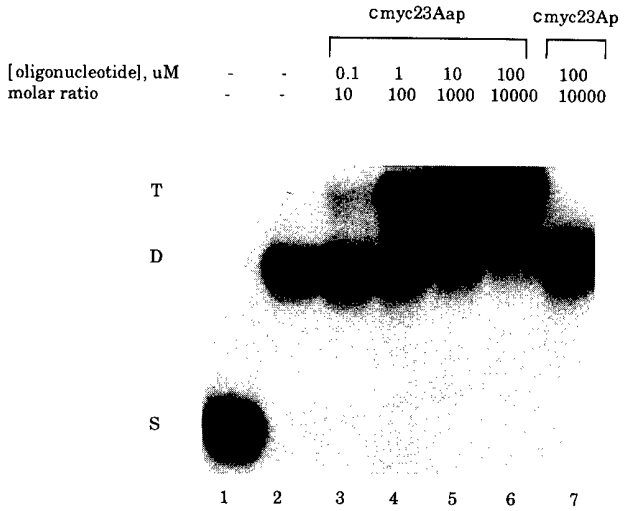

FIGURE 5: Gel mobility shift analysis showing triplex formation with the 23-bp c-*myc* promoter under protein binding conditions. The 23-bp target was incubated with oligonucleotide at the concentrations indicated under the protein binding conditions described in Materials and Methods.

transcripts are labeled by the incorporation of [α-^{32}P]GTP and correspond in size to the length of template DNA. The *Hin*dIII digest of the plasmid, pMyc-Luc containing 864 bp of the c-*myc* promoter, linearized the plasmid with 412 bp downstream of the transcription start site. After incubation of the promoter with the triplex-forming cmyc23Aap at 20 μM (1000-fold molar excess with respect to template), significant inhibition of transcription was observed, while the non-triplex-forming cmyc23Ap had little or no effect at the same concentration (Figure 6A). There are some longer bands seen in the gel. These may be due to nonspecific initiation of transcription from the upstream vector sequence in plasmids.

The effect of the c-*myc* P2-targeted triplex-forming oligonucleotide on the transcription process from a promoter unrelated to that of c-*myc* was examined by incubation of oligonucleotide with template DNA containing the cytomegalovirus immediately early promoter followed by *in vitro* transcription. Run-off transcription from the cytomegalovirus promoter yields a 363-nucleotide RNA transcript. As shown in Figure 6B, at the same concentration which inhibits c-*myc* transcription, triplex-forming oligonucleotide, cmyc23Aap has little effect on transcription from the cytomegalovirus promoter under the same conditions. These results suggest that inhibition of c-*myc* transcription by cmyc23Aap is due to sequence-specific triplex formation by the c-*myc* promoter.

DISCUSSION

Several reports have demonstrated that triplex-forming oligonucleotides targeted to positive regulatory factor binding sites inhibit transcription in cells. McShan et al. have demonstrated that a TFO targeted to the Sp1 binding sites in the human immunodeficiency virus long-terminal repeat inhibits viral transcription in infected cells. Grigoriev et al. have shown that a triplex-forming oligonucleotide targeted to the NF_kB site in the interleukin-2 receptor α regulatory sequence inhibits NF_kB-dependent transcription.

The human c-*myc* protooncogene P2 promoter is the predominant promoter for c-*myc* transcription. A detailed

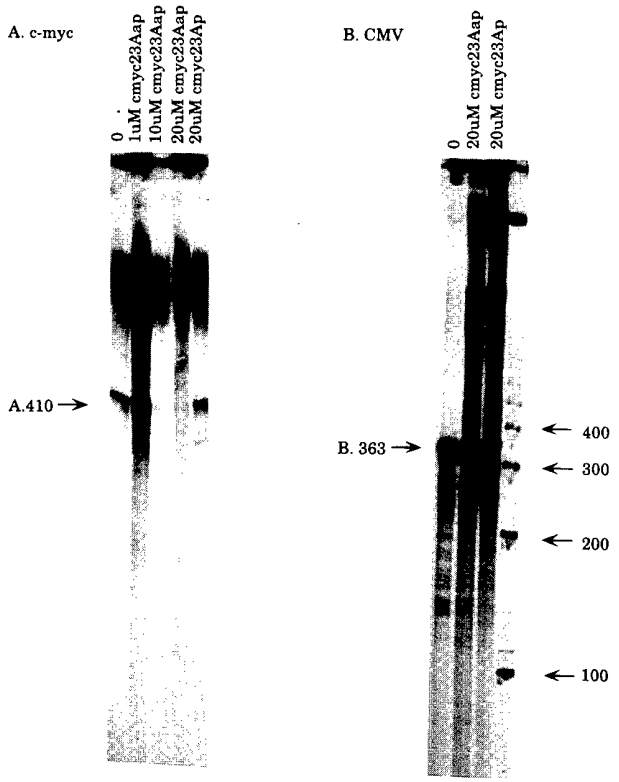

FIGURE 6: *In vitro* transcription assay demonstrating specific inhibition of c-*myc* transcription: (A) *in vitro* transcription from a plasmid containing the c-*myc* promoter region; (B) *in vitro* transcription from a purified CMV early promoter region. Oligonucleotides were added to the template DNA as described at concentrations indicated above each lane. *In vitro* transcription of the plasmid containing c-*myc* promoter yields a 412-base RNA transcript indicated by arrow A. The transcription is inhibited by triplex-forming oligonucleotide whereas the purine-rich control oligonucleotide has no effect on *in vitro* transcription. *In vitro* transcription using CMV promoter template yields a single 363-base transcript indicated by arrow B. Neither the c-*myc* TFO nor the control oligonucleotide has any effect on transcription from the CMV promoter. The 100-bp ladder was end-labeled with T4 PNK and used as the molecular weight marker.

analysis of the c-*myc* promoter regulatory elements have revealed multiple protein-binding sites within the P2 promoter of c-*myc*. Proteins binding to this region were designated MBP-1 (c-*myc* promoter binding protein) (Ray & Miller, 1991), MAZ (Bossene et al., 1992), and E2F (Thalmeier et al., 1989). Deletion studies have shown that MAZ is required for maximal P2 transcription. Deletion of the MAZ binding site increases P1 promoter usage (Asselin et al., 1989). The nuclear factor E2F is also involved in the transcriptional regulation of c-*myc*. This protein binds to two sequence elements within the P2 promoter in a region that is critical for promoter activity. Hiebert et al. (1989) have demonstrated in transient transfection assays that expression of adenovirus E1A gene products induces the transcription of c-*myc* gene and this E1A-dependent transactivation of the c-*myc* is mediated through E2F.

In an effort to provide sequence-specific DNA binding agents which may inhibit c-*myc* transcription, we have designed a triplex-forming oligonucleotide targeted to this region of c-*myc* P2 promoter. The target sequence for triplex formation in this region is not strictly homopurine−homopyrimidine but contains only a single C·G interruption. Previously it was shown by Beal and Dervan that G*GC, A*AT,

and T*AT triplets stabilize a triple helix to a greater extent than the other 13 natural triplets. They have also compared the relative cleaving ability of 15-mer oligonucleotides differing in sequence at a single position and are equipped with thymine−EDTA at each 3′ end so that binding could be monitored by the affinity cleaving method. Their results indicated that while oligonucleotides containing adenosine, cytosine, and guanine opposite a single C·G base pair did not provide cleavage, thymidine-substituted oligonucleotide gave weak but better cleavage than other oligonucleotides. On the basis of these facts, a potential triplex-forming oligonucleotide targeted to the human c-myc P2 pur·pyr motif was designed in parallel and antiparallel orientation with respect to the purine-rich strand, containing guanine to recognize GC (G*GC triplets), adenine to recognize AT (A*AT triplets), and thymine to recognize CG (T*CG triplets) (Figure 1B). The parallel oligonucleotide was used as a control oligonucleotide that would not form triplex with the target sequence. The oligonucleotide cmyc23Aap, which is oriented antiparallel to the purine-rich duplex, was shown to bind in a sequence-specific manner to the target site. A control oligonucleotide, cmyc23Ap, containing a sequence identical to cmyc23Aap but in a parallel orientation, does not form triplex. These results are consistent with those from studies by Beal and Dervan (1991) and Durland et al. (1991), which show that the third strand of the pur/pyr*pur·pyr triplex binds in an antiparallel orientation with respect to the purine-rich strand of the duplex target.

Giovannangeli et al. (1992) have also demonstrated that oligonucleotide containing three bases (thymine, cytosine, and guanine) is capable of binding to the target in a parallel orientation with respect to the homopurine sequence of a homopurine−homopyrimidine target of human immunodeficiency virus (HIV) proviral DNA.

We have shown that triplex formation in the c-*myc* P2 promoter inhibits the binding of a HeLa nuclear protein, presumably MAZ, and blocks *in vitro* transcription of the c-*myc* gene. The ability of triplex-forming oligonucleotides to compete with site-specific DNA binding proteins for binding to target sites was shown by Maher et al. (1989). They showed that the binding of *Ava*I, *Taq*I, and the transcription factor Sp1 to artificial recognition sites was inhibited by triplex formation. Gee et al. (1992) and Mayfield et al. (1993) have also shown that TFOs targeted to the Sp1 binding sites of human dihyrofolate reductase (DHFR) and Ha-Ras prevent Sp1 binding. It has also been demonstrated that TFOs targeted to the Ki-Ras and Her-2/Neu inhibit the binding of a protein in HeLa nuclear extract (Mayfield et al., 1994; Ebbinghaus et al., 1993). Postel et al. (1989) have fractionated HeLa cell nuclear extracts into components which support the transcription of c-*myc in vitro* and partially purified a HeLa cell transcription factor that is required for accurate c-*myc* transcription from the P2 promoter. This factor, named PuF (purine factor), binds to the −142 to −115 region upstream from the P1 start site by making contact with a GGGTGGG sequence motif. This group has also shown that a TFO targeted to the PuF binding site in the P1 promoter forms a triplex in HeLa cells and inhibits *in vivo* P1 transcription. Inhibition of P1 is approximately 10-fold greater than the inhibition of P2 under the same conditions (Postel et al., 1991). As mentioned above, P2 is the major promoter of c-*myc* expression and generates more than 75% of c-*myc* mRNA. Therefore, a TFO targeted to P1 promoter is unlikely to block c-*myc* expression completely. It has been shown by Maher et al. (1992) that triple-helical complexes assembled on the promoter inhibit *in vitro* transcription primarily by blocking assembly of the initiation complexes rather than occluding the positive regulatory factor. It is likely that cmyc23Aap, which interacts with a region close to the P2 TATA box, exerts its effect on formation of transcription initiation complex either by direct occlusion or by altering DNA flexibility. Therefore, it is plausible that inhibition of c-*myc* transcription by cmyc23Aap may result from direct blocking of MAZ and/or blocking the assembly of the preinitiation complex.

The identification and characterization of genes that are involved in human disease have provided important targets for modulation of gene expression. Because of their specificity to selectively inhibit transcription of their target genes in intact cells, triplex-forming oligonucleotides could be potential therapeutic agents. We have identified an oligonucleotide targeted to the human c-*myc* P2 promoter and demonstrated that the TFO binds to its target in a sequence-specific manner and inhibits nuclear protein binding and *in vitro* transcription. This is the first example of multiple distinct triplex-forming regions in the promoter of a single gene. The data presented in this report suggest the potential future application of this oligonucleotide on the specific modulation of c-*myc* expression *in vivo*.

ACKNOWLEDGMENT

The authors thank Charles Mayfield, Jimmy Reddoch, George Sanders, Scot Ebbinghaus, Nadarajah Vigneswaran, and Brian Hughes for their comments and advice in preparing the manuscript and John Caterina and David Donze for their technical assistance.

REFERENCES

Ashfield, R., Patel, A. J., Bossone, S. A., Brown, H., Campbell, R. D., Marcu, K. B., & Proudfoot, J. N. (1994) *EMBO J. 13*, 5656−5667.

Asselin, C., Nepveu, A., & Marcu, K. B. (1989) *Oncogene 4*, 549−558.

Battey, J., Moulding, C., Taub, R., Murphy, W., Stewart, T., Potter, H., Lenoir, G., & Leder, P. (1983) *Cell 34*, 779−787.

Beal, P. A., & Dervan, P. B. (1991) *Science 251*, 1360−1366.

Bentley, D. L., & Groudine, M. (1986) *Nature 321*, 702−706.

Bishop, J. M. (1987) *Science 235*, 305−311.

Boles, T. C., & Hogan, M. E. (1987) *Biochemistry 26*, 367−376.

Bossone, S. A., Asselin, C., Patel, A. J., & Marcu, K. B. (1992) *Proc. Natl. Acad. Sci. U.S.A. 89*, 7452−7456.

Colby, W. W., Chen, E. Y., Smith, D. H., & Levinson, A. D. (1983) *Nature 301*, 722−725.

Cole, M. D. (1986) *Ann. Rev. Genet. 20*, 361−384.

Cooney, M., Czernuszewicz, G., Postel, E. H., Flint, S. J., & Hogan, M. E. (1988) *Science 241*, 456−459.

Davis, T. L., Firulli, A. B., & Kinniburgh, A. J. (1989) *Proc. Natl. Acad. Sci. U.S.A. 86*, 9682−9686.

Durland, R. H., Kessler, D. J., Gunnell, S., Duvic, M., Pettitt, B. M., & Hogan, M. E. (1991) *Biochemistry 30*, 9246−9255.

Ebbinghaus, S. W., Gee, J. E., Rodu, B., Mayfield, C. A., Sanders, G., & Miller, D. M. (1993) *J. Clin. Invest. 92*, 2433−2439.

Fedorova, O. S., Knorre, D. G., Podust, L. M., & Zarytova, V. F. (1988) *FEBS Lett. 228*, 273−276.

Gee, J. E., Blume, S., Snyder, R. C., Ray, R., & Miller, D. M. (1992) *J. Biol. Chem. 267*, 11163−11167.

Giovannangeli, C., Rougee, M., Garestier T., Thuong, N. T., & Helene, C. (1992) *Proc. Natl. Acad. Sci. U.S.A. 89*, 8631−8635.

Grigoriev, M., Praseuth, D., Robin, P., Hemar, A., Saison-Behmoaras, T., Dautry-Varsat, A., Thuong, N. T., Helene, C., & Harel-Bellan, A. (1992) *J. Biol. Chem. 267*, 3389−3395.

Hall, D. J. (1990) *Oncogene 5*, 47−54.

Hanvey, J. C., Schimizu, M., & Wells, R. D. (1989) *Nucleic Acids Res. 18*, 157−161.

Helin, K., Lees, J. A., Vidal, M., Dyson, N., Harlow, E., & Fattaey, A. (1992) *Cell 70*, 337−350.

Hiebert, S. W., Lipp, M., & Nevins, J. R. (1989) *Proc. Natl. Acad. Sci. U.S.A. 86*, 3594−3598.

Lyamichev, V. I., Mirkin, S. M., Frank-Kamenetskii, M. D., & Cantor, C. R. (1988) *Nucleic Acids Res. 16*, 2165−2178.

Maher, L., III, Wold, B., & Dervan, P. B. (1989) *Science 245*, 725−730.

Maher, L., III, Dervan, P. B., & Wold, B. (1992) *Biochemistry 31*, 70−81.

Mayfield, C., Squibb, M., & Miller, D. (1994) *Biochemistry 33*, 3358−3363.

McShan, W. M., Rossen, R. D., Laughter, A. H., Trial, J., Kessler, D. J., Zendegui, J. G., Hogan, M. E., & Orson, F. M. (1992) *J. Biol. Chem. 267*, 5712−5721.

Moser, H. E., & Dervan, P. B. (1987) *Science 238*, 645−650.

Orson, F. M., Thomas, D. W., McShan, W. M., Kessler, D. J., & Hogan, M. E. (1991) *Nucleic Acids Res. 19*, 3435−3441.

Persson, H., & Leder, P. (1984) *Science 225*, 718−721.

Postel, E. H., Mango, S. E., & Flint, S. J. (1989) *Mol. Cell. Biol. 9*, 5123−5133.

Postel, E. H., Flint, S. J., Kessler, D. J., & Hogan, M. E. (1991) *Proc. Natl. Acad. Sci. U.S.A. 88*, 8227−8231.

Praseuth, D., Perrouault, L., Le Doan, T., Chassignol, M., Thuong, N., & Helene, C. (1988) *Proc. Natl. Acad. Sci. U.S.A. 85*, 1349−1353.

Ray, R., & Miller, D. M. (1991) *Mol. Cell. Biol. 11*, 2154−2161.

Sugiyama, A., Kume, A., Nemoto, K., Lee, S. Y., Asami, Y., Nemoto, F., Nishimura, S., & Kuchino, Y. (1989) *Proc. Natl. Acad. Sci. U.S.A. 86*, 9144−9148.

Thalmeier, K., Synovzik, H., Mertz, R., Winnacker, E. L., & Lipp, M. (1989) *Genes Dev. 3*, 527−536.

BI942685J

Oncogene (1995) 10, 2323-2330

Expression of β-galactosidase under the control of the human c-*myc* promoter in transgenic mice is inhibited by mithramycin

David E Jones Jr[1,3], Dong-Ming Cui[3] and Donald M Miller[1,2,3]

The [1]Department of Medicine, the [2]Department of Biochemistry and Molecular Genetics and the [3]Bolden Laboratory, the University of Alabama at Birmingham and the Birmingham Veterans Affairs Medical Center, Birmingham, Alabama, USA

In order to assess the functional contribution of the human c-*myc* promoter region in the expression of the c-*myc* gene, transgenic mouse lines containing a bacterial lac Z gene encoding β-galactosidase under the control of the human c-*myc* protooncogene promoter were generated. Transgenic mouse embryos heterozygous for the human c-*myc* Z transgene demonstrate high amounts of β-galactosidase activity as early as day 11 of embryogenesis by histochemical staining of whole embryos using 5-bromo-4-chloro-3-indolyl-β-D-galactopyranoside (X-Gal) as substrate, localizing specifically to early spinal cord tissue. β-galactosidase activity can be demonstrated by histochemical staining in brain tissue of day 14 embryos, localizing mainly to the prefrontal cortex region, while relative amounts of β-galactosidase in spinal cord tissue are reduced. Determination of specific activity of β-galactosidase using resorufin-β-galactopyranoside as substrate in homogenates of whole embryos heterozygous for the human c-*myc*/lac Z transgene demonstrates significantly elevated β-galactosidase activity over control embryos in day 11 and day 14 embryos. Surprisingly, cell homogenates of brain tissue from adult G_1 generation mice heterozygous for the human c-*myc*/lac Z transgene demonstrate greater than 10-fold higher specific activity of β-galactosidase over normal control brain tissue. Specific inhibition of the c-*myc*/lac Z transgene was also demonstrated in developing embryos using mithramycin given at a dose of 150 $\mu g\ kg^{-1}\ d^{-1}$ intraperitoneal to pregnant females on days 7-13 of gestation. Both histochemical staining of β-galactosidase and specific activity assays of day 14 embryos demonstrated significantly lower levels of β-galactosidase than untreated controls. These results are unique since we are able to detect expression of β-galactosidase in developing embryonic central nervous system tissue along with adult brain tissue of animals carrying the human c-*myc* Z transgene and we are able to specifically inhibit expression of the transgene using mithramycin administered *in utero*.

Keywords: c-*myc*; transcription; transgenic; mithramycin

Introduction

The c-*myc* protooncogene has been implicated in a number of different cellular functions including transcription control, oncogenesis, cell cycle entry, differentiation, apoptosis and DNA replication (for reviews see Cole, 1986; Marcu *et al.*, 1992). Despite the tremendous amount of work in this area, the precise target(s) of the c-*myc* gene product continues to elude researchers (Luseher and Eisenman, 1990; Marcu *et al.*, 1992). The discovery of *max* (Blackwood and Eisenman, 1991) and *mad* (Ayer *et al.*, 1993), the demonstration of sequence-specific binding of the *myc*/*max* heterodimer (Blackwood and Eisenman, 1991) and the functional antagonism of the *mad*/*max* complex to the *myc* protein (Ayer *et al.*, 1993) may eventually lead to defining specific roles and sites of action of the c-*myc* gene.

Much work has been done describing the transcriptional control of the c-*myc* gene. The human c-*myc* promoter region contain two predominant promoters, P1 and P2, separated by 174 nucleotides (Marcu *et al.*, 1992; DesJardins and Hay, 1993). Transcription initiation occurs primarily from the P2 promoter (Spencer and Groudine, 1991), although under certain physiologic conditions or in certain cell lines and malignancies, a shift in transcription promoter usage to the P1 promoter is seen (Taub *et al.*, 1984; Ruppert *et al.*, 1986; Chang *et al.*, 1991). It has been proposed that differential protein binding to the c-*myc* promoter results in differentiating utilization of the c-*myc* P1 and P2 promoters (Marcu *et al.*, 1992).

Previous work examining the expression of c-*myc* transgenic mice containing the human c-*myc* gene with its P2 promoter alone driven by the 5′ regulatory sequences of the class I H-2K, major histocompatibility promoter demonstrated that expression of the transgene was constitutive and did not change following partial hepatectomy (Morello *et al.*, 1990). More recent work using additional constructs of the c-*myc* gene alone with both P1 and P2 promoters (Lavenu *et al.*, 1994) or using a hybrid H-2K/c-*myc* P2 fusion promoter with various combinations of c-*myc* regulatory regions (Morello *et al.*, 1993) suggests that the *cis* elements regulating c-*myc* expression *ex vivo* are not sufficient for correct transcription and expression *in vivo*; however, these studies used the c-*myc* gene itself as a reporter with its inherent difficulty in quantitating expression accurately. Additionally, both transcriptional and post-transcriptional c-*myc* regulatory regions were included in all constructs, making assessment of discrete functional control elements of the c-*myc* gene very difficult.

Previous work in our laboratory has demonstrated that the human c-*myc* gene can be down-regulated by mithramycin, a drug used for treatment of certain myeloid malignancies and for the treatment of hypercalcemia of malignancy. Treatment of rats with mithramycin following a two-thirds partial hepatectomy prevents the characteristic increase in c-*myc* and

Correspondence: DM Miller
Received 7 October 1994; revised 20 February 1995; accepted 20 February 1995

c-Ha-*ras* transcription and blocks the increase in DNA synthesis characteristic of liver regeneration (Campbell *et al.*, 1994). The ability of mithramycin to block expression of c-*myc* and c-Ha-*ras* genes is thought to be its specific binding to G-C rich DNA promoter sequences (Miller *et al.*, 1987), thus preventing protein binding (Ray *et al.*, 1989; Blume *et al.*, 1991) and transcription initiation (Ray *et al.*, 1990; Snyder *et al.*, 1991).

The current study describes expression of β-galactosidase in transgenic mice under the control of the human c-*myc* promoter region alone. β-galactosidase activity can be demonstrated in developing embryos heterozygous for the c-*myc*/lac Z transgene as early as day 11 of gestation. Staining for β-galactosidase using 5-bromo-4-chloro-3-indolyl-β-D-galactopyranoside (X-Gal) as substrate localizes transgene activity to developing spinal cord tissue. At day 14 of gestation, β-galactosidase activity is seen in both spinal cord tissue and brain tissue, staining predominantly the prefrontal cortex area. Surprisingly, adult transgenic mice heterozygous for the human c-*myc*/lac Z transgene demonstrate elevated β-galactosidase activity in whole cell homogenates of brain tissue. These studies also demonstrate specific inhibition of transgene expression after treatment of pregnant females with intraperitoneal mithramycin by histochemical and by specific activity assay of β-galactosidase of mouse embryos, indicating that the transgene is being driven by the human c-*myc* promoter.

Results

The human c-*myc*/lac Z construct used for analysis of promoter activity in transgenic mice is shown in Figure 1. A 480 bp DNA fragment of the human c-*myc* promoter region generated by PCR was used to drive expression of β-galactosidase. The P1 and P2 transcription start sites synthesize transcripts beginning 252 nt and 78 nt upstream from the ATG start codon of the bacterial lac Z gene, respectively. The construct also contains 228 bp of 5′ non-transcribed sequences upstream from the human c-*myc* P1 promoter. The remainder of the construct contains 3 kb of DNA sequence encoding β-galactosidase, and 2.8 kb of sequence encoding the 3′ end of mouse β-globin exon 2 and the entire coding sequence of exon 3, along with intervening and 3′ non-translated sequences (Figure 1).

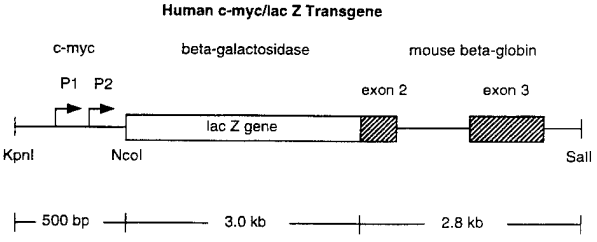

Figure 1 Diagram of the human c-*myc*/lac Z transgene. The human c-*myc* promoter region was generated by polymerase chain reaction (PCR) and cloned into a vector containing the lac Z gene and mouse β-globin exons two and three. A 6.3 kb KpnI/SalI restriction fragment was isolated and used to generate transgenic mouse lines as described in the Materials and methods section. Arrows represent human c-*myc* P1 and P2 transcription start sites; open box, lac Z coding sequences (the ATG start codon is contained within the NcoI site); hatched boxes, mouse β-globin exons two and three

A transgenic mouse line containing only 2–4 copies of the human c-*myc*/lac Z transgene per cell was examined for β-galactosidase activity during development and in adult transgenic mice. Day 10 embryos of this transgenic line did not possess demonstrable β-galactosidase by histochemical staining and day 14 embryos of this transgenic line demonstrated only minimal β-galactosidase activity, localizing mainly to the caudal spinal cord posterior brain and eye regions (data not shown). Because of the lack of easily demonstrable β-galactosidase activity within the central nervous system, this line was not studied further for this manuscript.

A second transgenic mouse line containing approximately 10–20 copies of the human c-*myc*/lac Z transgene per cell (data not shown) demonstrated β-galactosidase activity as early as day 11 of embryogenesis as shown in Figure 2. The intense histochemical staining using X-gal as substrate appears to stain developing spinal cord tissue (Figure 2A). Only one-half of each litter of embryos stained positive for β-galactosidase in agreement with Mendelian inheritance of the transgene (data not shown). A day 11 embryo which does not demonstrate β-galactosidase activity by histochemical staining is shown for comparison (Figure 2B).

β-galactosidase activity in developing embryos appears to follow that of developing neural tissues in the transgenic mouse line. As shown in Figure 3, β-galactosidase activity appears to decrease in intensity in developing spinal cord tissue of day 14 embryos (Figure 3A). However, an relative increase in activity is seen in developing brain tissue by histochemical staining (Figure 3A). The highest amount of activity appears to localize to the prefrontal cortex region (Figure 3A). Again, β-galactosidase activity is seen in only one-half of the embryos in each litter. An embryo which does not possess demonstrable β-galactosidase is shown in Figure 3B for comparison.

Specific activity of β-galactosidase was determined throughout embryogenesis using whole embyro homogenates derived from the mating of a male transgenic mouse heterozygous for the human c-*myc*/lac Z transgene to a normal, non-transgenic female mouse. As shown in Table 1, at least four out of eight day 11 embryos from this mating possess elevated β-galactosidase activity. Day 14 embryos appear to have to highest relative specific activity in mouse embryos which possess the human c-*myc*/lac Z transgene, as would be expected based on the histochemical staining of day 14 embryos for β-galactosidase (Figure 3A). Day 18 embryos possessing the human c-*myc*/lac Z transgene also demonstrate elevated β-galactosidase activity (Table 1), although not as striking as earlier embryos.

Adult mice heterozygous for the human c-*myc*/lac Z transgene were examined for β-galactosidase activity in various tissues as shown in Table 2. Brain tissue from the transgenic mouse line possesses greater than 10-fold higher β-galactosidase specific activity than control, non-transgenic mouse brain tissue in whole cell

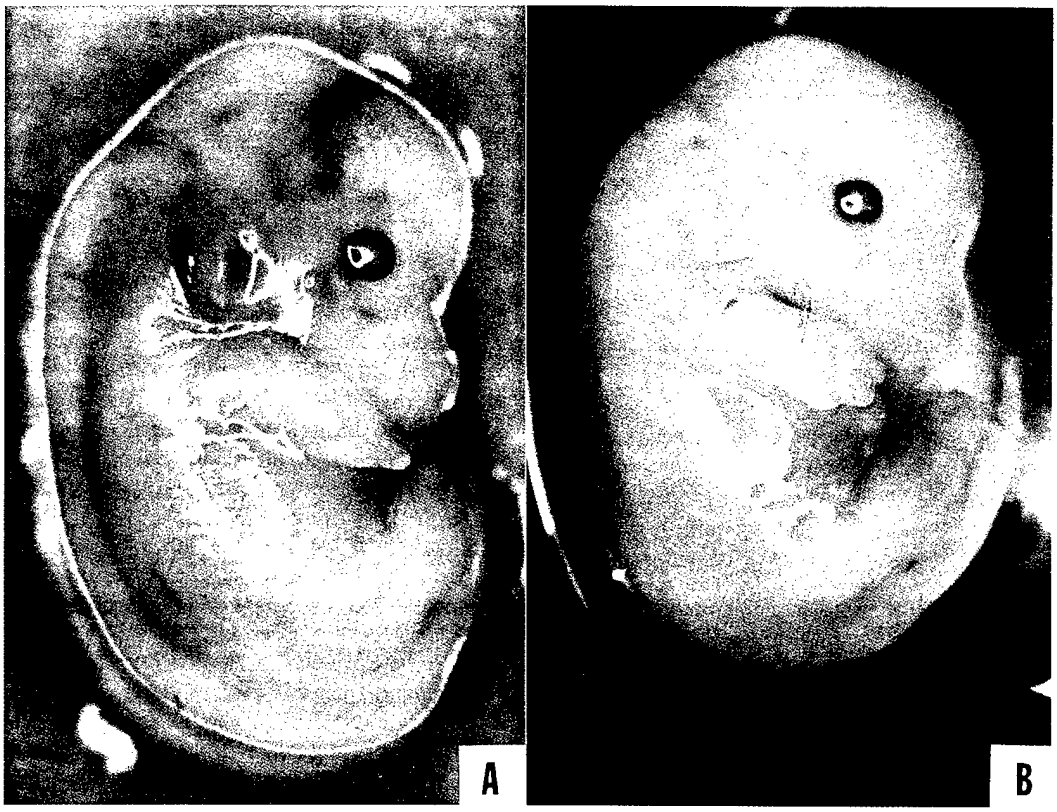

Figure 2 Day 11 embryo of a transgenic mouse line possessing 10–20 copies of the c-*myc*/lac Z transgene. Embryos were stained for β-galactosidase as described in the Materials and methods section. (**A**) day 11 embryo staining positive for β-galactosidase; (**B**) day 11 litter mate staining negative for β-galactosidase activity. Note β-galactosidase activity localizes to developing spinal cord tissue

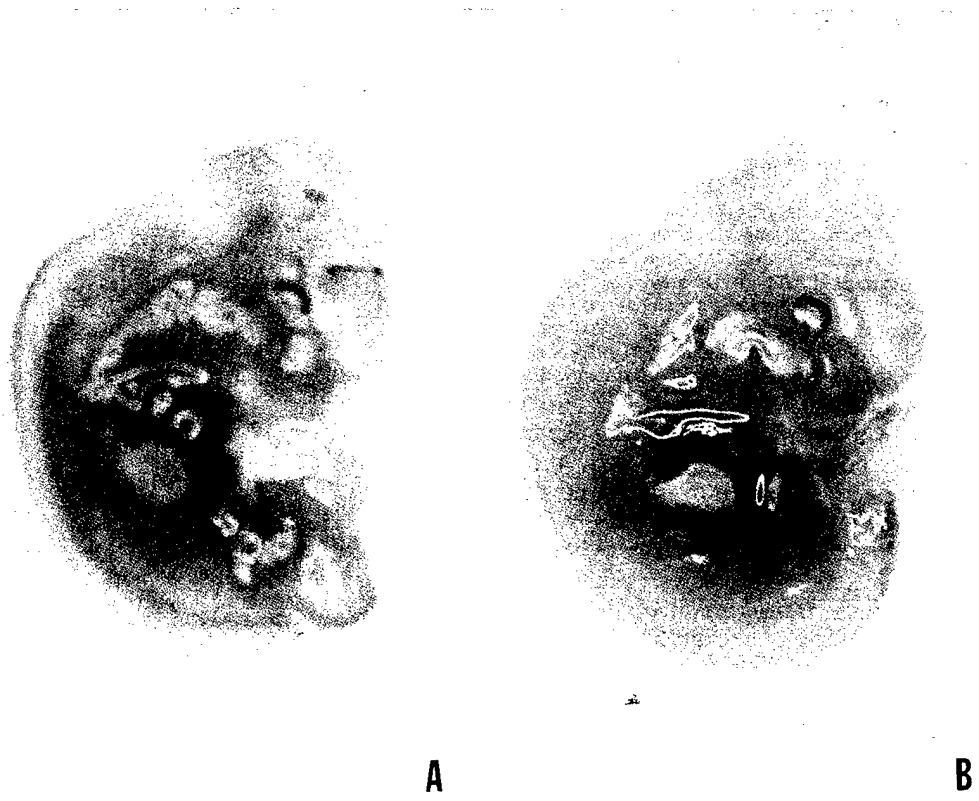

Figure 3 Day 14 embryos of a transgenic mouse line possessing 10–20 copies of the c-*myc*/lac Z transgene. Embryos were stained for β-galactosidase as described in the Materials and methods section. (**A**) Day 14 embryo staining positive for β-galactosidase; (**B**) day 14 litter mate staining negative for β-galactosidase. Note that β-galactosidase activity now appears in the prefrontal cortex region and spinal cord stains less intense than day 11 embryos (**A**)

Table 1 β-galactosidase activity of day 11, day 14 and day 18 embryos of transgenic mice

Animal Number	*Day 11*	*DNA Blot*	*Specific activity*[a] *Day 14*	*DNA*[b] *Blot*	*Day 18*	*DNA Blot*
1	277	N.D.[c]	792	+	110	+
2	168	N.D.	636	+	72	+
3	165	N.D.	364	–	61	+
4	140	N.D.	104	–	59	+
5	92	N.D.	205		47	+
6	39	N.D.	149		39	–
7	29	N.D.	118		21	–
8	13	N.D.	86		21	–
9					20	–
10					17	–
	Control[d] 75.8 (0-336)				*Control* 10.8 (2-21)	
			ositive 474.0		*Average Positive* 69.8	
			Average Negative 139.5		*Average Negative* 23.6	

[a]Specific activity of β-galactosidase [illegible] the change in OD_{572} over 2 h at 37°C using resorufin-β-galactosidase as substrate/protein concentration (g/ml by the micro-Bi[illegible]od). [b]The presence of the human c-*myc* /lacZ transgene was determined by DNA blot analysis in day 14 and day 18 embryos. + : pres[illegible] of the transgene; – : absence of the transgene. [c]N.D. not determined. [d]Control denotes the average β-galactosidase specific activity of day 11, day 14 and day 18 embryos from the mating of normal, non-transgenic mice (ranges are given in parentheses)

Table 2 Tissue distribution of β-galactosidase activity in adult tran[illegible] mice

Tissue	*Specific activity*[a] [illegible]	*Control*
Brain	2359 (1694–3204)	204 (32–195)
Liver	98 (81–117)	30 (16–54)
Kidney	207 (145–296)	125 (57–164)
Intestine	339 (216–414)	282 (143–495)
Lung	14 (0–31)	0
Muscle	58 (48–69)	43 (26–57)

[a]Specific activity of β-galactosidase measured as the change in OD_{572} over 2 h at 37°C using resorufin-β-galactosidase as substrate/protein concentration (g/ml by the micro-Biuret method). Each of these is the average specific activity of three mice. Ranges of specific activity are shown in parentheses. [b]Positive denotes a male transgenic male mice heterozygous for the human c-*myc*/lac Z transgene at 10–20 copies per cell. [c]Control denotes a normal, non-transgenic male mice used as a control for background β-galactosidase activity in normal mouse tissues

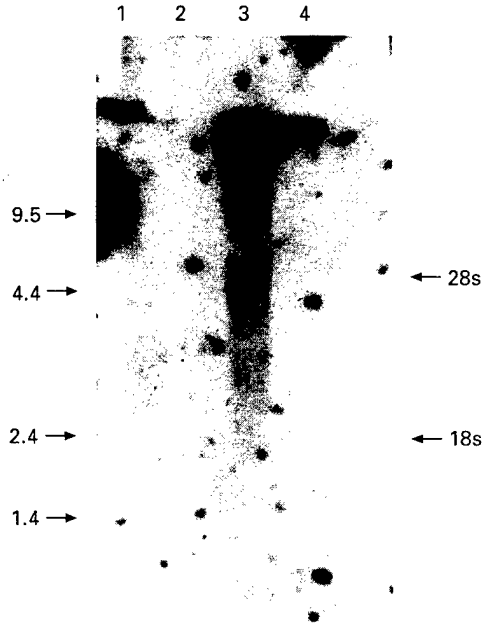

Figure 4 RNA blot analysis of normal and transgenic mouse tissues. RNA was isolated from normal mouse liver and transgenic mouse liver, brain, and kidney tissues, blotted to nitrocellulose, and probed with the lac Z gene as described in the Materials and methods section. Lane 1, normal mouse liver RNA; lane 2, transgenic mouse liver RNA; lane 3, transgenic mouse brain RNA; lane 4, transgenic mouse kidney RNA. Note that only transgenic brain RNA possesses transcripts which hybridize to the lac Z gene (one migrating greater than 9.5 kb and one at approximately 4.1 kb)

homogenates as shown in Table 2. Liver tissues appears to have only marginally elevated β-galactosidase specific activity, possessing approximately three-fold higher activity over normal, non-transgenic liver cell homogenates. No other tissues appear to possess significantly elevated β-galactosidase activity by specific activity assay of whole cell homogenates (Table 2).

To examine the specific transcription of the human c-*myc*/lac Z transgene, RNA blot analysis using RNA isolated from normal mouse liver tissue and transgenic animal liver, brain and kidney tissues was performed. A 3.0 Kb BamHI fragment of the lac Z gene was labelled as a probe for RNA blot analysis using random hexamers. As expected, no hybridization is seen in RNA isolated from normal mouse liver (Figure 4, lane 1). RNA isolated from transgenic mouse liver tissue does not demonstate mRNA transcripts which hybridize to the lac Z gene (Figure 4, lane 2). RNA isolated from transgenic brain tissue has two distinct RNA species, one migrating at greater than 9.5 kb and another at approximately 4.1 kb (Figure 4, lane 3). No lac Z transcripts are demonstrable in transgenic kidney RNA (Figure 4, lane 4), as expected, since transgenic kidney tissue does not possess significantly elevated β-

galactosidase activity over control kidney tissue by specific activity assay of whole cell homogenates (Table 2). Additionally, no transcripts for endogenous mouse c-*myc* mRNA were seen on the same RNA blot after probing with the mouse c-*myc* cDNA (data not shown).

To demonstrate c-*myc* promoter usage in transgenic mouse brain tissue, primer extension analysis was performed using the same RNAs examined by RNA blot analysis. The 3′ oligonucleotide primer used to synthesize the human c-*myc* promoter sequence by polymerase chain reaction (PCR) was used as primer for primer extension analysis. RNA isolated from normal mouse liver tissue hybridizes to the primer and gives extension products consistent with RNA transcripts of endogenous mouse c-*myc* mRNA beginning primarily at the P2 promoter with trace amounts initiating from the P1 promoter (Figure 5, lane 1). An identical pattern is seen in RNA isolated from transgenic mouse liver tissue (Figure 5, lane 2). These products represent endogenous mouse c-*myc* transcription with its characteristic transcriptional attenuation at the end of exon one (Bentley and Groudine 1988; Spencer *et al.*, 1990; Spencer and Groudine, 1991; Marcu *et al.*, 1992), since no lac Z mRNA transcripts are seen in transgenic mouse liver RNA (Figure 4, lane 2). Primer extension analysis of RNA isolated from transgenic brain tissue reveals a different promoter usage pattern of the human c-*myc*/lac Z transgene. The human c-*myc* P1 promoter is used primarily in the transcription of the human c-*myc* Z transgene (Figure 5, lane 3). This represents transcription from the human c-*myc*/lac Z transgene itself, since previous work (Ruppert *et al.*, 1986) demonstrates normal mouse brain tissue does not express c-*myc* mRNA to any detectable levels. The P1 promoter appears to be the preferential promoter over the P2 promoter in brain tissue expressing the c-*myc*/lac Z transgene, since this band is more intense than transcripts initiating from the P2 promoter (Figure 5, lane 3). Primer extension analysis of normal mouse brain RNA using the same 3′ human c-*myc* oligonucleotide demonstrates a primer extension product similar to normal mouse liver RNA, utilizing the mouse P2 promoter exclusively, although a much lower amount of the mouse c-*myc* 5′ extension product is seen (data not shown). RNA from transgenic kidney tissue does not demonstrate any detectable primer extension products (Figure 5, lane 4), as would be expected since no detectable lac Z transcripts are seen by RNA blot analysis (Figure 4, lane 4) and no β-galactosidase activity is seen in whole cell homogenates by specific activity assay (Table 2).

We wished to specifically inhibit the expression of β-galactosidase in transgenic mice heterozygous for the human c-*myc* Z transgene using mithramycin, a drug which binds to G-C rich regions of DNA (Miller *et al.*, 1987). Our laboratory has previously demonstrated that mithramycin can block the expression of the c-*myc* gene in rats following partial hepatectomy by binding to the c-*myc* promoter region (Campbell *et al.*, 1994). A normal pregnant female mouse mated to a transgenic male mouse heterozygous for the human c-*myc*/lac Z transgene was given mithramycin (150 $\mu g\ kg^{-1}\ d^{-1}$) intraperitoneal on days 7–13 of gestation. The pregnant females were sacrificed on day

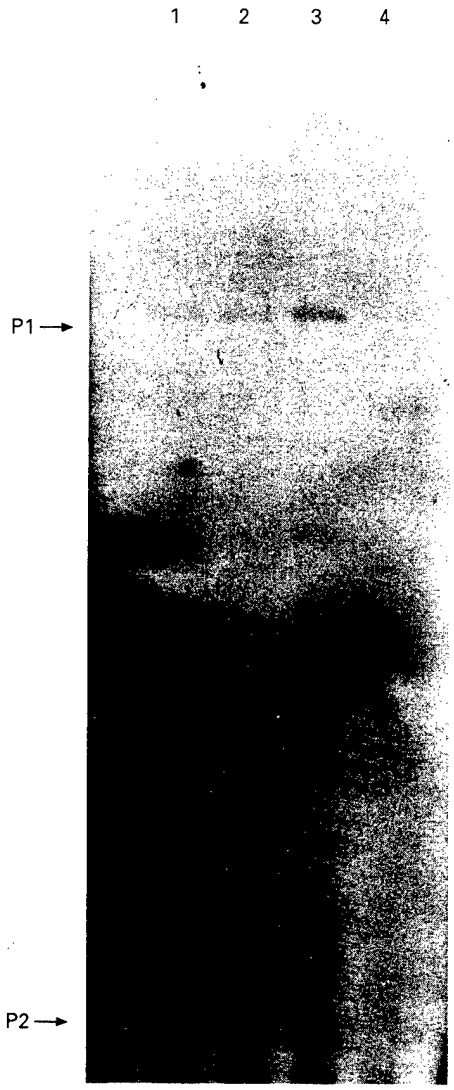

Figure 5 Primer extension analysis of normal mouse liver and transgenic mouse liver, brain, and kidney RNA. The 3′ c-*myc* oligonucleotide used to generate the human c-*myc* promoter region by PCR was hybridized to 10 μg of each RNA for primer extension analysis as described in the Methods section. Lane 1, normal mouse liver RNA; lane 2, transgenic mouse liver RNA; lane 3, transgenic mouse brain RNA; lane 4, transgenic mouse kidney RNA. Note that normal and transgenic mouse liver RNAs demonstrate predominantly P2 c-*myc* promoter use while transgenic mouse brain RNA uses the P1 promoter preferentially over the P2 promoter

14 of gestation and the embryos were examined for β-galactosidase activity by histochemical staining and specific activity assay of whole embryo homogenates. Embryos receiving mithramycin *in utero* stained qualitatively less intense than embryos from the saline control (data not shown). β-galactosidase staining of both the developing spinal cord and prefrontal cortex is decreased, indicating that the mithramycin effect is systemic (data not shown). To examine the effect of mithramycin in embryos which possess the human c-*myc*/lac Z transgene, β-galactosidase specific activity assay and DNA blot analysis of day 14 embryos were performed as shown in Table 3. β-galactosidase activity was inhibited approximately eight-fold by mithramycin given *in utero* in embryos possessing the human c-*myc*/lac Z transgene (average specific activity 57.2) as

Table 3 β-galactosidase activity of day 14 mouse embryos treated with mithramycin

Animal Number	*Specific Activity*[b]	*DNA Blot*[c]
1	82	+
2	79	+
3	67	+
4	67	+
5	58	+
6	27	–
7	24	–
8	22	–
9	7	–
10	2	–
11	0	–

Average Positive –57.2
Average Negative –13.7

[a]A non-transgenic pregnant mouse mated to an adult transgenic male mouse heterozygous for the human c-*myc*/lac Z transgene was ... mithramycin at 150 $\mu g\,kg^{-1}/d^{-1}$ intraperitoneal on day ... gestation and sacrificed on day 14. [b]Specif... galactosidase measured as the change in OD ... using resorufin-β-galactosidase as substrate/... ml by the micro-Biuret method). [c]The pres... c-*myc*/lac Z transgene was determined by DN... 14 and 18 embryos. +: presence of the transg... of the transgene

compared to untreated day 14 embryos (Table 1, average specific activity 474.0). Therefore, specific inhibition of the human c-*myc*/lac Z transgene can be demonstrated by administering mithramycin to transgenic mice *in utero*.

Discussion

The human c-*myc* promoter region was studied to determine its functional contribution to expression of the c-*myc* gene *in vivo* using β-galactosidase as a reporter gene. These studies demonstrate c-*myc* promoter-driven expression of β-galactosidase in central nervous system tissue and appears to correlate with the development of early spinal cord and brain tissue. However, expression of β-galactosidase in brain tissue of adult transgenic mice heterozygous for the human c-*myc*/lac Z transgene is constitutive. Expression in other tissues is absent by RNA blot analysis as expected from specific activity assay. Our results suggest that other *cis*-acting elements of the c-*myc* gene outside of the promoter region itself are responsible for correct expression in different tissue types and for normal down-regulation of the c-*myc* gene in terminally-differentiated cells *in vivo*, although chromosomal position-effect may also be responsible for its expression in central nervous system tissue.

We demonstrate selective inhibition of the human c-*myc*/lac Z transgene in developing mouse embryos using mithramycin. Treatment of a female mouse mated to a transgenic male mouse heterozygous for the c-*myc*/lac Z transgene with mithramycin results in an eight-fold decrease in β-galactosidase expression (Table 3). These results indicate that expression of the lac Z gene product is being driven by the human c-*myc* promoter alone and not surrounding DNA sequences at the integration site.

Other investigators have examined the expression of the c-*myc* gene in transgenic mice containing the human c-myc gene with its P2 promoter alone driven by the 5′ regulatory sequences of the class I H-2K, major histocompatibility promoter (Morello *et al.*, 1990). Their results indicate that expression of the transgene was constitutive and did not change following partial hepatectomy (Morello *et al.*, 1990). More recent work using additional constructs of the c-*myc* gene alone with both P1 and P2 promoters (Lavenu *et al.*, 1994) or using a hybrid H-2K/c-*myc* P2 fusion promoter with various combinations of c-*myc* regulatory regions (Morello *et al.*, 1993) suggests that the *cis* elements regulating c-*myc* expression *ev vivo* are not sufficient for correct transcri...on and expression *in vivo*. Our results suggests that ...e c-*myc* promoter region alone can direct expression of a reporter gene in transgenic mouse. ...ever, for correct tissue-specific and temporally-...ated expression of the c-*myc* gene. other regulatory ... of the c-*myc* gene may need to be included within ...e transgene.

Previous work (Ruppert *et al.*, 1986) examined expression of the c-*myc* protooncogene in cerebellar neurons at different developmental stages. An early post-natal wave of neuronal proliferation in the cerebellum was preceded by an approximately 25-fold increase in the steady state level of c-*myc* mRNA (Ruppert *et al.*, 1986). Their results indicate that increased expression most likely represents expression in two distinct neuronal populations. The c-*myc* promoter used predominantly in the postnatal period was the P2 promoter, with ratio of P2:P1 = 4 (Ruppert *et al.*, 1986). Promoter usage does not change even a 40-fold increase in c-*myc* expression (Kelley *et al.*, 1983; Ruppert *et al.*, 1986) and appears to be specific for individual cell lines and tissues (Kelley *et al.*, 1983). Our results indicate that transcription of the human c-*myc*/lac Z transgene initiates predominantly at the P1 human c-*myc* promoter, which has been demonstrated to be exempt from transcription termination at the end of exon one when expressed in *Xenopus* oocytes (Bentley and Groudine, 1988; Spencer *et al.*, 1990; Spencer and Groudine, 1991). Transcription initiation at the P1 promoter seen in our c-*myc*/lac Z transgene may reflect the lack of control elements responsible for normal c-*myc* promoter usage in adult brain tissue.

The steady state level of c-*myc* mRNA transcription is determined by at least three known mechanisms: (1) transcription initiation three (Marcu *et al.*, 1992; Shichiri *et al.*, 1993); (2) transcription attenuation/antitermination at the end of exon one (Spencer *et al.*, 1990; Spencer and Groudine, 1991; Marcu *et al.*, 1992); and (3) transcript degradation determined by the destabilizing sequences at the end of exon (Brewer and Ross, 1989; Brewer, 1991; Marcu *et al.*, 1992). The human c-*myc*/lac Z construct used for these studies contains only one of these three regions responsible for c-*myc* gene regulation. Previous work (Ruppert *et al.*, 1986) demonstrated very low levels of c-*myc* mRNA synthesis in adult mouse brain tissue and appears to localize mainly to Purkinje cells. These studies using the human c-*myc*/lac Z transgene suggest that other regulatory regions and possibly surrounding DNA sequences of the human c-*myc* gene are required for correct down-regulation of the c-*myc* gene seen in neural tissue *in vivo*.

Future studies will include the characterization of other structural regions within the human c-*myc* gene directing expression of β-galactosidase in transgenic

mice. These will encompass additional 5′ upstream regulatory sequences including a recently described transcriptional control region, FUSE (far upstream sequence element, Duncan *et al.*, 1994), attenuation sequences located at the end of exon one (Spencer *et al.*, 1990, Spencer and Groudine, 1991; Marcu *et al.*, 1992), and changing the 3′ splicing region of the transgene from mouse β-globin sequences to the 3′ c-*myc* sequences with its destabilizing effects on mRNA stability (Brewer and Ross, 1989; Brewer, 1991; Marcu *et al.*, 1992). These studies will detail the effects of known c-*myc* regulatory regions on the expression of β-galactosidase during development and help further define the roles of specific regulatory regions of the c-*myc* protooncogene during development.

Materials and methods

*Construction of the human c-*myc*/lac Z transgene*

The human c-*myc* promoter region was generated by polymerase chain reaction (PCR) using primers 280 bp upstream from the P1 c-*myc* promoter and 50 bp downstream from the P2 c-*myc* promoter. Oligonucleotide primers were synthesized containing a KpnI restriction site and a NcoI restriction site for 5′ and 3′ PCR primers, respectively. The PCR generated human c-*myc* promoter was ligated into a vector containing the bacterial lac Z gene (the ATG start codon contained within the NcoI site) and mouse β-globin exons two and three along with intervening sequences and the 3′ poly-A addition sequences (the parent plasmid, a generous gift from Dr Tim Townes, The University of Alabama at Birmingham, Birmingham, AL). A 6.3 kb restriction fragment containing the human c-*myc* promoter, the lac Z gene, and mouse β-globin sequences was purified on a 1.0% low-melting point agarose gel and used for injection of mouse embryos for transgenic mouse lines.

Animals

Two independent human c-*myc*/lac Z transgene mouse lines were obtained containing 2–4 copies per cell and 10–20 copies per cell, respectively. The transgenic mice were obtained by microinjection of a 6.3 kb KpnI/SalI restriction fragment (Figure 1), into the pronuclei of fertilized eggs derived from a C57BL/6 × SJL mating (G_0). Animals for all studies were obtained from the mating of a male G_1 offspring of founder transgenic animals to C57BL/6 × SJL hybrid normal, non-transgenic female mouse. Females were observed daily for a vaginal plug and counted as day 0 of gestation. Adult tissues analysed were from a G_1 male transgenic mouse heterozygous for the human c-*myc*/lac Z transgene, approximately 6 months old.

Histochemical analysis of β-galactosidase

Embryos stained for β-galactosidase (Cheng *et al.*, 1993) were fixed in PBS containing 2.0% formaldehyde and 0.2% glutaraldehyde at 4°C for 60 min. Embryos were rinsed in ice cold PBS twice and stained with 5-bromo-4-chloro-3-indolyl-β-D-galactopyranoside (X-gal) at 1 mg ml^{-1} in 5 mM $K_3Fe(CN)_6$ 5 mM $K_4Fe(CN)_6$ and 2 mM $MgCl_2$ in PBS at 37°C for approximately 24 h. Embryos were rinsed in PBS at 4% formaldehyde prior to photography.

Specific activity assay of β-galactosidase

Embryos were removed from sacrificed mothers, rinsed in ice-cold PBS, and placed on ice. The entire embryo was used for day 11 specific activity assays whereas only the upper two thirds (head and abdomen) were used for day 14 and day 18 embryos. The lower extremities were used for DNA blot analysis (Sambrook *et al.*, 1989) on day 14 and day 18 embryos to identify the presence or absence of the transgene in each embryo. Each embryo was homogenized in 250 μl of homogenization buffer (50 mM Tris-HCl, 7.4, 10 mM $MgCl_2$, 100 mM NaCl, and 0.01% Triton X-100) in a plastic microcentrifuge tube with a motor-driven Teflon homogenizer at 2500 r.p.m. Triton X-100 was added to 1% and incubated on ice for 15 min. Cellular debris was pelleted at 16 000 *g* for 10 min at 4°C in a table top microcentrifuge and the supernatant was transferred to a clean tube. β-galactosidase activity was determined using 50 μl of each sample added to 990 μl of homogenization buffer without Triton X-100. Ten μl of resorufin β-galactopyranoside (7.5 mg ml^{-1}) was added to each reaction and incubated at 37°C for 2 h. β-galactosidase enzyme activity was measured as the change in OD_{572} over 2 h. Specific β-galactosidase enzyme activity of each embryo was normalized for protein concentration using the micro-Biuret method (Sigma Chemical Company) expressed as g ml^{-1}.

Adult animals were sacrificed by CO_2 suffocation by the sublimation of dry ice in a closed container. Tissues were removed and rinsed in ice-cold saline. Approximately 3–5 volumes of ice-cold homogenation buffer (50 mM Tris-HCl, 7.4, 10 mM $MgCl_2$, 100 mM NaCl and 0.01% Triton X-100) was added to each tissue. Tissues were homogenized with 5–10 strokes of a motor-driven Teflon homogenizer at 2500 r.p.m. Triton X-100 was added to a final concentration of 1% and incubated on ice for 30 min. Cellular debris was pelleted at 48 000 *g* in a SW-50.1 rotor (Beckman Instruments). The supernatants were transferred to a clean tube and β-galactosidase specific activity was assayed as described above.

RNA blot analysis

Total RNA was extracted from tissue samples using RNAsol B (Tel-Test Inc., Friendswood, TX). RNA samples were electrophoresed on 1.2% formaldehyde gels and transferred to nitrocellulose (Sambrook *et al.*, 1989). RNA was cross-linked to the nitrocelulose filter with u.v. light and hybridized to a ^{32}P-labelled 3.0 kb BamHI DNA fragment encoding the bacterial lac Z gene at 42°C for 18–24 h. The filter was washed at final stringency of 0.2 × SSC and 0.5% sodium dodecyl sulfate at 45°C for 30 min and visualized by autoradiography.

Primer extension analysis

Ten μg of each RNA was used for primer extension analysis (Sambrook *et al.*, 1989). The 3′ oligonucleotide used for PCR generation of the human c-*myc* promoter region (see above) was also used for primer extension analysis. Primer extension products were electrophoresed on 8.0% denaturing acylanide gels and visualized by autoradiography.

Treatment of transgenic animals with mitramycin

Normal, non-transgenic female (F_2 hybrids of C57 BL/6X SJL mating) were mated to G_1 males heterozygous for the human c-*myc*/lac Z transgene. Vaginal plugs were identified (day 0) and pregnant females were treated with mithramycin (150 μg kg^{-1}/d^{-1} × 7d) on days 7–13 of gestation. Pregnant females were sacrificed the following day (day 14) and embryos were analysed for β-galactosidase activity by histochemical staining and specific activity assays as described above.

Acknowledgements

We wish to thank Ms Teresa McGaha for her assistance in the preparation of this manuscript. We would like to acknowledge Dr John Mountz, the Department of Medicine Division of Rheumatology and Dr Carl Pinkert, the Department of Comparative Medicine, The University of Alabama at Birmingham for injection of mouse embryos for transgenic mouse lines. We would also like to thank Dr Tim Townes, the Department of Biochemistry and Molecular Genetics, The University of Alabama at Birmingham, for the generous gift of the parent plasmid vector used for construction of the human c-*myc*/lac Z transgene. This work was supported by NIH Grants CA-42664 and CA-42337, the Department of the Army Grant DAMD 17-93-J-3018, and the VA Research Office.

References

Ayer DE, Kretzner L and Eisenman RN. (1993). *Cell*, **72,** 211–222.

Bentley DL and Groudine M. (1988). *Cell*, **53,** 245–256.

Blackwood EM and Eisenman RN. (1991). *Science*, **251,** 1211–1217.

Blume SW, *et al.* (1991). *J. Clin. Invest.*, **88,** 1613–1621.

Brewer G. (1991). *Mol. Cell. Biol.*, **11,** 2460–2466.

Brewer G and Ross J. (1989). *Mol. Cell. Biol.*, **9,** 1996–2006.

Campbell VW, *et al.* (1994). *Am. J. Med. Sci.*, **307,** 167–172.

Chang Y, Spicer DB and Sonenshein GE. (1991). *Oncogene*, **6,** 1979–1982.

Cheng T, Wallace MC, Merlie JP and Olson EN. (1993). *Science*, **261,** 215–218.

Cole MD. (1986). *Ann. Rev. Genet.*, **20,** 3834.

DesJardins E and Hay N. (1993). *Mol. Cell. Biol.*, **13,** 5710–5724.

Duncan R, *et al.* (1994). *Genes & Devel.*, **8,** 465–480.

Kelley K, Cochran BH, Stiles CD and Leder P. (1983). *Cell*, **35,** 603–610.

Lavenu A, Pournin S, Babinet C and Morello D. (1994). *Oncogene*, **9,** 527–536.

Luscher B and Eisenman RN. (1990). *Genes & Devel.*, **4,** 2025–2035.

Marcu KB, Bossone SA and Patel AJ. (1992). *Annu. Rev. Biochem.*, **61,** 809–860.

Miller DM, *et al.* (1987). *Am. J. Med. Sci.*, **30,** 388–394.

Morello D, Lavenu A, Pournin S and Babinet C. (1993). *Oncogene*, **8,** 1921–1929.

Morello D, Fitzgerald MJ, Babinet C and Fausto N. (1990). *Mol. Cell. Biol.*, **10,** 3185–3193.

Ray R, Thomas S and Miller DM. (1990). *Am. J. Med. Sci.*, **299,** 203–208.

Ray R, *et al.* (1989). *J. Clin. Invest.*, **83,** 2003–2007.

Ruppert C, Goldowitz D and Wille W. (1986). *EMBO J.*, **5,** 1897–1901.

Sambrook J, Fritsch EF and Maniatis T. (1989). *Molecular Cloning A Laboratory Manual*, 2nd ed. Cold Spring Harbor Laboratory Press, Cold Spring Harbor, New York.

Shichiri M, Hanson KD and Sedivy JM. (1993). *Cell Growth & Diff.*, **4,** 93–104.

Snyder RC, Ray R, Blume S and Miller DM. (1991). *Biochem.*, **30,** 4290–4297.

Spencer CA and Groudine M. (1991). *Advances Canc. Res.*, **56,** 1–48.

Spencer CA, *et al.* (1990). *Genes & Devel.*, **4,** 75–88.

Taub R, *et al.* (1984). *Cell*, **36,** 339–348.

Reprinted from Biochemistry, 1995, 34.

Inhibition of Nuclear Protein Binding to Two Sites in the Murine c-*myc* Promoter by Intermolecular Triplex Formation[†]

James F. Reddoch[‡] and Donald M. Miller*[,§]

Departments of Medicine and of Biochemistry and Molecular Genetics, University of Alabama at Birmingham, Birmingham, Alabama 35294

Received November 28, 1994; Revised Manuscript Received February 27, 1995[⊗]

ABSTRACT: The c-*myc* gene is overexpressed in a variety of tumor types and appears to play an important role in the abnormal growth of a number of cell types. In an effort to determine the ability of sequence- and species-specific triplex-forming oligonucleotides to inhibit expression of a targeted gene in animals, we have identified two novel triplex-forming sites in the murine c-*myc* promoter. One is homologous to the triplex-forming human PuF binding element located upstream of the P1 transcription start site. The other triplex-forming site is found in a region between P1 and P2 that encompasses the ME1a1 binding site and part of the E2F binding site and is highly homologous to the human sequence. Synthetic oligodeoxyribonucleotides designed to target these essential regulatory elements form sequence-specific triple helices as demonstrated by gel mobility shift analysis and DNase I footprinting. Polypurine:polypyrimidine regions in the P1 and P2 promoters form specific protein−DNA complexes upon incubation with a murine YC8 nuclear extract. Preincubation of each of the promoter fragments with its respective triplex-forming oligonucleotide results in the inhibition of nuclear protein binding. Non-triplex-forming oligonucleotides do not significantly affect protein binding. The data presented are a preliminary step toward generating an animal model for the phenotypic effects of triplex formation within the c-*myc* promoter.

The c-*myc* gene product plays an integral role in the cascade of signal transduction events following a mitogenic stimulus (Eisenman, 1989). Overexpression of c-*myc* is important in the tumorigenesis of a number of experimental and naturally occurring systems (Kato & Dang, 1992; Cole, 1986). The mechanisms responsible for c-*myc* overexpression include proviral insertion, gene amplification, and chromosomal translocation (Alt & Zimmerman, 1990; Cory, 1986). Although the protein has been localized to the nucleus (Hann et al., 1983), the precise cellular function of the c-Myc remains somewhat undefined. It is known, however, that Myc forms a heterodimer with Max (Blackwood & Eisenman, 1992; Prendergast et al., 1991) and that dimerization with Max is required for the oncogenic activity of Myc (Amati et al., 1993). The Myc/Max complex binds the first intron of prothymosin α to mediate transcription of that gene, supporting the role of Myc as a transactivator of gene expression (Gaubatz et al., 1994).

Regulation of c-*myc* transcription has been relatively well characterized. The highly conserved human and murine c-*myc* genes have three transcription initiation sites in common. In normal and resting cells, P2 is the dominant promoter in both species, giving rise to 75−90% of cytoplasmic c-*myc* mRNA (Taub et al., 1984; Bentley & Groudine, 1986; Eick & Bornkamm, 1989; Marcu et al., 1992). P1, located 164 bp upstream in mice (Bernard et al., 1983), generates 10−25% of c-*myc* transcripts in normal cells but may predominate in serum-stimulated and malignant cells (Siebenlist et al., 1984). P1 and P2 appear to be independently regulated by a composite of positive- and negative-acting factors binding within a 2.3 kb region upstream of the promoters (Yang et al., 1985; Ruppert et al., 1986; Hay et al., 1987). Recent evidence by Lavenu et al. (1994), however, showing that murine c-*myc* genomic constructs containing 3.5 kb upstream and 1.5 kb downstream are silent in the resultant transgenic mice, indicates that regulation may be even more complex than expected.

It has been suggested that inhibition of transcription initiation could provide an effective method of reducing expression from activated or amplified loci which participate in the malignant cell phenotype (Hélène, 1991). Mithramycin, an antibiotic which binds GC-rich regions of DNA (Van Dyke & Dervan, 1983), inhibits c-*myc* transcription initiation from both P1 and P2 by blocking the interaction of the transcription factor Sp1 with its target sites (Ray et al., 1990; Snyder et al., 1991). Unfortunately, mithramycin also inhibits the transcription of other genes containing similar GC-rich regulatory regions (Ray et al., 1989; Blume et al., 1991). Triplex DNA provides a gene-specific means of inhibiting transcription initiation since a triplex-forming oligonucleotide can interact with the targeted region in a sequence-specific manner. The relative sequence-specificity of triplex formation suggests that the oligonucleotide will not interfere with transcription factor binding to other genes.

Previous studies on intermolecular triplex formation by polypurine:polypyrimidine (pur:pyr) regions in gene promoters demonstrate the ability of a pyrimidine-rich third strand to form Hoogsteen hydrogen bonds with the purine-rich acceptor strand in the major groove of the target duplex (Lyamichev et al., 1988; de los Santos et al., 1989; Maher

[†] Supported by NIH Grant CA54380, by a research grant from the Share Foundation, and by U.S. Army Grant DAMD 17-93-J-3018.
* Author to whom correspondence should be addressed.
[‡] Department of Biochemistry and Molecular Genetics.
[§] Department of Medicine, Division of Hematology and Oncology.
[⊗] Abstract published in *Advance ACS Abstracts,* June 1, 1995.

0006-2960/95/0434-7659$09.00/0

et al., 1990; Pilch et al., 1990; Plume et al., 1990; Mergny et al., 1992; Lu & Ferl, 1993). The third strand in pyr·pur: pyr triple helices adopts a parallel orientation relative to the polypurine strand of the duplex (Moser & Dervan, 1987; Fedorova et al., 1988; Praseuth et al., 1988). The stability of a pyr·pur:pyr triplex is dependent on nonphysiological acidic conditions required by the C^+·G:C triplets responsible for sequence specificity (Wells et al., 1988; Rajagopal & Feigon, 1989). Recent studies have shown triplex formation by a purine-rich or mixed purine/pyrimidine third strand involving G·G:C and A·A:T or T·A:T triads at physiological pH (Beal & Dervan, 1991; Kolwi-Shigematsu & Kolwi, 1991; Postel et al., 1991; Durland et al., 1991). These triple helices arise through reverse-Hoogsteen bonding, resulting in an antiparallel orientation of the third strand (Beal & Dervan, 1991; Gee et al., 1992; Ebbinghaus et al., 1993; Mayfield et al., 1994a).

Cooney and co-workers (Cooney et al., 1988) have demonstrated triplex formation (pur·pur:pyr) by a nuclease-hypersensitive region upstream of the human c-*myc* P1 transcription start site. This hypersensitive element is coincident with the binding site of several nuclear proteins. Davis et al. (1989) have reported a ribonucleoprotein association that appears to involve RNA:DNA hybridization. Postel and co-workers (Postel et al., 1989, 1993) have demonstrated binding of a protein, PuF, which they later cloned and found that it was Nm23-H2, a putative suppressor of tumor metastasis (Steeg et al., 1988). The nuclear protein NSEP-1, which exhibits overlapping but distinct single- and double-stranded DNA binding specificities, has also been shown to interact with this sequence in the human c-*myc* promoter (Kolluri et al., 1992). Triplex-forming oligonucleotides directed to this region selectively suppress c-*myc* mRNA levels *in vitro* and in HeLa cells (Cooney et al., 1988; Postel et al., 1991).

The corresponding region of the murine *myc* promoter, roughly the area proximal to DNase I hypersensitive site III_1 (Siebenlist et al., 1984; Bentley & Groudine, 1986; Marcu et al., 1992), is highly homologous to the human sequence that binds the aforementioned proteins. Asselin et al. (1989) have demonstrated through deletion analysis that this region is essential for efficient transcription from the murine c-*myc* P1 transcription initiation site. The effect of this deletion on P2 activity was not addressed.

The presence of a nuclear factor binding site in the murine c-*myc* P2 promoter, composed entirely of pyr:pur sequence, in close proximity to DNase I hypersensitive site III_2, has been documented (Asselin et al., 1989). Deletional mutagenesis of this *cis* element showed that it is essential for transcription initiation from the murine start site P2. This region, designated ME1a1, is very highly conserved between humans and mice and has since been found to interact with a zinc-finger protein (termed Maz in humans) (Bossone et al., 1992). Three distinct *cis*-acting elements (5′ to 3′: ME1a2, E2F, and ME1a1) are required for optimal transcription initiation from P2 (Moberg et al., 1992). Hypersensitive site III_2 is situated almost exactly in the center of this positive regulatory element (Marcu et al., 1992). This pyr:pur region around site III_2 has not previously been shown to form triplex DNA.

The observations above suggest that these regions in the murine c-*myc* promoter, likely possessing similar functions as their human homologues, serve as ideal triplex target regions for determining the effect of triplex-forming oligonucleotides on endogenous gene expression in an animal model. We have demonstrated here that two regions in the murine c-*myc* gene promoter corresponding to binding sites for essential nuclear factors in the human c-*myc* promoter bind murine nuclear proteins with a high degree of specificity. We have shown triple helix formation with these murine P1 and P2 promoter sequences by gel mobility shift analysis and DNase I footprinting. The inhibition of nuclear factor binding by triplex formation is established by a decrease in protein−DNA interaction, also shown by gel shift, following preincubation of the target region with triplex-forming oligonucleotides. This is the first report of triplex formation in a murine gene promoter and, as such, is the foundation for a murine model allowing assessment of the effects of triplex-forming oligonucleotides directed to the endogenous c-*myc* gene.

MATERIALS AND METHODS

Oligonucleotide Synthesis. Oligonucleotides were synthesized by standard phosphoramidite chemistry on a Milligen Cyclone Plus DNA synthesizer and purified by reverse phase chromatography over a Clontech Oligonucleotide Purification/Elution Cartridge. Concentrations were determined by absorption measurements at 260 nm by using molar extinction coefficients. Oligonucleotide integrity was verified by 5′ end-labeling with [γ-^{32}P]ATP and T_4 polynucleotide kinase followed by gel electrophoresis under denaturing conditions. Radiolabeled duplexes of 27 and 30 bp were prepared by 5′ end-labeling one strand with [γ-^{32}P]ATP and T_4 kinase and annealing the labeled strand with its unlabeled complement.

Protein Binding Assays. For protein shifts, ^{32}P-labeled double-stranded target sequence oligonucleotides representing a section of the murine c-*myc* promoter were incubated with a YC8 nuclear extract (Dignam et al., 1983) for 30 min at 22 °C in a buffer consisting of 20 mM Tris (pH 7.9), 2.5 mM $MgCl_2$, 140 mM KCl, 1 mM DTT, and 8% glycerol. The final total protein concentration was 265 ng/μL. For competition studies, unlabeled murine myc P1 or P2 duplex target (27 or 30 bp, respectively), 22 bp nonspecific duplex DNA, or duplex DNA representing the homologous region in the human c-myc P1 or P2 promoter (27 or 23 bp, respectively) was mixed with the ^{32}P-labeled murine myc duplex target prior to adding extract. Samples were electrophoresed on 5% native polyacrylamide gels at 100 V. Both gel and running buffer contained 90 mM Tris−borate (pH 8.5), 2 mM EDTA. Bands were visualized by autoradiography.

Sequences of the competitors for protein binding are as follows (nucleotide positions are relative to P1):

NS22: 5′ G C A T A T T A C T G G T G C A G G A C C A 3′
3′ C G T A T A A T G A C C A C G T C C T G G T 5′

P1 specific (−177 to −151):

5′ T C C T C C T C C T C T T T C C C C G G C T C C C C A 3′
3′ A G G A G G A G G A G A A A G G G G C C G A G G G G T 5′

P2 specific (+89 to +118):

5′ T T G G C G G G A A A A A G A A G G G A G G G G A G G G A T 3′
3′ A A C C G C C C T T T T T C T T C C C T C C C C T C C C T A 5′

P1 human (−142 to −116):

5′ C C T T C C C C A C C C T C C C C A C C C T C C C C A 3′
3′ G G A A G G G G T G G G A G G G G T G G G A G G G G T 5′

P2 human (+99 to +121):

5′ G G G A A A A A G A A C G G A G G G A G G G A 3′
3′ C C C T T T T T C T T G C C T C C C T C C C T 5′

Gel Mobility Shift Analysis of Triplex Formation. Potential triplex-forming oligonucleotides were heated at 65 °C for 5−10 min to reduce self-aggregation. After quick-cooling, the oligonucleotides were added to their respective radiolabeled double-stranded target in 20 mM Tris (pH 7.9), 2.5 mM $MgCl_2$, 140 mM KCl, 1 mM DTT, and 8% glycerol (except for Figure 4C) and incubated at 37 °C for 2 h. The reactions in Figure 4C were conducted in 20 mM Tris (pH 7.9), 10 mM $MgCl_2$ and incubated at 37 °C for 3 h. Samples were electrophoresed on 16% native polyacrylamide gels at 100 V. Both gel and running buffer contained 90 mM Tris−borate (pH 8.0), 10 mM $MgCl_2$. Bands were visualized by autoradiography.

DNase I Footprinting Analysis. "P1" triplex formation was conducted as follows: oligonucleotides of 61 and 56 nucleotides were synthesized, purified, and quantitated as described above. After annealing, the resulting duplex, representing the mouse *myc* promoter region from −199 to −138 with respect to P1, was Klenow-labeled with [α-^{32}P]-dATP. This labeled fragment was incubated with triplex-forming oligonucleotide (preheated to 65 °C and quick-cooled) or poly[d(I-C)] and incubated overnight at 37 °C in 20 mM Tris (pH 7.9), 10 mM $MgCl_2$.

"P2" triplex formation was conducted as follows: a 775-bp fragment of the murine c-*myc* gene was PCR-amplified, using *Taq* polymerase, from the plasmid pMMTV-Stu (American Type Culture Collection) which harbors 9.3 kb of the murine myc locus. The 5′ PCR primer was designed with a *Kpn*I restriction endonuclease recognition sequence and the 3′ primer with a *Bgl*II recognition sequence. The PCR-amplified fragment was purified from a 1% low melting point agarose gel and ligated into the vector pCR (Invitrogen). This plasmid was digested with *Kpn*I and *Bgl*II, and the liberated fragment was again gel-purified and subcloned into pGLII (Promega). The resulting plasmid yields four fragments upon digestion with *Sca*I and *Hin*dIII. The 343 bp fragment, with an upstream *Sca*I blunt end and a downstream *Hin*dIII sticky end, was resolved and excised from a 3% low melting point agarose gel. This fragment was end-labeled with [α-^{32}P]dCTP using the Klenow fragment and incubated overnight with oligonucleotide (preheated to 65 °C and cooled) in 20 mM Tris (pH 7.9), 10 mM $MgCl_2$ at 37 °C. The sequence of the target purine-rich region was confirmed by chemical cleavage sequencing (Maxam & Gilbert, 1980).

After triplex formation, samples were allowed to cool to room temperature and then were digested with DNase I on ice (20 s for the P1 fragment, 30 s for the P2 fragment). Digestion was terminated by the addition of 20 mM EDTA in 90% formamide followed by heating to 95 °C for 5 min. Samples were electrophoresed on 8 M urea/polyacrylamide gels at 42 W.

Analysis of Inhibition of Protein Binding. Potential triplex-forming oligonucleotides were heated at 65 °C for 5−10 min, quick-cooled, and then added to their respective labeled double-stranded target oligonucleotides in 20 mM Tris (pH 7.9), 2.5 mM $MgCl_2$, 140 mM KCl, 1 mM DTT, and 8% glycerol. Incubation at 37 °C proceeded for 2 h. Samples were then allowed to cool to room temperature, at which point YC8 nuclear extract was added to achieve a final concentration of 265 ng of protein/μL. Incubation at 22 °C proceeded for 30 min. Samples were then electrophoresed on 5% native polyacrylamide gels at 100 V. Both gel and running buffer contained 90 mM Tris−borate (pH 8.5), 2 mM EDTA. Bands were visualized by autoradiography.

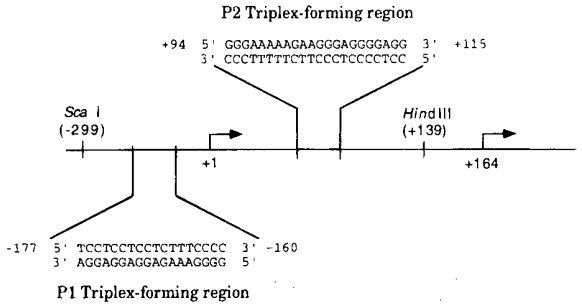

FIGURE 1: Map of the murine c-*myc* promoter showing the P1 and P2 targets for protein binding and triplex formation. The P1 transcription initiation site is designated "+1". The P2 initiation site is located 164 bp downstream. Restriction endonucleases *Sca*I and *Hin*dIII (cutting site positions relative to the P1 start site) were used to prepare a DNase I footprinting template.

RESULTS

Nuclear Protein Binding. The c-*myc* locus contains two major transcription initiation sites, P1 and P2 (Figure 1). Purine-rich elements upstream of each of these sites have been shown to bind factors that are essential for efficient transcription initiation. Synthetic duplexes representing c-*myc* promoter pur:pyr motifs are illustrated "P1 Triplex-forming region" (27 bp) and "P2 Triplex-forming region" (30 bp) in Figure 1. Protein binding was demonstrated by gel mobility shift experiments (Figure 2). The murine T lymphoma cell line YC8 (Ghanta et al., 1993) was chosen as a source of nuclear proteins based on its high level of c-*myc* expression (data not shown). Incubation of the 27 bp P1 probe (panel A) with a YC8 nuclear extract results in the formation of a highly retarded major band indicating the formation of a protein−DNA complex (arrow). The specificity of this interaction is demonstrated by the fact that the 27 bp P1 duplex, in its unlabeled form, competes for binding. This specific competition is shown by the significant decrease in the amount of labeled DNA that shifts, reflecting the binding of the protein of interest to this unlabeled DNA of the same sequence. Competition of the unlabeled P1 sequence is accompanied by the increasing presence of free probe in lanes 3, 4, and 5. Whereas a 50-fold excess of specific competitor results in decreased nuclear protein−DNA interaction, the same concentration of nonspecific competitor probe is unable to compete, as evidenced by the persistence of a shifted protein−DNA complex in lane 8 of the same intensity as that in lane 2. The results of the specific and nonspecific competitions demonstrate that nuclear factor binding to this P1 region involves a sequence-specific interaction. When a 27 bp duplex representing the corresponding human P1 pur:pyr motif is used as a competitor (lanes 9, 10, and 11), the pattern of protein displacement closely resembles that observed when the unlabeled probe itself is used as a competitor (lanes 3, 4, and 5). These results suggest that there is adequate homology between the two duplexes to allow binding of the same protein, and that the human sequence possesses similar affinity for this nuclear proteins.

Panel B of Figure 2 illustrates similar specificity of nuclear factor binding to the 30 bp probe representing the polypyrimidine:polypurine region upstream of P2. As shown in lane 2, a specific protein−DNA complex (arrow) is formed

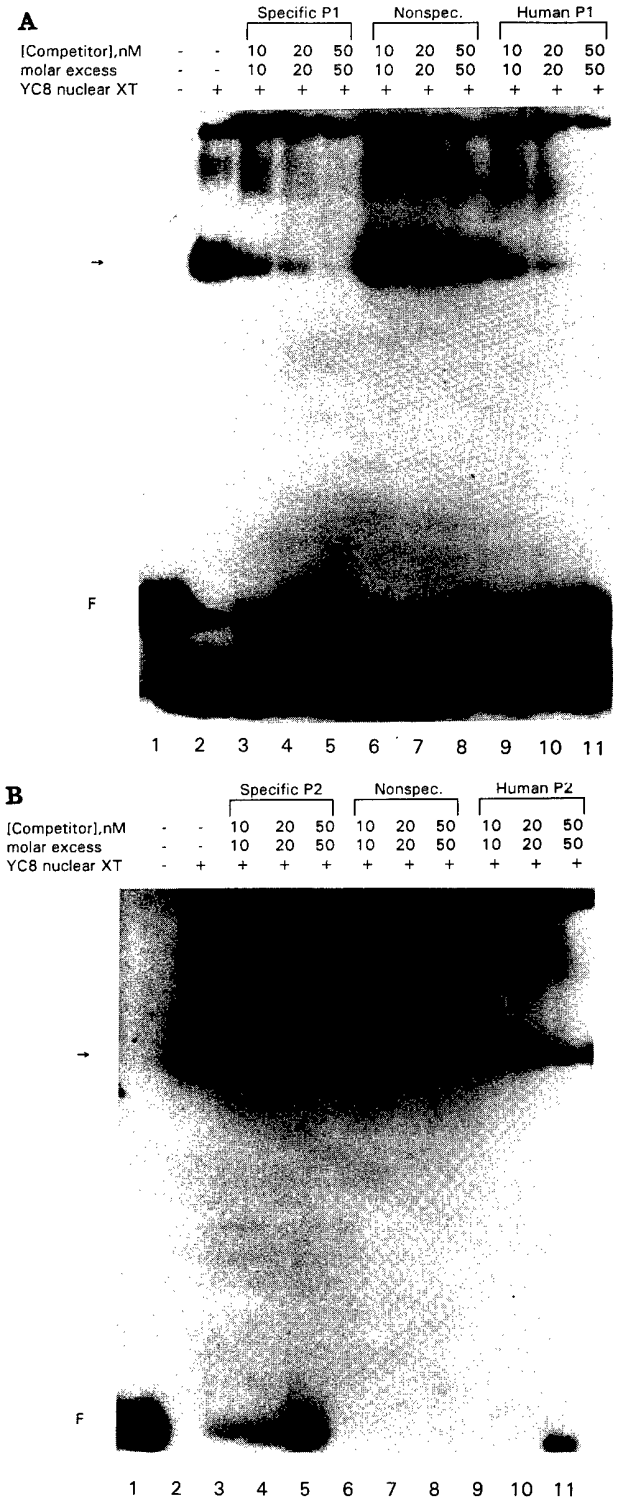

FIGURE 2: Gel mobility shift analysis demonstrating sequence-specific nuclear protein binding to the P1 purine:pyrimidine and the P2 pyrimidine:purine motifs in the murine c-*myc* promoter. Except for lanes 1 and 2 in each panel, synthetic ^{32}P-kinase-labeled 27 bp (A) and 30 bp (B) murine c-*myc* fragments were incubated with competitor duplexes and YC8 nuclear extract as described. "Molar excess" refers to the stoichiometric quantity of competitor DNA with respect to labeled probe. Lane 1 (both panels) does not contain either competitor DNA or extract. Lane 2 (both panels) does not contain competitor DNA. Arrows indicate specific protein−DNA complexes. "F" indicates free probe.

following incubation of the labeled probe with YC8 nuclear extract. Upon addition of increasing amounts of unlabeled specific murine competitors (lanes 3, 4, and 5), the labeled DNA−protein complexes disappear accompanied by a corresponding increase in the amount of the faster-migrating free probe. The unlabeled duplex representing the analogous region of the human promoter (lanes 9, 10, and 11) also competes, suggesting, as with the P1 sequence, a functional conservation of this *cis*-acting element between mice and humans. The nonspecific competitor does not affect the formation of protein complexes with the labeled probe (lanes 6, 7, and 8). These data demonstrate that the nuclear factor binding to this P2 pyr:pur motif, as with the P1 pur:pyr motif, involves a sequence-specific interaction.

Oligonucleotide Design and Triplex Formation with the P1 Target. Figure 3A illustrates the 27 bp pur:pyr P1 target duplex and the oligonucleotides that were assessed for their ability to form triplex with this sequence. Oligonucleotide sequences were designed to allow guanine recognition of G:C base pairs in the target, thus forming G•G:C triads, and thymine recognition of A:T base pairs, forming T•A:T triads. Potential triplex-forming oligonucleotides targeted to this pur:pyr motif were designed with identical sequences, but in both parallel (P1−18p) and antiparallel (P1−18ap) orientation with respect to the polypurine strand (i.e., the strand to which the reverse Hoogsteen hydrogen bonds form) of the target duplex. Because the target sequence is highly asymmetrical, the parallel oligonucleotide can bind only in the parallel orientation (improbable under these conditions), and the antiparallel oligonucleotide can bind only in the antiparallel fashion in order to form the defined triads.

The relative ability of each oligonucleotide to form triplex with the target duplex is determined by gel mobility shift analysis and confirmed by DNase I footprinting. In order to approximate more closely the ionic conditions *in vivo*, the gel shift reactions were conducted in the presence of 140 mM K^+, a concentration which has previously been shown to inhibit purine third-strand intermolecular triple helix formation (Milligan et al., 1993; Cheng & Van Dyke, 1993; Olivas & Maher, 1995). As illustrated in the gel shift in panel B, the P1−18ap oligonucleotide causes a shift of duplex (D) to a distinct, slower migrating complex (T) indicating triplex formation (Durland et al., 1990). A 1 μM concentration (a 10^3-fold molar excess) of this antiparallel oligonucleotide is sufficient to shift approximately half of the labeled target to the triple-helical form (lane 3). A 10^4-fold molar excess of the antiparallel oligonucleotide reveals a near-complete shift to triplex (lane 4). Lane 5, in contrast, features a 10^4-fold excess of parallel oligonucleotide (P1−18p) and demonstrates this oligonucleotide's failure to form triplex as all of the labeled target continues to migrate as a duplex. The use of oligonucleotides of the same sequence but opposite orientation is designed to illustrate the high degree of sequence-specificity with which the third strand binds its duplex ligand.

The endonuclease DNase I is less effective in cleaving the A form of DNA, which accompanies triplex formation (Arnott & Selsing, 1974), than the B form (Rhodes & Klug, 1986). A DNase I footprint experiment was conducted to ensure that the oligonucleotide binds the region to which it is directed and affords protection from DNase cleavage to the entire 18 bp sequence, thus conclusively proving antiparallel triplex formation (Figure 3C). Lane 4 shows digestion of the Klenow-labeled target after incubation with an excess of the P1−18ap. Triplex formation protects the polypurine stretch (displayed in lane 2) from cleavage, demonstrating the localization of the oligonucleotide to the correct target sequence. P1−18p (lane 5), in the same

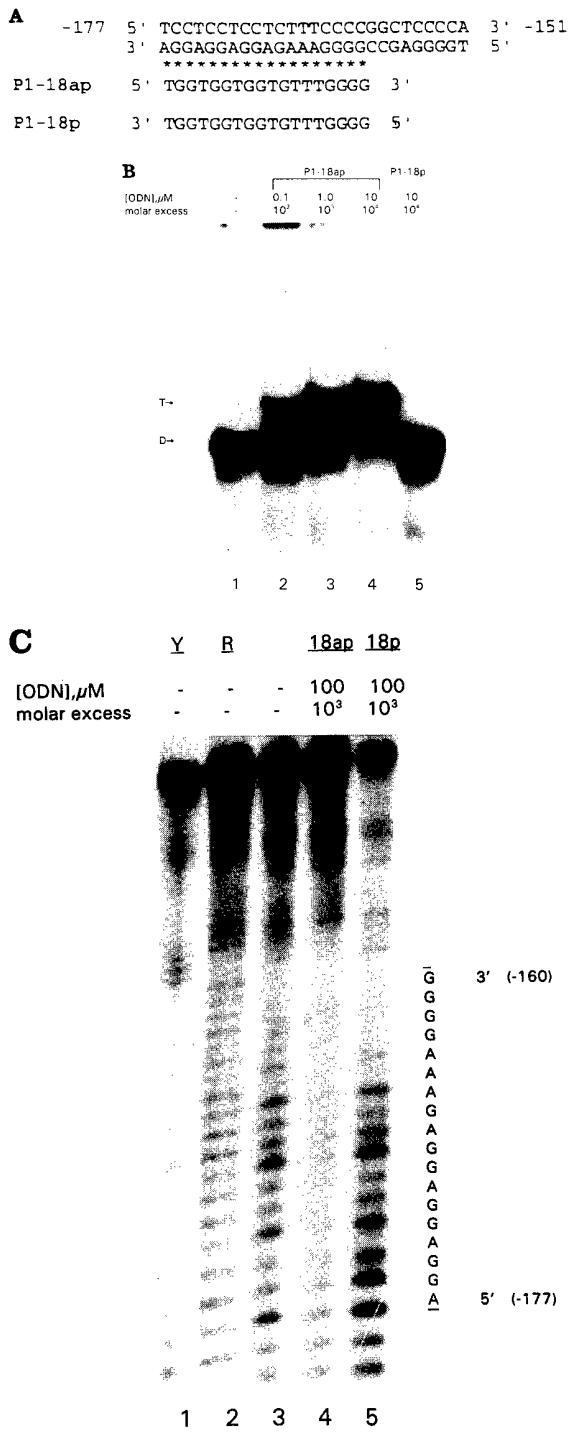

FIGURE 3: (A) Oligonucleotide sequences and their alignment with the 27 bp murine c-*myc* P1 target site. The "ap" and "p" notations refer to the orientation (antiparallel and parallel, respectively) of the oligonucleotide with respect to the purine-rich target strand. Asterisks denote reverse-Hoogsteen hydrogen bonds. (B) Gel mobility shift analysis demonstrating oligonucleotide-directed triplex formation in the P1 promoter target. The concentration of oligonucleotide (ODN), as well as the excess of oligonucleotide, is indicated above each lane. The buffer for triplex formation is identical to that used in protein binding. Lane 1 is a control migration of the labeled target without oligonucleotide. "T" and "D" indicate the electrophoretic positions of triplex and duplex DNA, respectively. (C) DNase I footprinting analysis of triplex formation in the P1 promoter target. Lanes 1 and 2 are Maxam–Gilbert sequencing reactions (pyrimidine-specific and purine-specific, respectively) conducted with the synthetic ^{32}P-Klenow-labeled 61 bp P1 target duplex. This duplex was incubated in the absence (lane 3) or presence (lanes 4 and 5) of oligonucleotides. The polypurine target sequence is shown vertically at left.

concentration, does not afford protection as demontrated by a cleavage pattern similar to that in the lane 3 control digestion. The data in panel C are consistent with those obtained from gel mobility shift analysis (panel B), further demonstrating that triplex formation occurs with the third strand in an antiparallel orientation relative to the polypurine target strand.

Oligonucleotide Design and Triplex Formation with the P2 Target. Figure 4A shows the P2 target polypyrimidine: polypurine duplex and the oligonucleotides assessed for their ability to form triplex. Panel B is a gel mobility shift analysis used to follow the change in mobility following triplex formation. Again, incubation of oligonucleotides with the target duplex was conducted in the presence of 140 mM K^+. The antiparallel oligonucleotide, P2−22ap, shifts nearly all of the labeled duplex to triplex at a 10^4 molar excess (lane 5). Lane 6 exhibits the inability of P1−18p, which bears sequence similarities to P2−22ap, to shift the labeled target to the triple-helical form, thus underscoring the specificity of the interaction between P2−22ap and the target. The parallel oligonucleotide, P2−22p, is capable of forming triplex with this particular target (panel C). The results in panel C were achieved in TM buffer (see Materials and Methods), but were entirely reproducible in the physiological approximation buffer used above (data not shown). The unique sequence of P2−22p suggests that the orientation of the third strand is antiparallel to the target purine strand in triplex formation. Panel D shows the 12 consecutive hydrogen bonds that would result from an antiparallel, reverse-Hoogsteen interaction of P2−22p with the P2 target duplex.

A DNase I footprint analysis illustrates the sequence-specificity of triplex formation by the P2 promoter (Figure 4, panel E). The sequence lanes (1 and 2) highlight the distinctive stretch of all pyrimidines in the coding strand and all purines in the noncoding strand. It is to this unique motif that the P2 oligonucleotide is directed. Lane 3 is a control for DNase I digestion in the absence of oligonucleotide. Lanes 4, 5, and 6 show the protection afforded by increasing concentrations of P2−22ap oligonucleotide, demonstrating triplex formation within the target region. The cleavage pattern following incubation of the target with the P1−18ap oligonucleotide displays fragments resulting from cleavage within the target region of a greater intensity than those in the P2−22ap-treated reactions, indicating the failure of the P1−18ap oligonucleotide to form triplex within this region. Because of uneven levels of total radioactivity in each lane, the extent of cleavage in the target region must be judged in a non-triplex-forming region context. The lanes with the triplex-forming oligonucleotide show a greater non-target region:target region band intensity ratio than that of the no-oligo and non-triplex-forming controls. Taken together, the gel mobility shift analysis and the footprint experiment conclusively demonstrate the specificity of the interaction of the P2−22ap oligonucleotide with its polypyrimidine: polypurine target.

Effect of Triplex Formation on Nuclear Protein Binding. The effect of triplex formation within the P1 and P2 target regions on nuclear protein binding was determined by gel mobility shift analysis. Figure 5A indicates a concentration-dependent inhibition of protein binding to the P1 probe following incubation of the probe with the triplex-forming oligonucleotide, P1−18ap. A 10 μM P1−18ap concentration (lane 5), sufficient to shift nearly all of the probe to the triplex

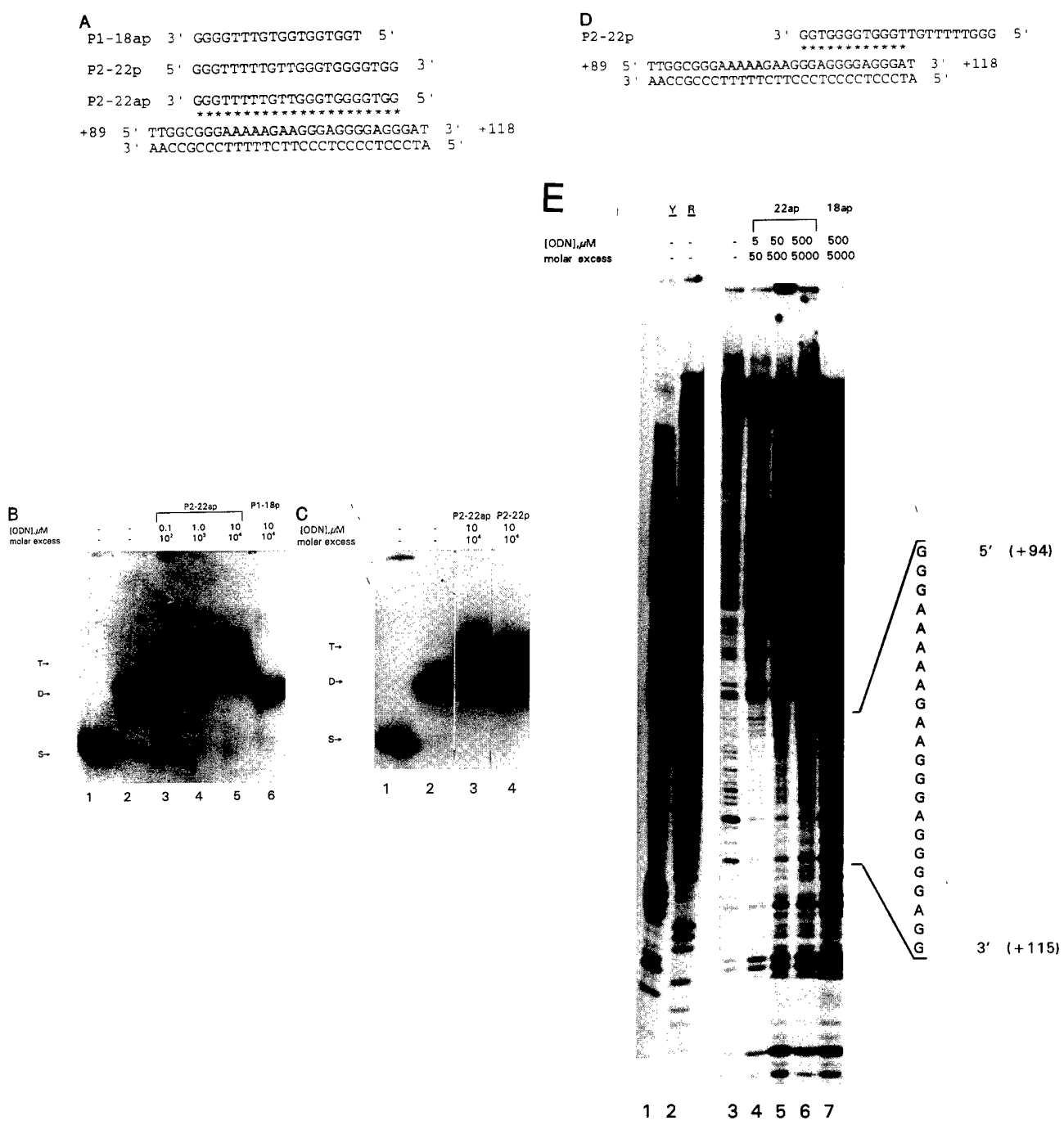

FIGURE 4: (A) Oligonucleotide sequences and their alignment with the 30 bp murine c-*myc* P2 target site. The "ap" and "p" notations refer to the orientation (antiparallel and parallel, respectively) of the oligonucleotide with respect to the purine-rich target strand. Asterisks denote reverse-Hoogsteen hydrogen bonds. (B) Gel mobility shift analysis demonstrating oligonucleotide-directed triplex formation in the P2 promoter target. The concentration of oligonucleotide (ODN), as well as the excess of oligonucleotide, is indicated above each lane. The buffer for triplex formation is identical to that used in protein binding. Lane 1 is a control for the migration of the labeled polypurine strand component of the target duplex. Lane 2 is a control for the migration of the target duplex without oligonucleotide. "T" = triplex; "D" = duplex; "S" = single-stranded DNA. (C) Gel mobility shift analysis demonstrating the ability of parallel oligonucleotide to form triplex with the P2 promoter target. The concentration of oligonucleotide (ODN), as well as the excess of oligonucleotide, is indicated above each lane. This experiment was conducted in TM buffer. Lane 1 is a control for the migration of the labeled polypurine strand component of the target duplex. Lane 2 is a control for the migration of the target duplex without oligonucleotide. "T" = triplex; "D" = duplex; "S" = single-stranded DNA. (D) Sequence of the parallel P2 oligonucleotide and the reverse-Hoogsteen hydrogen binding pattern (asterisks) it would assume in forming antiparallel triplex. (E) DNase I footprinting analysis of triplex formation in the P2 promoter target. Lanes 1 and 2 are Maxam−Gilbert sequencing reactions (pyrimidine-specific and purine-specific, respectively) conducted with the ^{32}P-Klenow-labeled 343 bp P2 target duplex. This duplex was incubated in the absence (lane 3) or presence (lanes 4−7) of oligonucleotides. The polypurine target sequence is shown vertically at left.

form in Figure 3B, results in a near-complete inhibition of protein binding. Protein binding to the labeled probe is not inhibited by the same concentration of P1−18p, shown to be unable to form triplex with this target. The difference in protein bound to the labeled target in lane 2 (binding in the absence of oligonucleotide) and lane 5 is sufficient to illustrate the inhibitory effect of triplex formation within this P1 pur:pyr motif on nuclear factor binding.

Triple helix formation with the P2 target has a similar effect (Figure 5, panel B). Again, a 10 μM concentration

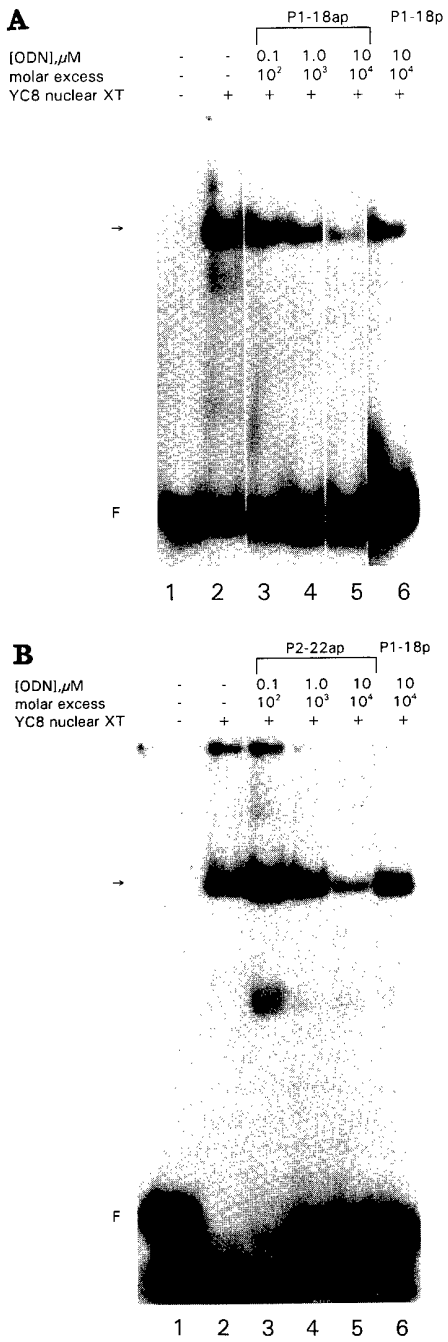

FIGURE 5: Gel mobility shift analysis demonstrating inhibition of nuclear protein binding to the murine c-*myc* P1 and P2 promoters by triplex formation. The 27bp P1 target (A) and the 30 bp P2 target (B) were incubated with their respective third-strand oligonucleotides and then with YC8 nuclear extract as described. Arrows indicate protein−DNA complexes. "F" indicates free probe. Labeled probe which has adopted the triplex confomer cannot be distinguished from duplex labeled probe as a result of the low percentage (5%) of acrylamide in these gels as opposed to the gels used to demonstrate triplex formation.

of the triplex-forming oligonucleotide, P2−22ap in this case, is sufficient to block nearly all protein−DNA complex formation (lane 5). This concentration of oligonucleotide was instrumental in shifting roughly 95% of the probe to the triple-helical form in Figure 4B. At the same concentration, P1−18p, which does not form triplex, has little effect upon protein binding (lane 6). Although triplex formation with the probe cannot be resolved on this gel due to the low polyacrylamide percentage (5%), it is presumed that the triplex is stable throughout the protein binding period since the buffers for triplex formation and protein binding are identical. Therefore, panel B in Figures 3 and 4 is a suitable reference as to the degree of triplex formation in each of the protein binding reactions. As expected, a near-complete shift of the probe to the triple-helical form is required to prohibit the binding of protein to the probe. The data above suggest that triplex formation is directly responsible for the inhibition of nuclear factor binding to duplexes representing both the P1 and P2 polypurine- and polypyrimidine- rich regions of the murine c-*myc* promoter.

DISCUSSION

The ability of triplex formation to inhibit transcription of a target gene was first demonstrated with an oligodeoxynucleotide targeted to a polypurine:polypyrimidine nuclease-hypersensitive region upstream of the P1 start site in the human c-*myc* oncogene in a cell-free system (Cooney et al., 1988). Subsequent work has shown that c-*myc* transcription is repressed in human cervical carcinoma (HeLa) cells by treatment with the triplex-forming oligonucleotide directed to the nuclease-hypersensitive site (Postel et al., 1991). Helm et al. (1993) demonstrated that a triplex-forming oligonucleotide targeted to this same region of the c-*myc* promoter inhibits the growth of ovarian carcinoma (SKOV-3) cells and HeLa cells in culture, in keeping with the necessity for c-*myc* in proliferation (Kelly et al., 1983; Luscher & Eisenman, 1990). Although the mechanism for transcription inhibition has not been elucidated, it has been suggested that triplex formation prevents binding of essential regulatory factors (Maher et al., 1989; Gee & Miller, 1992). In the case of human c-*myc*, the triplex target is the PuF/Nm23 binding site (Postel et al., 1989; 1993). Similarly, a triplex-forming oligonucleotide known to block NFκB binding to an enhancer element (Grigoriev et al., 1992) represses transcription of the interleukin-2 receptor α-subunit gene in cultured lymphocytes (Orson et al., 1991). Triplex-induced inhibition of nuclear protein binding also inhibits transcription from the HER-2/*neu* promoter *in vitro* (Ebbinghaus et al., 1993). Blocking Sp1 binding by the formation of triplex DNA in the human Ha-*ras* promoter (Mayfield et al., 1994b; Mayfield & Miller, 1994) is sufficient to inhibit *in vitro* transcription initiation. These studies demonstrate *in vitro* and *in vivo* gene-specific transcription repression accompanying triplex targeted to nuclear protein binding sites.

The results presented here are the first to demonstrate triplex formation by the murine c-*myc* promoter. Two important regulatory regions in the *myc* promoter have been the object of our attention. The first is the polypurine: polypyrimidine region upstream of the P1 transcription initiation site that exhibits nuclease hypersensitivity. The *cis*-acting importance of this region in transcription from both the human P1 and P2 c-*myc* promoter is well documented (Lipp et al., 1987; Postel et al., 1989). A recent model proposes that it is the ability of this peculiar DNA sequence to form *intra*molecular triple helices that lends it transcriptional significance (Firulli et al., 1994). We demonstrate here that a stable antiparallel intermolecular triple helix is formed upon addition of a mixed purine/pyrimidine third strand to a duplex representing the murine P1 pur:pyr nuclease hypersensitive element.

The model mentioned above (Firulli et al., 1994), designating the triplex-forming ability of the human c-*myc* nuclease sensitive element as a positive indicator of promoter

strength, seems to contradict the prevailing notion that triplex mediates an inhibitory effect on transcription by blocking the interaction of regulatory proteins. The transcriptionally active stable triplexes in that study involve C^+•G:C and T•A:T triplets in an intramolecular complex that includes a single-stranded portion of approximately 25 bases and a parallel orientation of the polypyrimidine triplex-forming strand. The authors suggest that one or more of the proteins known to bind this nuclease hypersensitive element could function to stabilize this structure at neutral pH. The likelihood of this type of triplex occurring is not incompatible with the potential down-regulatory role of our triplex. The antiparallel triplex-forming oligonucleotide may function in skewing the equilibrium of intramolecular triplex formation such that intermolecular triplex prevails. Its repressive effect might arise by not allowing the interaction of proteins that would bind to the intramolecular triplex-induced structure in a transcriptionally-active locus. If this hypothesis is correct, the task of achieving and maintaining large molar excesses of oligonucleotide in the nucleus becomes that much more critical in down-regulating c-*myc* expression. The scenario is made exponentially more complicated by the presumed association of various proteins able to bind single- and double-stranded nucleic acids. The fact that a ribonucleoprotein binds this region of the human *myc* promoter suggests that intermolecular interactions might exist that involve the recruitment of regulatory nucleic acids by proteins to a particular subnuclear locale. As of yet, intramolecular triple helix formation has not been demonstrated in the murine c-*myc* promoter, although sequence motifs that are involved in triplex formation in the Firulli model are conserved between human and mouse.

The second important regulatory region in the c-*myc* promoter with which we have formed triplex DNA is coincident with the binding site for several activating proteins. Roussel et al. (1994) have postulated that *ets* family members and E2F-1 may independently regulate c-*myc* expression through the same binding site within this region at different times following a mitogenic stimulus. The adjacent ME1a1 element has been shown to increase initiation of c-*myc* transcription *in vitro* (Hall, 1990) and to be essential for initiation of P2 *in vivo* (Asselin et al., 1989). A zinc finger protein, termed Maz in humans, was shown to bind this site (Pyrc et al., 1992; Bossone et al., 1992). Moberg et al. (1992) named the E2F and Maz binding sites as two of the three distinct elements within the murine c-*myc* promoter that are required for transcription. Our novel triplex-forming site encompasses half of the E2F and all of the ME1a1 canonical *cis* elements. We demonstrate here that nuclear protein−DNA interaction, which we have shown through DNA competitions to be sequence-specific, is inhibited upon triplex formation between the P2 target duplex and the antiparallel oligonucleotide.

Our decision to target both the P1 and P2 promoters was based on the *in vivo* work of Postel and co-workers (Postel et al., 1991). In that study, they achieved an impressive oligonucleotide concentration of 0.35 μM in the nucleus, demonstrated decreased DNase I cleavage at the appropriate hypersensitive site, and documented a decrease in c-*myc* RNA levels. While the level of transcripts originating from P1 decreased by over 80%, the number of P2 transcripts dropped by only about 40%, in keeping with the positive regulatory role of the region from −101 to −293 in P1 transcription (Hay et al., 1987). The disparity between P1 and P2 repression levels prompted our targeting both P1 and P2 promoters, as a triplex-forming oligonucleotide directed to the P1 promoter may be sufficient in inhibiting a majority of initiation events from the P1 start site, but repression of transcription from the entire locus may additionally require triplex formation between P1 and P2.

The apparent ability of a parallel oligonucleotide to form triplex is not without precedent. Durland et al. (1990) noted that a lack of asymmetry in their target duplex allowed a 37-mer parallel oligonucleotide to reverse its orientation and thereby form triplex in an antiparallel fashion. Eosin cleavage data indicated that only 27 bp of the target were protected and that the 3′ 10 bases of the triplex-forming oligonucleotide remained unbound. Our P2 parallel oligonucleotide is highly asymmetrical and is therefore not likely to reverse its orientation and form triplex with the same bases as that of the antiparallel oligonucleotide. However, the 12 potential triplets of canonical reverse-Hoogsteen hydrogen bonding suggest that it might indeed reverse its orientation, albeit to adopt a tailed triple-helical structure similar to that described above. Further evidence supporting a reverse-Hoogsteen structure is the fact that the P2 parallel oligonucleotide featuring adenines substituted for thymines also forms triplex (data not shown). Giovannangeli et al. (1992) have demonstrated that A•A:T triplets adopt only the reverse-Hoogsteen bonding pattern, which corresponds to an antiparallel orientation in the case of a third strand with bases in the *anti* conformation. Our result differs from the Durland et al. (1990) study in that their parallel triplex with a tail displayed reduced mobility relative to that of the antiparallel triplex while our P2 parallel triplex shows slightly increased migration in comparison to the P2 antiparallel triplex.

Both the P1 and P2 murine c-*myc* targets for triplex formation are highly homologous to their equivalent regions in the human *myc* promoter. This sequence homology suggests a conserved role for these elements. Our data demonstrate the ability of the analogous human sequences (both P1 and P2) to compete for murine nuclear protein binding. That the binding is specific is shown by the inability of a nonspecific fragment of DNA to compete. The fact that the human sequences compete suggests that there are proteins with similar DNA binding specificities in the human *myc* transcription system and enhances the potential of a whole animal murine model in that it may more accurately predict human responses to triplex-forming oligonucleotides targeted to human c-*myc*.

Ultimately, we seek to generate a model for the efficacy of triplex-forming oligonucleotides to alter c-*myc* expression. One possible alternative approach might have been a transgenic mouse expressing human c-*myc* for determining the effect of human *myc*-directed triplex-forming oligonucleotides on human *myc* expression in a mouse. We chose instead to construct a whole animal model to examine the effect of targeting a native gene that is instrumental in normal cell proliferation as well as oncogenesis. Another version of this latter approach might be to test human c-*myc* oligonucleotides in a whole animal context. However, the specificity of triplex formation lessens the possibility that human *myc*-targeted oligonucleotides will form triplex with the murine *myc* promoter and turn off the endogenous gene. It is necessary, therefore, to use oligonucleotides with proven triplex-forming ability with murine DNA as well as the ability to block murine nuclear factors from binding their specific targets. Most important, though, is to assess the

effect of triplex-forming oligonucleotides on murine c-*myc* expression within a murine whole animal context.

ACKNOWLEDGMENT

We are grateful to K. Shrestha for preparation of YC8 nuclear extracts. We thank C. A. Mayfield and H. G. Kim for technical assistance and helpful discussion. We also thank B. Hughes for computer time and assistance.

REFERENCES

Alt, F. W., & Zimmerman, K. (1990) *Crit. Rev. Oncog. 2*, 75−95.
Amati, B., Brooks, M. W., Levy, N., Littlewood, T. D., Evan, G. I., & Land, H. (1993) *Cell 72*, 233−245.
Arnott, S., & Selsing, E. (1974) *J. Mol. Biol. 88*, 509−521.
Asselin, C., Nepveu, A., & Marcu, K. B. (1989) *Oncogene 4*, 549−558.
Beal, P. A., & Dervan, P. B. (1991) *Science 251*, 1360−1363.
Bentley, D. L., & Groudine, M. (1986) *Nature 321*, 702−706.
Bernard, O., Cory, S., Gerondakis, S., Webb, E., & Adams, J. M. (1983) *EMBO J. 2*, 2375−2383.
Bossone, S. A., Asselin, C., Patel, A. J., & Marcu, K. B. (1992) *Proc. Natl. Acad. Sci. U.S.A. 89*, 7452−7456.
Blackwood, E. M., Luscher, B., & Eisenman, R. N. (1992) *Genes Dev. 6*, 71−80.
Blume, S. W., Snyder, R. C., Ray, R., Thomas, S., Koller, C., & Miller, D. M. (1991) *J. Clin. Invest. 88*, 1613−1621.
Cheng, Y.-K., & Pettitt, B. M. (1992) *Prog. Biophys. Mol. Biol. 58*, 225−257.
Cheng, A.-J., & Van Dyke, M. W. (1993) *Nucleic Acids Res. 21*, 5630−5635.
Cole, M. D. (1986) *Annu. Rev. Genet. 20*, 361−384.
Cooney, M., Czernuszewicz, G., Postel, E., Flint, S. J., & Hogan, M. E. (1988) *Science 241*, 456−459.
Cory, S. (1982) *Adv. Cancer Res. 47*, 189−234.
Degols, G., Clarenc, J.-P., Lebleu, B., & Leonetti, J.-P. (1994) *J. Biol. Chem. 269*, 16933−16937.
Dignam, J. D., Lebovitz, R. M., & Roeder, R. G. (1983) *Nucleic Acids Res. 11*, 1475−1481.
Durland, R. H., Kessler, D. J., Duvic, M., & Hogan, M. E. (1990) in *Molecular Basis of Specificity in Nucleic Acid−Drug Interactions* (Pullman, B., & Jortner, J., Eds.) pp 565−578, Kluwer Academic, Boston, MA.
Durland, R. H., Kessler, D. J., Gunnell, S., Duvic, M., Pettitt, B. M., & Hogan, M. E. (1991) *Biochemistry 30*, 9246−9255.
Ebbinghaus, S. W., Gee, J. E., Rodu, B., Mayfield, C. A., Sanders, G., & Miller, D. M. (1993) *J Clin. Invest. 92*, 2433−2439.
Eick, D., & Bornkamm, G. W. (1989) *EMBO J. 8*, 1965−1972.
Eisenman, R. N. (1989) in *Oncogenes and the Molecular Origins of Cancer* (Weinberg, R. A., Ed.) pp 175−221, Cold Spring Harbor Laboratory Press, Cold Spring Harbor, NY.
Fedorova, O. S., Knorre, D. G., Podust, L. M., & Zarytova, V. F. (1988) *FEBS Lett. 228*, 273−276.
Firulli, A. B., Maibenco, D. C., & Kinniburgh, A. J. (1994) *Arch. Biochem. Biophys. 310*, 236−276.
Gaubatz, S., Meichle, A., & Eilers, M. (1994) *Mol. Cell. Biol. 14*, 3853−3862.
Gee, J. E., & Miller, D. M. (1992) *Am. J. Med. Sci. 304*, 366−372.
Gee, J. E., Blume, S., Snyder, R. C., Ray, R., & Miller, D. M. (1992) *J. Biol. Chem. 267*, 11163−11167.
Ghanta, V. K., Hiramoto, N. S., Soong, S.-J., Miller, D. M., & Hiramoto, R. H. (1993) *Int. J. Neurosci. 71*, 251−265.
Giovannangeli, C., Rougée, M., Garestier, T., Thuong, N. T., & Hélène, C. (1992) *Proc. Natl. Acad. Sci. U.S.A. 89*, 8631−8635.
Grigoriev, M., Praseuth, D., Robin, P., Hemar, A., Saison-Behmoaras, T., Dautry-Varsat, A., Thuong, N. T., Hélène, C., & Harel-Bellan, A. (1992) *J. Biol. Chem. 267*, 3389−3395.
Hall, D. J. (1990) *Oncogene 5*, 47−54.
Hann, S. R., Abrams, H. D., Rohrschneider, L. R., & Eisenman, R. N. (1983) *Cell 34*, 789−798.
Hay, N., Bishop, J. M., & Levens, D. (1987) *Genes Dev. 1*, 659−671.
Hélène, C. (1991) *Eur. J. Cancer 27*, 1466−1471.
Helm, C. W., Shrestha, K., Thomas, S., Shingleton, H. M., & Miller, D. M. (1993) *Gynecol. Oncol. 49*, 339−343.
Kato, G. J., & Dang, C. V. (1992) *FASEB J. 6*, 3065−3072.
Kelly, K., Cochran, B. H., Stiles, C. D., & Leder, P. (1983) *Cell 35*, 603−610.
Kolluri, R., Torrey, T. A., & Kinniburgh, A. J. (1992) *Nucleic Acids Res. 20*, 111−116.
Kolwi-Shigematsu, T., & Kolwi, Y. (1991) *Nucleic Acids Res. 19*, 4267−4271.
Lavenu, A., Pournin, S., Babinet, C., & Morello, D. (1994) *Oncogene 9*, 527−536.
Lipp, M., Schilling, R., Wiest, S., Laux, G., & Bornkamm, G. W. (1987) *Mol. Cell. Biol. 7*, 1393−1400.
Lu, G., & Ferl, R. J. (1993) *Int. J. Biochem. 25*, 1529−1537.
Luscher, B., & Eisenman, R. N. (1990) *Genes Dev. 4*, 2025−2035.
Maher, L. J., Dervan, P. B., & Wold, B. (1989) *Science 245*, 725−730.
Marcu, K. B., Bossone, S. A., & Patel, A. J. (1992) *Annu. Rev. Biochem. 61*, 809−860.
Mayfield, C., & Miller, D. (1994) *Nucleic Acids Res. 22*, 1909−1916.
Mayfield, C., Squibb, M., & Miller, D. (1994a) *Biochemistry 33*, 3358−3363.
Mayfield, C., Ebbinghaus, S., Gee, J., Jones, D., Rodu, B., Squibb, M., & Miller, D. (1994b) *J. Biol. Chem. 269*, 18232−18238.
Maxam, A., & Gilbert, W. (1980) *Methods Enzymol. 65*, 499−560.
Mergny, J. L., Duval-Valentin, G., Nguyen, C. H., Perroualt, L., Faucon, B., Rougée, M., Montenay-Garestier, T., Bisagni, E., & Hélène, C. (1992) *Science 256*, 1681−1684.
Milligan, J. F., Krawczyk, S. H., Wadwani, S., & Matteucci, M. D. (1993) *Nucleic Acids Res. 21*, 327−333.
Moberg, K. H., Logan, T. J., Tyndal, W. A., & Hall, D. J. (1992) *Oncogene 7*, 411−421.
Moser, H. E., & Dervan, P. B. (1987) *Science 238*, 645−650.
Olivas, W. M., & Maher, L. J., III (1995) *Biochemistry 34*, 278−284.
Orson, F. M., Thomas, D. W., McShan, W. M., Kessler, D. J., & Hogan, M. E. (1991) *Nucleic Acids Res. 19*, 3435−3441.
Postel, E. H., Mango, S., & Flint, S. J. (1989) *Mol. Cell. Biol. 9*, 5123−5133.
Postel, E. H., Flint, S. J., Kessler, D. J., & Hogan, M. E. (1991) *Proc. Natl. Acad. Sci. U.S.A. 88*, 8227−8231.
Postel, E. H., Berberich, S. J., Flint, S. J., & Ferrone, C. A. (1993) *Science 261*, 478−480.
Praseuth, D., Perrouault, L., LeDoan, T., Chassignol, M., Thuong, N., & Hélène, C. (1988) *Proc. Natl. Acad. Sci. USA 85*, 1349−1353.
Prendergast, G. C., Lawe, D., & Ziff, E. B. (1991) *Cell 65*, 395−407.
Pyrc, J. J., Moberg, K. H., & Hall, D. J. (1992) *Biochemistry 31*, 4102−4110.
Rajagopal, P., & Feigon, J. (1989) *Nature 339*, 637−640.
Ray, R., Snyder, R. C., Thomas, S., Koller, C. A., & Miller, D. M. (1989) *J. Clin. Invest. 83*, 2003−2007.
Ray, R. S., Thomas, S., & Miller, D. M. (1990) *Am. J. Med. Sci. 299*, 203−208.
Roussel, M. F., Davis, J. N., Cleveland, J. L., Ghysdael, J., & Hiebert, S. W. (1994) *Oncogene 9*, 405−415.
Ruppert, C., Goldwitz, D., & Wille, W. (1986) *EMBO J. 5*, 1897−1903.
Siebenlist, U., Hennighausen, L., Battey, J., & Leder, P. (1984) *Cell 37*, 381−391.
Snyder, R. C., Ray, R., Blume, S., & Miller, D. M. (1991) *Biochemistry 30*, 4290−4297.
Steeg, P. S., Bevilacqua, G., Kopper, L., Thorgeirsson, U. P., Talmadge, J. E., Liotta, L. A., & Sobel, M. E. (1988) *J. Natl. Cancer Inst. 80*, 200−204.
Strobel, S. A., & Dervan, P. B. (1990) *Science 249*, 73−75.
Taub, R., Moulding, C., Battey, J., Murphy, W., Vasicek, T., Lenoir, G. M., & Leder, P. (1984) *Cell 36*, 511−526.
Van Dyke, M. W., & Dervan, P. B. (1983) *Biochemistry 22*, 2373−2377.
Wells, R. D., Collier, D. A., Hanvey, J. C., Shimizu, M., & Wohlrab, F. (1988) *FASEB J. 2*, 2939−2949.
Yang, J., Bauer, S. R., Mushinsky, J. F., & Marcu, K. B. (1985) *EMBO J. 4*, 1441−1447.

BI942740O

Reprinted from Biochemistry, 1995, 34.

Appendix 6

The c-*myc* Promoter Binding Protein (MBP-1) and TBP Bind Simultaneously in the Minor Groove of the c-*myc* P2 Promoter†

Divya Chaudhary‡ and Donald M. Miller*,‡,§,||

Department of Medicine and Department of Biochemistry and Molecular Genetics, Comprehensive Cancer Center, University of Alabama at Birmingham, Birmingham, Alabama 35294-3300, and Birmingham Veterans Affairs Medical Center, Birmingham, Alabama 35294-0001

Received July 22, 1994; Revised Manuscript Received November 29, 1994⊗

ABSTRACT: The c-*myc* promoter binding protein (MBP-1) is a DNA binding protein which negatively regulates the expression of the human c-*myc* gene. MBP-1 binds to a sequence which overlaps the binding site for the general transcription factor TBP, within the c-*myc* P2 promoter region. Since TBP binds in the minor groove, MBP-1 might inhibit c-*myc* transcription by preventing the formation of a functional preinitiation complex. In support of this hypothesis, we have demonstrated that MPB-1 is a minor groove binding protein. In order to characterize MBP-1 binding, we substituted A-T base pairs in the MBP-1 binding site with I-C base pairs, which changes the major groove surface without altering the minor groove surface. This substitution did not inhibit the sequence-specific binding of MBP-1 and TBP. On the other hand, G-C to I-C substitution within the MBP-1 binding site alters the minor groove and prevents MBP-1 binding. Competitive electrophoretic mobility shift assays were used to show that berenil, distamycin, and mithramycin, all of which bind in the minor groove, compete with MBP-1 for binding to the MPB-1 binding site. These minor groove binding ligands also effectively inhibit the simultaneous DNA binding activity of both MBP-1 and TBP. We conclude that both MBP-1 and TBP can bind simultaneously in the minor groove of the TATA motif on the c-*myc* P2 promoter. This suggests that MBP-1 may negatively regulate c-*myc* gene expression by preventing efficient transcription initiation.

The c-*myc* protooncogene plays an important role in the regulation of cellular proliferation and differentiation (Marcu *et al.*, 1992; Spencer & Groudine, 1991). The level of c-*myc* expression correlate with the rate of cell proliferation in most cell types, and induction of c-*myc* expression has been associated with the entry of cells into the cell cycle. Overexpression of the c-*myc* gene is common in the phenotypic abnormalities of many maglignant cell types (Cole, 1986); therefore, the mechanisms regulating c-*myc* expression are central to understanding the role of c-*myc* in cell transformation.

In mouse plasmacytomas and in human Burkitt's lymphoma cell lines, the translocated form of the c-*myc* gene is often the only allele which is transcribed, usually in a constitutive and elevated manner (Cory, 1986). This may be caused by the loss of a negative regulatory region during translocation. The explanation correlates with the observations of Grignani *et al.* (1990), who showed that c-*myc* is involved in an autoregulatory loop which is operative in primary and nontumorigenic cell lines but lost in transformed cell lines. They reported that this autoregulation occurs at the level of transcriptional initiation and involves a stable intermediate. This evidence further suggests that the negative regulation of c-*myc* expression may play a very important role in oncogenesis.

The human c-*myc* promoter binding protein, MBP-1, binds the c-*myc* P2 promoter and negatively regulates c-*myc* promoter function in cotransfection assays with *myc*−CAT constructs (Ray & Miller, 1991). Most studies have shown that the P1 and P2 promoters of the c-*myc* gene, which are separated by 160 bp, are subject to independent regulation (Broome *et al.*, 1987; Lipp *et al.*, 1989). MBP-1 is a 37 kDa protein and has been shown to bind in a region +123 to +153 bp relative to P1 on the c-*myc* P2 promoter. The binding site for MBP-1 on the c-*myc* P2 promoter region includes the transcription factor TBP binding site. These features suggest a possible mechanism by which MBP-1 might function and prompted us to compare the groove binding properties of MBP-1 to those of TBP.

The DNA binding antibiotic mithramycin binds as a dimer and spans 6 bp in the minor groove of G-C-rich sequences (Cons & Fox, 1989; Sarker & Chen, 1989; Sastry & Patel, 1993). Mithramycin has been shown to bind the c-*myc* promoter and block transcription initiation *in vitro* (Snyder *et al.*, 1991). One of the strongly protected regions within the c-*myc* promoter is from +110 bp to +128 bp relative to P1 promoter. The large region of the P2 promoter which binds mithramycin indicates that several drug molecules bind adjacent to one another. This region overlaps the first 5 bp of the MBP-1 binding site on the c-*myc* P2 promoter.

Distamycin, berenil, netropsin, and the Hoechst dye 33258 are nonintercalating minor groove binding ligands characterized by their B-DNA and A-T-specific interactions. Distamycin binding spans 5 bp in the minor groove (Coll *et al.*,

† This work was supported by NIH Grants RO1 CA42664 and RO1 CA42337, by a Veterans Administration Merit Review Grant, and by a Share Foundation Grant (to D.M.M.).

* Correspondence should be addressed to this author at the Division of Hematology/Oncology, University of Alabama at Birmingham. Phone: 205-934-1977. Fax: 205-975-6911.

‡ Department of Biochemistry and Molecular Genetics, University of Alabama at Birmingham.

§ Department of Medicine, University of Alabama at Birmingham.

|| Birmingham Veterans Affairs Medical Center.

⊗ Abstract published in *Advance ACS Abstracts*, March 1, 1995.

0006-2960/95/0434-3438$09.00/0

1987; Ford & Rickwood, 1984) and causes changes in the width of the helical minor groove (Fox & Waring, 1984). X-ray analysis of the netropsin−DNA complex has shown that netropsin binds within the minor groove by displacing the water molecules of the spine of hydration, by similar interactions as in the distamycin−DNA complex (Kopka *et al.*, 1985). NMR studies of the DNA binding characteristics of berenil show large changes in the chemical shift for protons in the DNA minor groove (Jenkins *et al.*, 1993). X-ray crystallographic studies on a berenil−DNA complex by Brown *et al.* (1992) have shown that there is no significant alteration in the B-type DNA after berenil binding.

Several investigators have reported the use of minor groove binding ligands as competitors in DNA binding assays with DNA binding proteins for ascertaining their groove binding characteristics (Mattes, 1990; Grokhovskii *et al.*, 1989; Sidorva *et al.*, 1991). Dickinson *et al.* (1992) used distamycin as a competitor for DNA binding of a tissue-specific nuclear matrix/scaffold associating protein, SATB1, using drug−protein competition to study its minor groove recognition characteristics. Distamycin and netropsin as well as Hoechst 33258 effectively compete with HMG-I proteins for binding in the minor groove of DNA (Reeves & Nissen, 1990). Other examples that have been studied by this method include human DNA ligase (Ciarrocchi *et al.*, 1991), binding of polyamines in the minor groove of B-DNA (Schmid & Behr, 1991), sequence-specific synthetic DNA binding peptides which bind in the minor groove (Grokhovsky *et al.*, 1991), topoisomerase I−DNA interaction (Mortenson *et al.*, 1990), and minor groove recognition by histone H1 (Kas *et al.*, 1989).

Starr and Hawley (1991) used a novel approach to show that the general transcription factor TBP binds in the minor groove of the TATA box motif. An artificial TATA box sequence was used in which all of the adenine and thymine residues were replaced by inosines and cytosines. These substitutions alter the surface of the major groove but do not change the surface of the minor groove. The interaction of TBP with the sequence substituted from TATAAA to CICIII was the same as that of the wild-type sequence, confirming minor groove binding. This approach has also been used in studies to elucidate the minor groove binding of the HMG box-containing regulatory proteins: lymphoid enhancer factor 1 by Giese *et al.* (1992) and the high mobility group protein HMGI(Y) by Thanos and Maniatis (1992).

We have used this approch, as well as competition for DNA binding with minor groove binding ligands, to show that MBP-1, like TBP, binds in the minor groove of the c-*myc* P2 promoter. This result lends strong support to the hypothesis that negative regulation of the c-*myc* promoter by MBP-1 is mediated through disrupting or preventing the formation of the transcription initiation complex.

EXPERIMENTAL PROCEDURES

Probes. A 50 bp oligonucleotide (−52 to +2 relative to the P2 start site on the c-*myc* promoter) and its complement oligonucleotide were synthesized and purified by reverse-phase oligonucleotide purification/elution cartridges (Clontech). The oligonucleotide was radiolabeled using [γ-^{32}P]-dATP with T4 polynucleotide kinase (Gibco BRL). It was then annealed to its complement by heating at 90 °C for 10 min in 20 mM Tris-HCl (pH 7.4), 10 mM $MgCl_2$ and slow-cooling at room temperature to form a radiolabeled double-stranded probe.

The A:T to I:C substitution of the TATA motif was made by substituting TATAA for CICIII; 50 bp oligonucleotides were synthesized and purified in the same manner as the wild-type oligonucleotides. They were then used to make radiolabeled probe as described above, for electrophoretic mobility shift analysis. The mutant DNA fragment used as a competitor in the protein binding assays has been described previously (Ray & Miller, 1991). The G:C to I:C substitution was done at the GC bp −33 relative to the P2 start site, and the complementary 34 bp oligonucleotides with this sequence change were synthesized. The 34 bp oligonucleotides were purified and annealed as before to be used as a competitor in protein binding assays.

The NFkB binding site double-stranded oligonucleotide was purchased from Promega. End-labeling was performed as before, and the DNA fragment was purified by ethanol precipitation.

Minor Groove Binding Ligands. Distamycin A, berenil (diminiazine aceturate), and mithramycin were purchased from Sigma Chemical Co. These compounds were prepared in distilled water as 10^{-2} M stock solutions and stored at −20 °C.

Protein Extracts. The MBP-1 cDNA was cloned in both orientations in the prokaryotic expression vector pGemex-1 (Promega). The pGemex-MBP-1 clones and the pGemex plasmid alone were used to transform the JM109(DE3) *Escherichia coli* strain. Protein extracts were prepared from these transformed strains as follows. The induced bacterial extracts were partially purified by ammonium sulfate fractionation and precipitation. Cells were grown to an OD_{600} of 0.6 and induced with 0.4 mM IPTG for 3 h followed by lysis and fractionation as described by Pognonec *et al.* (1991). The extracts from the MBP-1 cDNA-containing strains had a total protein concentration of 1 μg/μL, and the extracts from the strains containing the plasmid alone had a total protein concentration of 0.5 μg/μL, as estimated by the colorometric Bradford assay (Bradford, 1976).

The bacterial extract containing recombinant TBP was prepared from the BL21(DE3) *E. coli* strain containing the TBP cDNA cloned in a pET expression vector (provided by Dr. R. G. Roeder). Purified TBP and NFkB proteins were purchased from Promega.

Binding Assays for MBP-1. The DNA−protein binding reactions were carried out in 10 mM Tris-HCl (pH 7.5), 100 mM NaCl, 1 mM EDTA, 1 mM DTT, 4% glycerol, and 5 μg of poly[d(I-C)] for 30 min at 37 °C. In some cases, the binding reactions were carried out in the same buffer conditions as for the TBP−DNA binding reactions (described below). Each reaction contained approximately 0.02 pmol of radiolabeled DNA and 1 μL of bacterial extract from the MBP-1 cDNA-transformed strains or 2 μL of bacterial extract from the cells transformed with plasmid alone, in a final volume of 10 or 20 μL. Unlabeled DNA competitor for protein binding was added (wherever mentioned) in 100-fold excess of labeled probe DNA. The protein−DNA binding reactions were analyzed by electrophoresis on a 6% nondenaturing polyacrylamide gel containing 89 mM Tris−borate and 2 mM EDTA.

In the MBP-1−DNA binding assays containing mithramycin, the reactions were performed as above, but with 6.5 mM $MgCl_2$ and at 37 °C for 20 min. The control protein

binding reactions for this set of assays were also done under identical conditions. The MBP-1−DNA binding reactions in the presence or absence of distamycin and berenil were carried out in 20 mM Tris-HCl (pH 8.0), 1.5 mM $MgCl_2$, 25 mM KCl, 1 mM DTT, 4% glycerol, and 5 μg of poly-[d(I-C)] at room temperature for 20 min with the same DNA and protein concentrations as above. All binding reactions were resolved on 6% nondenaturing polyacrylamide gels as described earlier.

Binding Assays for TBP and NFkB. The DNA binding assays for NFkB were carried out in 10 mM Tris-HCl (pH 7.5), 50 mM NaCl, 1 mM $MgCl_2$, 0.5 mM DTT, 0.5 mM EDTA, 4% glycerol, and 0.5 μg of poly[d(I-C)] at room temperature for 30 min; 0.02 pmol of radiolabeled DNA probe and 1 gsu of NFkB (Promega) were used for each binding reaction. The NFkB−DNA binding assays which were performed in the presence or absence of mithramycin were carried out in the same buffer with 6.5 mM $MgCl_2$ at 37 °C for 20 min. All reactions were analyzed by nondenaturing polyacrylamide gel electrophoresis as noted above.

The TBP−DNA binding assays, which were performed in the presence or absence of minor groove binding ligands, were carried out in 20 mM Tris-HCl (pH 7.9), 80 mM KCl, 10 mM $MgCl_2$, 2 mM DTT, and 4% glycerol for 15 min at 37 °C (Promega); 0.02 pmol of radiolabeled DNA and 4 ng of TBP (Promega) were used per reaction. The TBP−DNA binding reactions were analyzed on a 6% nondenaturing polyacrylamide gel containing 2.5 mM $MgCl_2$, 0.05% NP-40, 89 mM Tris−borate, and 2 mM EDTA.

Simultaneous Protein Binding Assays. The simultaneous MBP-1 and TBP DNA binding assays, which were performed in the absence or presence of minor groove binding ligands, were carried out in the TBP−DNA binding reaction buffer. All reactions contained 0.02 pmol of radiolabeled DNA probe, 1 μL of bacterial extract containing recombinant MBP-1, and/or 4 ng of TBP (Promega) as before. These reactions were carried out at 37 °C for 20 min and analyzed by nondenaturing polyacrylamide gel electrophoresis as described for the TBP−DNA binding reactions.

RESULTS

Electrophoretic Mobility Shift Analysis. The MPB-1 binding site of the c-*myc* P2 promoter is a 34 bp region which overlaps the TBP binding site. This region was used as a probe in electrophoretic mobility shift assays to study the binding characteristics of MBP-1. Recombinant MBP-1-containing bacterial extracts from cells containing the pGemex-MBP-1 clone were able to specifically retard the electrophoretic mobility of the P2 promoter fragment as shown by the experiment in Figure 1. Induced bacterial extracts from cells which contained the MBP-1 cDNA clone in the negative orientation as well as induced extracts from cells which contained the parent pGemex plasmid did not cause a MBP-1-specific electrophoretic mobility shift (Figure 1, lanes 2, 5, and 7). The induced extract generates a specific and a nonspecific electrophoretic mobility shift when lower nonspecific DNA concentrations are used in the binding reaction. Increasing the concentration of nonspecific DNA as target DNA, in the binding reaction, competes with the nonspecific DNA binding activity in the protein extract but does not affect the specific DNA binding activity by recombinant MBP-1 (data not shown and Figure 6, lanes 2 and 3). Specificity of binding was also determined by competing the MBP-1-specific binding with excess unlabeled DNA fragment, whereas an excess of a mutated unlabeled DNA fragment did not compete for binding (data not shown and Figure 3). The P2 promoter fragment used above was also used in electrophoretic mobility shift assays which demonstrated binding to the TATA binding protein, TBP (Figure 1, lane 3).

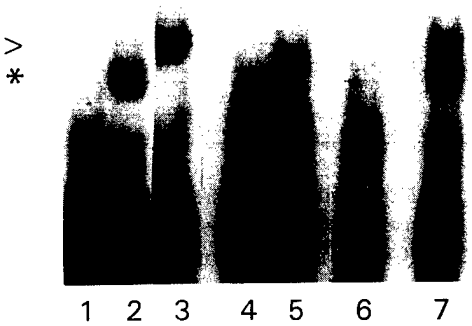

FIGURE 1: Gel mobility shift assay of a 50 bp duplex oligonucleotide containing thec-*myc* P2 promoter region. Lanes 1, 4, and 6, DNA control; lane 2, binding reaction with partially purified extract from cells containing the MBP-1 cDNA cloned in the negative orientation; lane 3, binding reaction with TBP; lane 5, binding reaction with partially purified extract from cells containing the vector plasmid alone; lane 7, binding reaction with partially purified bacterial extract containing recombinant MBP-1 protein. The arrow shows the specific TBP-bound DNA shift in lane 3 and specific MBP-1-bound DNA shift in lane 7, and the asterisk shows the nonspecific protein-bound DNA shifts in lanes 2, 5, and 7.

Recombinant MBP-1 from the pGemex-MBP-1 clone was used to characterize DNA binding at different temperatures and for different binding reaction times. MBP-1−DNA binding was found to be similar at room temperature, 4 or 37 °C, and the binding activity was observed after incubation periods as short as 5 min (data not shown).

Protein Binding to IC-Substituted Oligonucleotides. To determine whether MBP-1 binds to the major groove on the DNA, we substituted the TATAAA motif of the P2 promoter fragment with CICIII, thereby altering the major groove surface and leaving the minor groove surface as before in terms of hydrogen donors and acceptors. TBP was used as a control, since TBP has been shown to bind to the IC-substituted TATA box region on the adenovirus major late promoter (Starr & Hawley, 1991). For the experiment shown in Figure 2A, an induced extract containing recombinant MBP-1 was used in an electrophoretic mobility shift analysis of protein binding to the radiolabeled CICIII-substituted P2 promoter fragment. The electrophoretic mobility shift (Figure 2A, lane 1) indicates that alteration of the major groove had no effect on the DNA binding activity of MBP-1. Figure 2B,C shows the control experiments in which the same DNA fragment can generate an electrophoretic mobility shift by extract containing recombinant TBP and commercially available purified TBP, respectively. These experiments suggest that MBP-1, like TBP, binds on the minor groove surface of the DNA.

As a further test of minor groove binding, the converse experiment was also performed. A single G-C base pair on the MBP-1 binding site in the P2 promoter fragment was substituted by an I-C base pair. This substitution specifically alters the minor groove surface at that base pair but leaves the major groove identical to the normal binding site. The

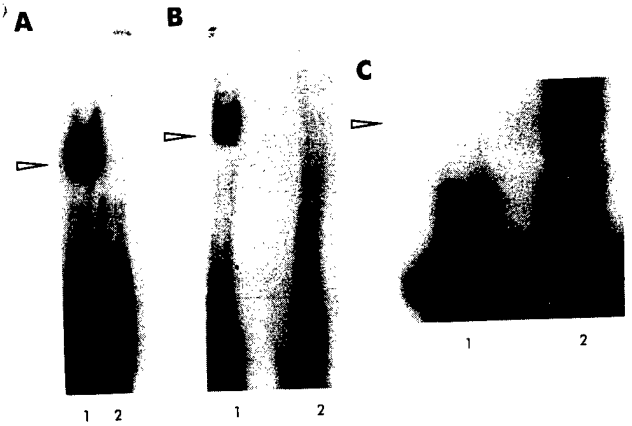

FIGURE 2: Gel mobility shift assay of a 50 bp duplex oligonucleotide containing the c-*myc* P2 promoter fragment with the core TATAAA sequence motif substituted to CICIII. (A) Lane 1, binding reaction with extract containing recombinant MBP-1 protein; lane 2, DNA control. (B) Lane 1, binding reaction with extract containing recombinant TBP protein; lane 2, DNA control. (C) Lane 1, DNA control; lane 2, binding reaction with TBP (Promega).

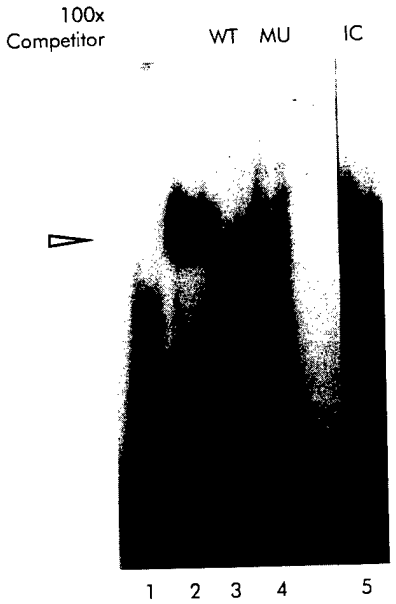

FIGURE 3: Competitive gel mobility shift assays with a 50 bp duplex oligonucleotide c-*myc* P2 promoter fragment (as in Figure 2). Lane 1, DNA control. Lane 2, binding reaction with extract containing recombinant MBP-1 protein. Lanes 3−5, competition for MBP-1 binding by adding excess cold 34 bp duplex oligonucleotides. WT, containing the MBP-1 binding site (lane 3); MU, containing a mutant MBP-1 binding site (lane 4); IC, containing the MBP-1 binding site with a single GC to IC substitution (lane 5).

electrophoretic mobility shift assay with the CICIII-substituted P2 promoter fragment and extract containing recombinant MBP-1 was performed in a competition experiment (Figure 3) using excess unlabeled wild-type binding site (lane 3), mutant binding site (lane 4), and G-C- to I-C-substituted binding site (lane 5). MBP-1 binding is specifically competed only when excess unlabeled wild-type binding site is used, but not when an excess unlabeled mutant binding site or minor groove altered binding site is used. The binding properties exhibited by MBP-1 in these experiments clearly suggest minor groove recognition of the c-*myc* P2 promoter.

Effect of Minor Groove Binding Ligands on MBP-1−DNA Binding. The compounds mithramycin, distamycin, and

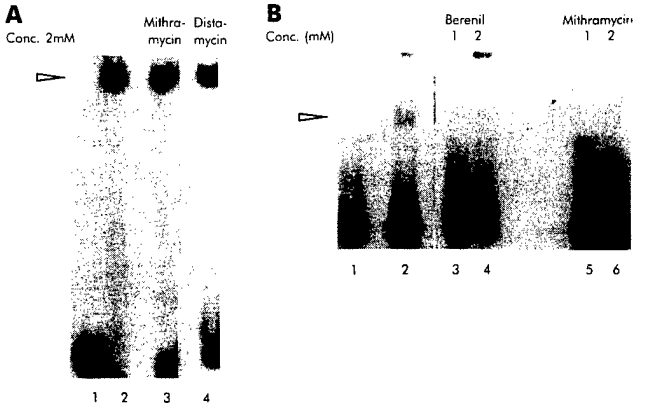

FIGURE 4: Gel mobility shift assay in the presence or absence of minor groove binding ligands. (A) Lane 1, DNA control (NFkB binding site duplex); lane 2, NFkB alone; lane 3, NFkB binding in the presence of 2×10^{-3} M mithramycin; lane 4, NFkB binding in the presence of 2×10^{-3} M distamycin. (B) Lane 1, DNA control; lane 2, TBP alone; lanes 3 and 4, TBP binding in the presence of 1×10^{-3} and 2×10^{-3} M berenil; lanes 5 and 6, TBP binding in the presence of 1×10^{-3} and 2×10^{-3} M mithramycin.

berenil possess and property of minor groove recognition for DNA binding. This property has been used to ascertain the groove binding characteristics of MBP-1. In order to conclusively prove this, a major groove binding protein, NFkB, and a minor groove binding protein, TBP, have been used in a parallel study. Similar DNA concentrations have been used in electrophoretic mobility shift experiments, and the abilities of minor groove binding ligands to compete for DNA binding at similar ligand concentrations have been compared for all three proteins. Partially purified recombinant MBP-1 was used for all ligand binding competition assays.

Figure 4A shows that neither distamycin nor mithramycin is able to compete with NFkB−DNA binding at a concentration of 2 mM. On the other hand, lower ligand concentrations (1 and 2 mM) effectively compete with TBP−DNA binding (Figure 4B). Figure 5B shows that an even lower concentration (0.2 mM) of distamycin and berenil can significantly compete with TBP−DNA binding. Similarly, distamycin and berenil have an inhibitory effect on DNA binding by recombinant MBP-1 in an electrophoretic mobility shift assay at concentrations as low as 0.2 mM (Figure 5A). This further suggests that MPB-1, like TBP, recognizes the minor groove surface on the DNA. We have also successfully tested the ability of two other minor groove binding ligands (netropsin and Hoecsht dye 33258) to compete with the DNA binding activity of recombinant MBP-1 (data not shown).

Effect of Minor Groove Binding Ligands on MBP-1−TBP−DNA Binding. The minor groove binding ligands have been effective in competing with both MBP-1 and TBP for DNA binding, suggesting that both proteins bind on the same surface of the c-*myc* P2 promoter region. Although the MPB-1 binding site is larger and includes the TBP binding site, both proteins bind together on the c-*myc* P2 promoter (Figure 6), raising the question of whether the simultaneous binding of two minor groove binding proteins on the same DNA region can be competed by minor groove binding ligands. This was tested in a competition electrophoretic mobility shift assay, which allows both MBP-1 and TBP to bind simultaneously to the target DNA (Figure 6, lanes 5−12).

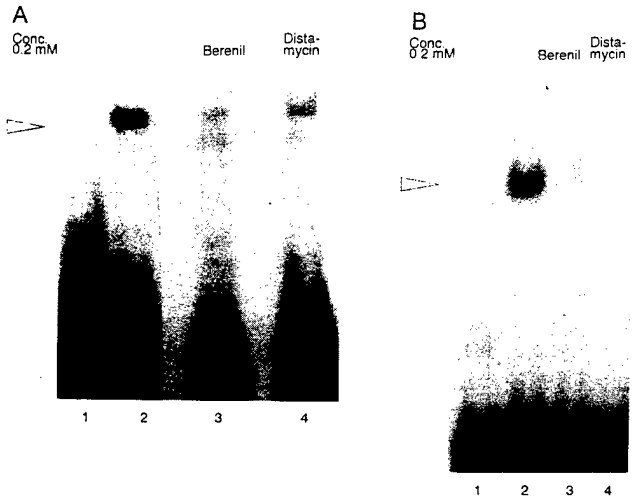

FIGURE 5: Distamycin and berenil compete with MBP-1 and TBP for DNA binding. (A) Lane 1, DNA control (as in Figure 1); lane 2, binding reaction with recombinant MBP-1 alone; lanes 3 and 4, MBP-1 binding reaction with 0.2×10^{-3} M berenil and distamycin, respectively. (B) Lane 1, DNA control; lane 2, binding reaction with TBP alone; lanes 3 and 4, TBP binding reaction with 0.2×10^{-3} M berenil and distamycin, respectively.

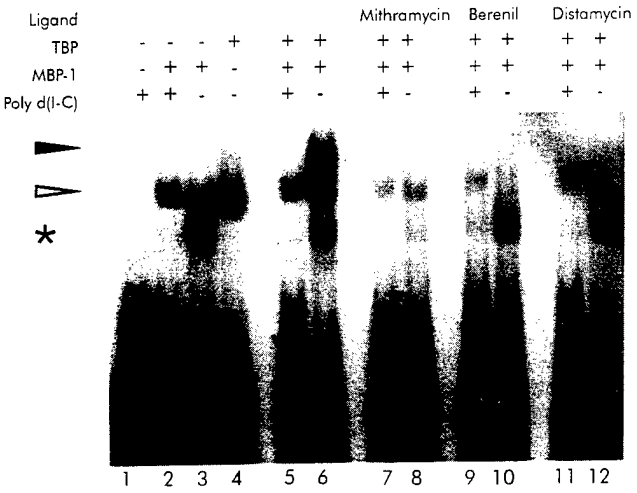

FIGURE 6: Minor groove binding ligands inhibit the simultaneous binding of MPB-1 and TBP on the c-*myc* P2 promoter. Lane 1, DNA control (as in Figure 1); lanes 2 and 3, binding reaction with recombinant MBP-1 in the presence and absence of poly[d(I-C)], respectively; lane 4, binding reaction with TBP; lanes 5−12, binding reaction with both TBP and MBP-1 in the presence of poly-[d(I-C)] (lanes 5, 7, 9, and 11) or in the absence of poly[d(I-C)] (lanes 6, 8, 10, and 12), and with 1×10^{-3} M mithramycin (lanes 7 and 8), berenil (lanes 9 and 10), or distamycin (lanes 11 and 12). The solid arrow shows the dual protein-bound DNA shift, the open arrow shows the single protein-bound DNA shift, and the asterisk shows the nonspecific protein-bound DNA shift.

Partially purified bacterial extracts containing recombinant MBP-1 give a nonspecific band in an electrophoretic mobility shift assay when the binding reaction is carried out in the absence of poly[d(I-C)] (Figure 6, compare lanes 2 and 3; Figure 1). Partially purified bacterial extracts from cells containing the parent pGemex plasmid result in the same nonspecific band upon electromobility shift analysis (Figure 1, lane 5). Figure 7 shows the results of simultaneous protein binding assays using purified TBP and partially purified extracts from cells containing the pGemex vector. The two electromobility shifts seen are the TBP-bound DNA and the

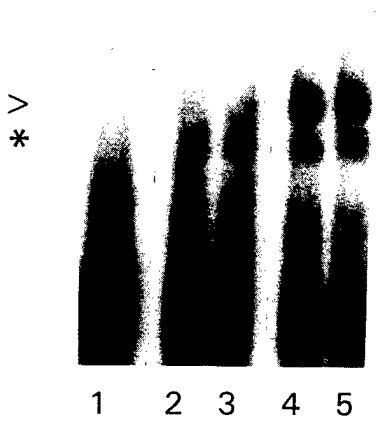

FIGURE 7: Partially purified protein extracts that do not contain recombinant MBP-1 do not form dual protein-bound DNA complex with TBP upon DNA binding. Lane 1, DNA control; lanes 2 and 3, binding reactions with 2 and 4 μL, respectively, of protein extract (0.5 μg/μL total protein) from bacterial cells that contain the vector plasmid without the MBP-1 cDNA; lanes 4 and 5, dual protein binding reactions (as in Figure 6) with TBP and the same concentration of protein extracts as in lanes 2 and 3. The arrow shows the specific TBP-bound DNA shift, and the asterisk shows the nonspecific DNA binding activity.

nonspecific DNA binding activity present in these partially purified extracts. Commercially available purified TBP binds DNA in the absence of any poly[d(I-C)] in the binding reaction (Figure 6, lane 4) as per the manufacturer (Promega). Therefore, simultaneous protein binding reactions for Figure 6 were done both in the presence (lane 5) and in the absence (lane 6) of poly[d(I-C)]. When comparing lanes 3 and 6, the composition of the binding reactions differs only in the absence and presence of purified TBP, respectively. In the absence of poly[d(I-C)], there is a supershift obtained (lane 6), and this is due to the simultaneous binding of MBP-1 and TBP to the 50 bp P2 promoter fragment. The presence of poly[d(I-C)] is not optimal for DNA binding by purified TBP, so no supershift for dual protein binding is seen in the presence of poly[d(I-C)] in lane 5. Mithramycin, berenil, and distamycin (1 mM) are able to inhibit this supershift caused by dual protein binding (lanes 8, 10, and 12) and to some extent the single protein-bound shift (lanes 7−12). The effect of these minor groove binding ligands differs in the competition for minor groove binding as seen in Figure 6, and this can be explained and correlated with the differing DNA recognition properties for these ligands (see Discussion). Berenil is more effective than distamycin and mithramycin in terms of specifically inhibiting the formation of protein−DNA complexes.

Berenil can specifically inhibit both the single protein shift and the dual protein-bound supershift (Figure 8B) at concentrations as low as 0.1 mM (lane 3) and 0.2 mM (lane 4). In a control experiment, berenil is ineffective in a competitive electrophoretic mobility shift assay with the major groove binding NFkB−DNA binding activity (Figure 8A). The experiments here show that both MBP-1 and TBP bind the P2 promoter region simultaneously and do not compete with each other for DNA binding under *in vitro* conditions. These observations lead us to conclude that the minor groove of the c-*myc* P2 promoter region is the common recognition motif for simultaneous binding by both the general transcription factor TBP and MBP-1, a negative regulator of c-*myc* expression.

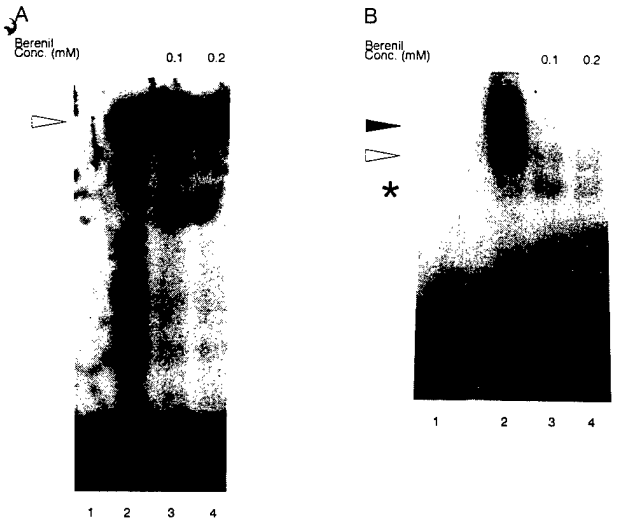

FIGURE 8: Berenil inhibits the DNA binding activity of both MBP-1 and TBP but not NFkB. (A) Lane 1, DNA control (as in Figure 4A); lane 2, binding reaction with NFkB; lanes 3 and 4, NFkB binding reaction with 0.1×10^{-3} and 0.2×10^{-3} M berenil, respectively. (B) Lane 1, DNA control (as in Figure 1); lane 2, binding reaction with recombinant MBP-1 and TBP; lanes 3 and 4, MBP-1 and TBP binding reaction with 0.1×10^{-3} and 0.2×10^{-3} M berenil, respectively. The solid arrow shows the dual protein-bound DNA shift, the open arrow shows the single protein-bound shift, and the asterisk shows the nonspecific protein-bound shift.

DISCUSSION

MBP-1 Binds in the Minor Groove of the c-myc P2 Promoter. This paper presents evidence that MBP-1 binds in the minor groove surface of the c-*myc* P2 promoter TATA box motif. One line of evidence supporting this conclusion is the major and minor groove alteration experiments. These experiments utilize a well-characterized approach (Starr & Hawley, 1991) which takes advantage of the dissimilarity of major groove surface for A-T and I-C base pairs and the dissimilarity of minor groove surface for G-C and I-C base pairs. The hydrogen acceptors and donors for the G-C to I-C base substitution are identical in the major groove but differ in the minor groove. The converse applies for the A-T to I-C substitution. The TATA box motif of the c-*myc* promoter is flanked by several G-C base pairs, so the sequence of the MBP-1 binding site was optimal for this strategy. MBP-1 binding was unaffected when the major groove was altered and inhibited when the minor groove was altered. This finding has several important implications as discussed below.

Some studies have linked the minor groove recognition property of a protein to its ability to bend the DNA upon binding (Suck *et al.*, 1988; White *et al.*, 1989; Giese *et al.*, 1992). Since many of the sequence-specific DNA binding proteins recognize the major groove at their binding site (Suzuki, 1993), bending of the DNA may well be necessary to accommodate for minor groove binding. A recent example which supports this correlation is TBP, which binds the minor groove and induces bending upon DNA binding (Horikoshi *et al.*, 1992). It has now become of interest to determine whether MBP-1 binding induces any such conformational change. Although the predominant effect of A-T to I-C substitutions is to change the groove characteristics, it is possible that there is an effect on the overall flexibility of the DNA due to these base changes. That such an effect might occur implies that the change in flexibility of the DNA did not alter minor groove recognition by the proten to any detectible degree.

Minor Groove Binding Ligands Inhibit MBP-1−DNA Binding. The second line of evidence supporting our conclusion that MBP-1 binds in the minor groove comes from the ability of minor groove binding ligands to compete for DNA binding. DNA binding by the well-characterized major groove binding protein NFkB (Baldwin & Sharp, 1988) is not inhibited by ligand concentrations higher than those that effectively compete out DNA binding by MBP-1 and TBP (Figures 4 and 5). Each of the ligands used in this study differs slightly in the mechanism of their minor groove recognition.

Distamycin binding to DNA induces a cooperative structural transition that can be transmitted to over about 100 bp (Hogan *et al.*, 1979). Most of the recent studies indicate that distamycin recognizes potential binding sites more by the shape of the DNA than by the sequence (Churchill *et al.*, 1990) and requires at least four consecutive A-T base pairs (Zimmer & Wahnert, 1986). In a mithramycin dimer bound to its 6 bp minor groove binding site, the central cytidine is reported to adopt an A-DNA sugar pucker and glycosidic torsion angle (Sastry & Patel, 1993). Mithramycin and distamycin have been used to compete for the binding of proteins in the major groove as well, such as Sp1 (Snyder *et al.*, 1991) and homeodomain peptides (Dorn *et al.*, 1992).

However, in the same competition studies of major groove binding peptides (Dorn *et al.*, 1992), berenil was shown to be ineffective in competing for the binding of peptides in the major groove. Also, Oakley *et al.* (1992) have shown that netropsin does not affect the binding of the major groove binding protein GCN4. Detailed studies of DNA-bound berenil have shown that berenil is closely isohelical with the floor of the minor groove (Hu *et al.*, 1992; Lane *et al.*, 1992; Yoshida *et al.*, 1990). Several NMR studies have confirmed that binding of berenil does not have any structural or conformational effect on the DNA.

Thus, each of the minor groove binding ligands used in this study differs in its minor groove recognition properties. Mithramycin and distamycin are not as highly specific for minor groove recognition as berenil is. In order to correctly interpret the results from these ligand competition assays, an appropriate set of control assays is necessary. The control assays used as a basis for comparison were competition assays with each ligand and the use of both a previously characterized, minor groove binding protein (TBP) and a major groove binding protein (NFkB). Additional minor groove binding ligands (Hoechst dye 33258 and netropsin) were also used in similar competition assays to arrive at the same result (data not shown). The fact that the nonspecific DNA binding activity, which occurs in the absence of nonspecific target DNA in the binding reactions, is not altered by berenil (Figure 6, lanes 3, 6, and 10; Figure 8B), but is slightly affected by distamycin and mithramycin (Figure 6, lanes 3, 6, 8, and 12), agrees with the above discussion on DNA structural implications of ligand binding and DNA recognition. Berenil−DNA binding does not affect major groove binding proteins (Dorn *et al.*, 1992, and Figure 8A) but can affect minor groove binding proteins at concentrations as low as 0.1 mM (Figure 8B). This finding also supports the previous structural studies which had concluded

that there is no conformational change on the DNA due to berenil binding.

MBP-1 and TBP Simultaneously Bind in the Minor Groove. Based on the fidelity of base pair recognition due to the hydrogen donors and acceptors on the groove surfaces, it was proposed that six potential recognition sites occur in the major groove as compared to three in the minor groove of the DNA (Seeman *et al.*, 1976). These interactions allow proteins to differentiate between all four base pairs in the major groove and only three in the minor groove. An increasing number of specific and nonspecific minor groove binding proteins have been reported in the past several years including HMG family proteins (Reeves & Nissen, 1990; Giese *et al.*, 1992; Thanos & Maniatis, 1992), nuclear scaffold protein SATB1 (Dickinson *et al.*, 1992), TBP (Starr & Hawley, 1991; Lee & Horikoshi, 1991), DNase I (Suck *et al.*, 1988), *Escherichia coli* IHF protein (Yang & Nash, 1989), and now MBP-1. In dual protein−DNA binding conditions, the presence of the minor groove binding ligands competes away the supershifted dual protein−DNA complex more effectively than the single protein−DNA complex (Figure 6, lanes 6, 8, 10, and 12, and Figure 8B). This demonstrates that the minor groove of the c-*myc* P2 promoter can allow MBP-1 and TBP to bind together and the simultaneous protein binding to the same minor groove can be effectively inhibited by minor groove binding ligands. Thus, this is the first evidence of the simultaneous recognition of the same DNA minor groove by two different proteins.

Biological Significance of Minor Groove Recognition by MBP-1. The c-*myc* P2 promoter is the stronger promoter for the c-*myc* protooncogene and accounts for 80% of the c-*myc* gene expression. This study has important implications on the efficiency of transcriptional initiation from the P2 promoter, since the TATA box motif is the binding site for the general transcription factor TBP. Binding of TBP occurs in the absence of other proteins in vitro and is an early step in the assembly of a multiprotein preinitiation complex at the promoter. The stabilization of this higher order complex has been attributed largely to the ability of TBP to bend the DNA upon minor groove binding (Horikoshi *et al.*, 1992). Both MBP-1 and TBP are about the same size and can simultaneously bind on the same face of the c-*myc* P2 promoter. Since MBP-1 has been shown to negatively regulate the c-*myc* promoter activity (Ray & Miller, 1991), the results from this paper provide an insight into the mechanism by which MBP-1 exerts its effect.

A model for the regulation of the c-*myc* P2 promoter by MBP-1 can be suggested, involving the simultaneous binding to the minor groove by both MBP-1 and TBP. Lieberman and Berk (1994) have recently shown that a transcriptional activator can stabilize the DNA−protein interactions of TAFs (transcription cofactors in the TFIID complex) and produce a change in the DNase I digestion pattern upstream and downstream in addition to the TBP footprint over the TATA box. It can be hypothesized that the binding of MBP-1 along with TBP to the TATA box on the c-*myc* P2 promoter can disrupt or prevent the assembly of other factors required for efficient transcription. It will be very important to study the molecular effect of this binding in terms of binding of other transcription factors, the base contacts, as well as TBP contacts that are affected. We are currently addressing relevant questions that arise as a result of this study.

ACKNOWLEDGMENT

We thank Dr. R. G. Roeder for the generous gift of the human cDNA clone of TBP in the pET expression vector. We are also grateful to Dr. R. B. Ray for her assistance during the early stages of this work and to David Donze for providing helpful advice.

REFERENCES

Baldwin, A. S., & Sharp, P. A. (1988) *Proc. Natl. Acad. Sci. U.S.A. 85*, 723−727.
Bradford, M. M. (1976) *Anal. Biochem. 72*, 248−254.
Broome, M. E., Reed, J. C., Godillot, E. P., & Hoover, R. G. (1987) *Mol. Cell. Biol. 7*, 2988−2993.
Brown, D. G., Sanderson, M. R., Garman, E., & Neidle, S. (1992) *J. Mol. Biol. 226(2)*, 481−490.
Churchill, M. E., Hayes, J. J., & Tullius, T. D. (1990) *Biochemistry 29(25)*, 6043−6050.
Ciarrocchi, G., Fontana, M., Spadari, S., & Montecucco, A. (1991) *Anticancer Res. 11(3)*, 1317−1322.
Cole, M. D. (1986) *Annu. Rev. Genet. 20*, 361−384.
Coll, M., Fredrick, C. A., Wang, A. H., & Rich, A. (1987) *Proc. Natl. Acad. Sci. U.S.A. 84(23)*, 8385−8389.
Cons, B. M., & Fox, K. R. (1989) *Anti-Cancer Drug Des. 5(1)*, 93−97.
Cory, S. (1986) *Adv. Cancer Res. 47*, 189−234.
Dickinson, L. A., John, T., Kohwi, Y., & Kohwi-Shigematsu, T. (1992) *Cell 70*, 631−645.
Dorn, A., Affotter, M., Muller, M., Gehring, W. J., & Leupin, W. (1992) *EMBO J. 11*, 279−286.
Ford, T. C., & Rickwood, D. (1984) *Nucleic Acids Res. 12(2)*, 1219−1226.
Fox, K. R., & Waring, M. J. (1984) *Nucleic Acids Res. 12(24)*, 9271−9285.
Giese, K., Cox, J., & Grosschedl, R. (1992) *Cell 69*, 185−195.
Grignani, F., Lombardi, L., Inghirami, G., Sternas, L., Cehova, K., & Dalla-Favera, R. (1990) *EMBO J. 9*, 3913−3922.
Grokhovskii, S. L., Surovaia, A. N., Sidorova, N., & Gurskii, G. V. (1989) *Mol. Biol. (Engl. Transl.) 23(6)*, 1558−1580.
Grokhovsky, S. L., Surovaya, A. N., Brussov, R. V., Chernov, B. K., Sidorova, N., & Gursky, G. V. (1991) *J. Biomol. Struct. Dyn. 8(5)*, 989−1025.
Hogan, M., Dattagupta, N., & Crothers, D. M. (1979) *Nature 278*, 521−524.
Horikoshi, M., Bertuccioli, C., Takada, R., Wang, J., Yamamoto, T., & Roeder, R. G. (1992) *Proc. Natl. Acad. Sci. U.S.A. 89*, 1060−1064.
Hu, S. H., Weisz, K., James, T. L., & Shafer, R. H. (1992) *Eur. J. Biochem. 204(1)*, 31−38.
Jenkins, T. C., Lane, A. N., Neidle, S., & Brown, D. (1993) *Eur. J. Biochem. 213(3)*, 1175−1184.
Kas, E., Iazurralde, E., & Laemmle, U. K. (1989) *J. Mol. Biol. 210(3)* 587−599.
Kopka, M. L., Yoon, C., Goodsel, D., Pjura, P., & Dickerson, R. E. (1985) *Proc. Natl. Acad. Sci. U.S.A. 82*, 1376−1380.
Lane, A. N., Jenkins, T. C., Brown, T., & Neidle, S. (1991) *Biochemistry 30(5)*, 1372−1385.
Lee, D. K., & Horikoshi, M. (1991) *Cell 67*, 1241−1250.
Lieberman, P. M., & Berk, A. J. (1994) *Genes Dev. 8*, 995−1006.
Lipp, M., Schilling, R., & Bernhart, G. (1989) *Oncogene 4*, 535−541.
Marcu, K. B., Bossone, S. A., & Patel, A. J. (1992) *Annu. Rev. Biochem. 61*, 809−860.
Mattes, W. B. (1990) *Nucleic Acids Res. 18(13)*, 3723−3730.
Mortensen, U. H., Stevnsner, T., Krogh, S., Olesen, K., Westergaard, O., & Bonven, B. J. (1990) *Nucleic Acids Res. 18(8)*, 1983−1989.
Oakley, M. G., Mrksich, M., & Dervan, P. V. (1992) *Biochemistry 31(45)*, 10969−10975.
Pognonec, P., Kato, H., Sumimoto, H., Kretzchmar, M., & Roeder, R. G. (1991) *Nucleic Acids Res. 19(23)*, 6650.
Ray, R., & Miller, D. M. (1991) *Mol. Cell. Biol. 11(4)*, 2154−2161.

Reeves, R., & Nissen, M. S. (1990) *J. Biol. Chem. 265(15)*, 8573–8582.
Sarker, M., & Chen, F. M. (1989) *Biochemistry 28(16)*, 6651–6657.
Sastry, M., & Patel, D. J. (1993) *Biochemistry 32(26)*, 6588–6604.
Schmid, N., & Behr, J. P. (1991) *Biochemistry 30(17)*, 4357–4361.
Seeman, N. C., Rosenberg, J. M., & Rich, A. (1976) *Proc Natl. Acad. Sci. U.S.A. 73*, 804–808.
Sidorova, N., Nikolaev, V. A., Surovaia, A. N., Zhuze, A. L., & Gurskii, G. V. (1991) *Mol. Biol. (Engl. Transl.) 25(3)*, 706–717.
Snyder, R. C., Ray, R., Blume, S., & Miller, D. M. (1991) *Biochemistry 30*, 4290–4297.
Spencer, C. A., & Groudine, M. (1991) *Adv. Cancer Res. 56*, 1–48.
Starr, D. B., & Hawley, D. K. (1991) *Cell 67*, 1231–1240.
Suck, D., Lahm, A., & Oefner, C. (1988) *Nature 332*, 464–468.
Suzuki, M. (1993) *EMBO J. 12(8)*, 3221–3226.
Thanos, D., & Maniatis, T. (1992) *Cell 71*, 777–789.
White, S. W., Appelt, K., Wilson, K. S., & Tanaka, I. (1989) *Proteins: Struct., Funct., Genet. 5*, 281–288.
Yang, C. C., & Nash, H. A. (1989) *Cell 57*, 869–880.
Yoshida, M., Banville, D. L., & Shafer, R. H. (1990) *Biochemistry 29(28)*, 6585–6592.
Zimmer, C., & Wahnert, U. (1986) *Prog. Biophys. Mol. Biol. 47*, 31–112.

BI941671A